MULTI-SENSOR NAVIGATION SYSTEM DESIGN

by

David Royal Downing

B.S., The University of Michigan
(1962)

M.S., The University of Michigan
(1963)

SUBMITTED IN PARTIAL FULFILLMENT
OF THE REQUIREMENTS FOR THE
DEGREE OF DOCTOR OF SCIENCE

at the

MASSACHUSETTS INSTITUTE OF TECHNOLOGY

May 1970

Signature of Author: _____
Department of Aeronautics
and Astronautics, May 1970

Certified by: _____
Thesis Supervisor

Certified by: _____
Thesis Supervisor

Certified by: _____
Thesis Supervisor

Certified by: _____
Thesis Supervisor

Accepted by: _____
Chairman, Departmental
Graduate Committee

Archives
MASS. INST. TECH.
APR 22 1971
LIBRARIES

Thesis
A.M.
1970
Sm

All physical phenomena are governed by a set of simple principles and logic. The apparent complexity of these phenomena is due to our limited knowledge and understanding of them.

David Royal Downing
May 1970

ACKNOWLEDGEMENTS

The author would like to express his deepest appreciation to the following individuals who have made contributions to this thesis.

To Professor Wallace Vander Velde, who as Chairman of the Thesis Committee, provided encouragement and guidance. He always found time in his very heavy schedule to discuss the thesis problems. Also his thorough reading and critical comments of the final draft has contributed greatly to the clarity of the presentation.

To Professor Walter Hollister and Dr. Frank Tung, who as members of the Thesis Committee, provided technical assistance and encouragement throughout the thesis. Special mention is a also due these gentlemen for their insistence early in the thesis that the author solve an example problem. The example became a focal point for communication between the author and the committee and contributed greatly to the clarification of the basic concepts of the thesis.

To Professor James Potter, who as a member of the thesis committee, gave of his expertise in the areas of optimal estimation theory and control.

To the employees and administration of the National Aeronautics and Space Administration's Electronics Research Center for their support. This support included financial aid, use of digital computer and the interest and encouragement of my fellow workers. Of special note are Dr. Richard Hayes and Mr. Robert Wedan who as the authors supervisors provided encouragement and interest throughout the preparation of the thesis. Also, special thanks go to Dr. Arthur H. Lipton and Dr. John Bortz, Sr., who throughout the author's doctoral program, have provided encouragement, interest and technical counsel which were invaluable. They also deserve a great deal of thanks for the many hours spent making technical comments and proofreading the entire final draft.

To Miss Diane Maguire for her thoroughly professional typing of the final draft and for her patience and cheerful disposition.

To the author's wife Barbara who deserves the most special recognition of all. She has been a source of encouragement throughout the authors graduate schooling. Only she knows the sacrifices she has made.

CONTENTS

Chapter		Page
	ACKNOWLEDGEMENTS	iii
	ABSTRACT	1
	SYMBOLS	3
	GENERAL NOTATION	5
1	INTRODUCTION	6
2	FUNCTIONAL DESCRIPTION OF MULTI-SENSOR SYSTEM DESIGN PROCEDURE	10
	2.1 INTRODUCTION	10
	2.2 FRAMEWORK OF DESIGN PROCESS	10
	2.3 ANALYTIC DESIGN PROCEDURE	12
3	FORMULATION OF THE DESIGN PROBLEM	16
	3.1 INTRODUCTION	16
	3.2 MODEL OF A NAVIGATION SYSTEM	16
	3.2.1 Mission Related Parameters	17
	3.2.2 System Related Parameters	18
	3.2.3 Mission Objective Parameters	22
	3.3 MATHEMATICAL FORMULATION	24
4	OPTIMAL SCHEDULING OF NAVIGATION MEASUREMENTS	28
	4.1 INTRODUCTION	28
	4.2 THEORETICAL DEVELOPMENT	28
	4.2.1 Continuous Measurement Formulation	28
	4.2.2 Necessary Conditions	30
	4.2.3 Formulation of Special Measurement Processes	37
	4.3 COMPUTATION ALGORITHM	39
	4.3.1 Algorithm Selection	39
	4.3.2 Computer Mechanization	41
	4.4 NUMERICAL EXAMPLE: OPTIMAL SCHEDULING OF DME MEASUREMENTS	46

CONTENTS (Continued)

Chapter			Page
		4.4.1 Problem Statement.	50
		4.4.2 Optimization Results	52
		4.4.3 Optimization Procedure Characteristics .	56
5	DESIGN PROCEDURE		59
	5.1 INTRODUCTION.		59
	5.2 EVALUATION TECHNIQUES		59
	5.3 DESIGN OPTIONS.		66
		5.3.1 Minimal System	66
		5.3.2 Set of Minimal Systems	69
		5.3.3 Satisfactory Systems	72
		5.3.4 Suboptions	76
	5.4 AUXILIARY DATA.		76
		5.4.1 Design Data.	76
		5.4.2 Utilization Data	82
	5.3 SUMMARY		84
6	AVIONICS SYSTEM DESIGN		85
	6.1 INTRODUCTION.		85
	6.2 PROBLEM STATEMENT AND CONVERSION TO ENGINEERING TERMS		85
		6.2.1 Mission Data	85
		6.2.2 Mission Objective.	87
		6.2.3 System Data.	87
	6.3 DESIGN PROCEDURE RESULTS.		89
		6.3.1 Minimal System	89
		6.3.2 Set of Minimal Systems	93
		6.3.3 Satisfactory Systems	103
	6.4 SUMMARY		110
7	SUMMARY AND RECOMMENDATIONS.		111
	7.1 SUMMARY		111
	7.2 RECOMMENDATIONS		113
		7.2.1 Procedure Efficiency and Flexibility . .	113
		7.2.2 Related Applications	114

CONTENTS (Continued)

Appendix		Page
A	THEORMS RELATING TO THE SWITCHING FUNCTIONS AND THE COVARIANCE PROPAGATION.	116
B	NAVIGATION IN A BENIGH ENVIRONMENT.	119
C	CHARACTERISTICS OF DIGITAL PROGRAM.	121
D	MODEL OF ENVIRONMENTAL DISTURBANCES	122
E	MEASUREMENT SENSITIVITY	126
F	PERFORMANCE INDEX SENSITIVITY FOR VARIATIONS IN CONTROL HISTORY	129
G	DESIGN PROCEDURE SYSTEM LISTING AND ANALYSIS SUMMARY	131
	REFERENCES.	136
	BIOGRAPHICAL SKETCH	139

MULTI-SENSOR NAVIGATION SYSTEM DESIGN

by

David Royal Downing

Submitted to the Department of Aeronautics and Astronautics in May 1970 in partial fulfillment of the requirements for the degree of Doctor of Science in Instrumentation.

ABSTRACT

This thesis treats the design of navigation systems that collect data from two or more on-board measurement subsystems and process this data in an on-board computer. Such systems are called Multi-Sensor Navigation Systems.

The design begins with the definition of the design requirements and a list of n sensors and c computers. A Design Procedure is then developed which automatically performs a systematic evaluation of the $(2^n-1) \times c$ candidate systems that may be formed. This procedure makes use of a model of the navigation system that includes sensor measurement errors and geometry, sensor sampling limits, data processing constraints, relative computer loading, and environmental disturbances. The performance of the system is determined by its terminal navigation uncertainty and dollar cost. The Design Procedure consists of three design options, three levels of evaluation, and a set of auxiliary data. By choosing from among the design options and the auxiliary data, the designer can tailor the Design Procedure to his particular application.

A design option is developed to answer each of the following three questions: (1) Which candidate system meets the system accuracy specification and has the lowest system cost? (2) For each sensor or computer chain, which is defined as the set of all systems containing that component, what is the system that satisfies the accuracy requirements and has the lowest cost? (3) Which systems satisfy the design accuracy requirements?

The system evaluation is accomplished using one optimal and two nonoptimal techniques. The optimal performance evaluation uses the measurement schedule that minimizes the

terminal uncertainty. A first-order optimization procedure is developed to determine this schedule. This uses optimal sampling logic derived by applying the Maximum Principle. One non-optimal analysis uses the idea that the addition of a sensor or the increase of the computer processing capability can not degrade the system's performance. The second non-optimal technique obtains approximate values of the system's accuracy by assuming measurement schedules that do not satisfy the processing constraint.

The Procedure is applicable to a large class of air or space missions for which a nominal trajectory can be defined. To illustrate how the Procedure would be used, the design of an aircraft navigation system for operation in the NE corridor is presented. This problem considers the configuration of a system starting with four candidate sensors and three candidate computers. The outputs from all three design options are presented and discussed.

Thesis Supervisor: Wallace VanderVelde, Sc.D.
Title: Professor of Aeronautics and Astronautics

Thesis Supervisor: Walter Hollister, Sc.D.
Title: Associate Professor of Aeronautics and Astronautics

Thesis Supervisor: James Potter, Ph.D.
Title: Associate Professor of Aeronautics and Astronautics

Thesis Supervisor: Frank Tung, Ph.D.
Title: Chief, Microcircuit Technology Division, NASA/ERC

SYMBOLS

A	constant weighting matrix used in definition of System Performance Index.
CC	computer capacity (measurements/hour)
C1, C2, . . .	short hand designation of candidate computers
DT	time step used in numerical integration
DT_i	sampling interval for i^{th} sensor
$\overline{DT}_i$	minimum allowed DT_i
F	system linearized dynamics matrix
H	linearized measurement sensitivity matrix
$\mathscr{H}$	system Hamiltonian
$\dot{I}$	information rate
J	system performance index
J_{LC}	value of J computed using Limiting Case Analysis
J_{req}	value of J from system design specification
J^*	value of J computed using Optimal Measurement Schedule
K_i	Computer Loading factor for processing i^{th} sensor data (non-dimensional)
M/H	abbreviation for measurements/hour
N	measurement sample rate matrix (measurements/hour)
$N_i = N_{ii}$	sample rate for i^{th} sensor

NM_i	maximum allowed value of N_i
P	covariance matrix of the errors in the estimate of the state vector x.
Q	intensity matrix of system disturbances.
R	covariance matrix of measurement errors
SW	switching function matrix
S1, S2, . . .	shorthand designation of candidate sensors
t	time
T	time of flight
x	nx1 state vector
$\hat{x}$	estimated value of x
z	linearized measurement vector
z	special costate matrix ($P \wedge P$)
ε	estimation error vector
$\varepsilon 1$ and $\varepsilon 2$	parameters used in time step generation
$\varepsilon 3$, $\varepsilon 4$ and $\varepsilon 5$	parameters used in control iteration scheme
	costate matrix
$\wedge$	costate matrix
$\phi\ (t_1, t_2)$	state transition matrix

GENERAL NOTATION

Vectors are indicated by a small underlined letter; matrices are designated capital letters.

Δ ( )	incremental change in ( ).
δ ( )	variational change in ( ).
$( )_{nom}$	the variable ( ) evaluated along the nominal trajectory
cov [ ]	covariance matrix of [ ].

Chapter 1

INTRODUCTION

This work proposes that it is possible to formulate the design of a class of Multi-Sensor Navigation Systems in such a way as to allow a major portion of the total design process to be accomplished analytically. The term "Multi-Sensor Navigation System" is used in the present work to denote a navigation system which collects and processes information from two or more measurement subsystems, as shown in Figure 1. Throughout this work, these measurement subsystems, whether a simple chronometer or a complicated inertial measurement unit, are referred to as "sensors."

Multi-Sensor Navigation Systems are used for one or a combination of three reasons. The most basic reason is to permit the determination of the minimum set of navigation variables, i.e., to provide measurements that span the navigation space of interest. Multi-Sensor Navigation Systems of this type are as old as navigation itself. An example of such a system is the sextant and chronometer used to navigation on the open seas. Each instrument by itself provides the capability of determining only one of the two navigation parameters of interest; the sextant gives latitude and the chronometer, the determination of longitude. A second reason for using several sensors is concerned with the question of system reliability. In this case, either several identical sensors or several different sensors that measure related navigation parameters are used so that the total system reliability is increased over any minimum set of sensors, i.e., the mission objectives can be achieved even though a number of the sensors may fail during the mission. An example of this kind of system is the use of three identical inertial navigation systems in the Boeing 747 aircraft. A third reason for having two or more sensors in the system is to improve the systems performance. Performance here deals primarily with accuracy. It is known that the combination of data from several different sensors can result in an accuracy that would be impossible or too costly to achieve from a single sensor. An example of this type of behavior is the combination of an inertial measurement unit and an independent position measurement. It has been shown (ref. 1) that with a relatively simple position measurement to correct at discrete times the growing inertial error, such a multi-sensor system can achieve accuracies beyond the capability of a pure inertial system that has the same total system cost.

The design of a Multi-Sensor Navigation Systems is complicated by two facts. First, the system's performance is measured by a combination of several items including navigation accuracy, cost, reliability, maintainability, and the availability of components. Each of these items is also a function of a group of parameters. As an example, the system's accuracy is affected by

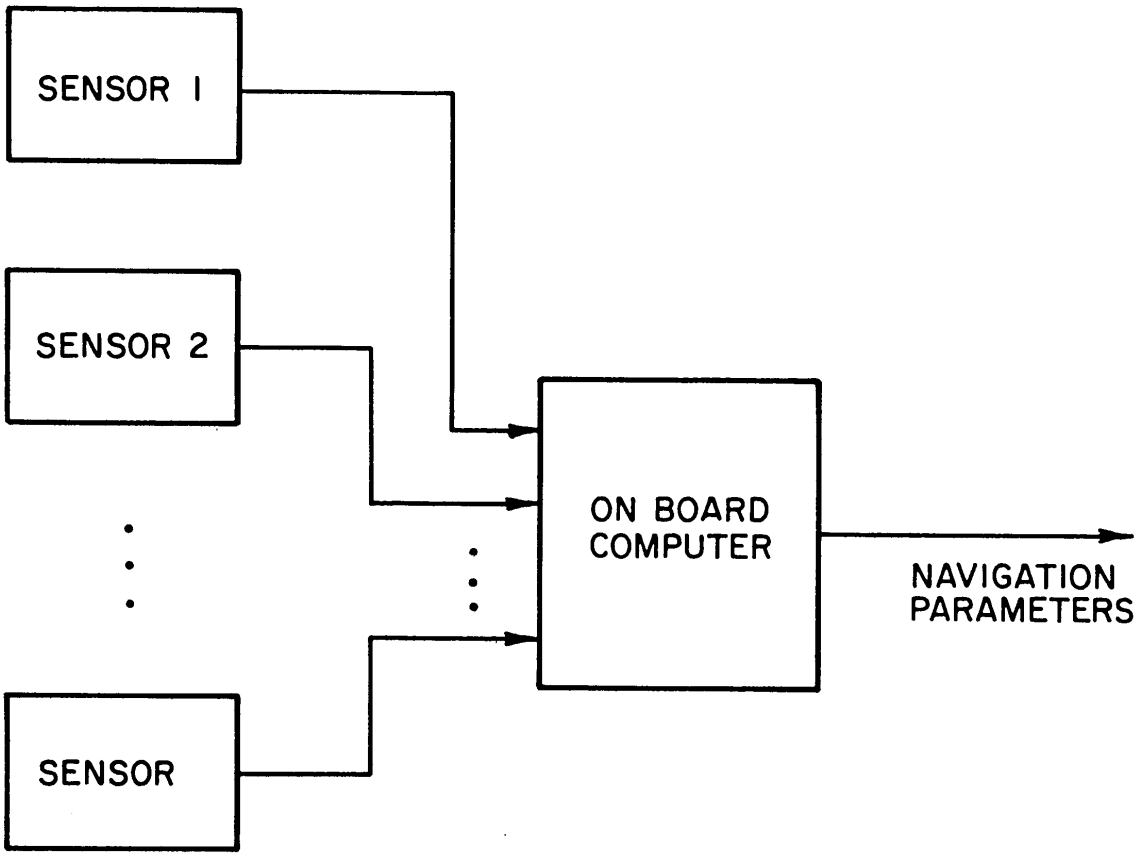


Figure 1.- Multi-sensor navigation system

the characteristics of the on-board sensors and computer, the external information sources, the vehicle and nominal trajectory, and the environmental disturbances. For all but the simplist of applications, it is virtually impossible to keep track of all these factors. A second complication arises due to the large number of candidate configurations. If n sensors and C computers are identified as candidate components, there are $(2^n - 1) \times C$ candidate systems. It is generally not feasible, due to limited resources, to perform detailed analyses on all the candidate systems. In the past, therefore, the designer has selected a subset of candidate systems based on his experience and then has analyzed these systems at a detailed level. From the results of these analyses, the designer selected the best in this subset, and if this system met the requirements, it was the final design. Using this technique, the possibility always exists of overlooking a better system.

To alleviate these difficulties, a Design Procedure (a design tool) has been developed which permits a major portion of the design process to be accomplished using automatic computation. Three desired characteristics of the Design Procedure are: (1) the incorporation of a framework in which the important design parameters are accounted for automatically, (2) the development of an efficient set of logic and evaluation analysis that permit the evaluation of all systems, and (3) sufficient flexibility enabling the designer to tailor the Design Procedure to his particular problem.

The first task in the development of the Design Procedure is the selection of the portion of the design process and the measures of system performance that are best adaptable to automatic computation. This work is presented in Chapter 2. In Chapter 3, a mathematical model of the navigation system and a general mathematical framework are generated. The model of the navigation system includes the sensor characteristics of accuracy, geometry and limited sample rates. The computer is characterized by a limit on the amount of data that can be processed per unit time and by a set of weighting constants that recognize the difference in the computer loading of the various navigation data. The mission is characterized by the vehicle, nominal trajectory, and environmental disturbances. To establish an analytic structure, it is assumed that the navigation measurements will be processed by a Least-Squares Estimation routine. In the process of the formulation of the design problem, the concept of maximum system accuracy is seen to be important. To determine the maximum terminal navigation accuracy of a system requires the determination of the optimal measurement schedule. In Chapter 4, an iterative optimization procedure is developed to accomplish this. In this development, the discrete measurement process is reformulated in terms of continuous measurement rates. This formula-

tion allows the sensor sampling limitations and the processing limits to assume a convenient form. The technique then calls for a series of iterations on the sensor sampling rates to arrive at the optimal measurement schedule. To illustrate the optimazation technique, the first example problem is presented. In this simple problem, the optimal measurement schedule is determined for a system which could measure range to two seperate ground stations.

The Design Procedure is presented in Chapter 5. It consists of three design options, a set of selection logic for each option, three system evaluation techniques, and a set of auxiliary design data.

Each design option provides the designer with a different list of systems. The first option determines the Minimal System, i.e., the system that satisfies the design accuracy requirements and has the lowest total cost. Defining a component chain as a list of all systems that contain a given component, the second option determines the Minimal System for each sensor and computer chain. The third option determines all those candidate systems that satisfy the system accuracy requirements. The auxiliary data include the time histories of the estimation errors, the optimal measurement schedules and the corresponding sensor switching functions, and computer sensitivity data. By selecting from among the design options and auxiliary data, the designer can tailor the Design Procedure to his application.

The first evaluation technique makes use of the optimization procedure presented in Chapter 4. The second evaluation technique exercises the system using non-optimal measurement schedules that ignore the computer constraint to determine the system's limiting performance. The third technique uses the fact that a system's performance is never degraded if the system is augmented by additional sensors or computer capacity. Application of the two non-optimal evaluation techniques often allows candidate systems to be eliminated without the need of determining the optimal measurement schedule. To make efficient use of these three evaluation techniques, a different selection logic is generated for each of the design options. These sets of logic determine both the order in which the candidate systems are evaluated and also the order in which the evaluation techniques are applied to each system. An example problem is presented in Chapter 6 to demonstrate the Design Procedure. This design problem is the determination of the en-route navigation system to be used on a V/STOL aircraft for flights between Boston and Washington, D. C. Four candidate sensors and three candidate computers are considered.

Finally, Chapter 7 presents a summary of the present work and a discussion of several areas which are recommended for further study.

Chapter 2

FUNCTIONAL DESCRIPTION OF MULTI-SENSOR SYSTEM DESIGN PROCEDURE

2.1 INTRODUCTION

The proposition of this work is that it is possible to formulate the design of a class of multi-sensor navigation systems in a way that allows a major portion of the total design process to be accomplished by automatic computation.

In this chapter, the portion of the total design process performed by the Multi-Sensor Design Procedure will be identified. To make this functional identification, a general framework for the total design process is presented and examined to determine which of the various functions could be performed automatically. Areas are identified in this chapter in which specific analysis is required. Then, in a later chapter, these analyses are performed.

2.2 FRAMEWORK OF DESIGN PROCESS

The procedure by which an engineer designs a complicated system is a very individualistic process that depends on the designer's experience and the particulars of the application. It is, however, possible to identify a set of logical functions that are common in all cases and that form a basic framework for the design process. This framework shown in Figure 2 is composed of five logical functions and two iterative paths. The process begins when the designer is presented with the problem statement. The problem statement is in the general form "Design the best navigation system for Mission A," where Mission A is described in words. The first task the designer must do is to convert the word statement into engineering concepts and parameters. The problem statement suggests a logical division of this formulation into three areas. The first of these is indicated by the word "best". This established the need for a set of parameters which are measures of the objectives of the design, i.e., measures of system performance and efficiency. The second set of parameters of importance is indicated by the word "systems". The system refers to the collection of navigation hardware (measurement subsystems and computer) and the software required to process the measurements. Finally, the word "mission" requires a third set of parameters. The mission parameters define the specifics of such factors as the nominal trajectory, vehicle, and physical environment.

Having converted the problem into engineering terms, it is next necessary to list the navigation sensors and computers which are candidates for inclusion in the final design.

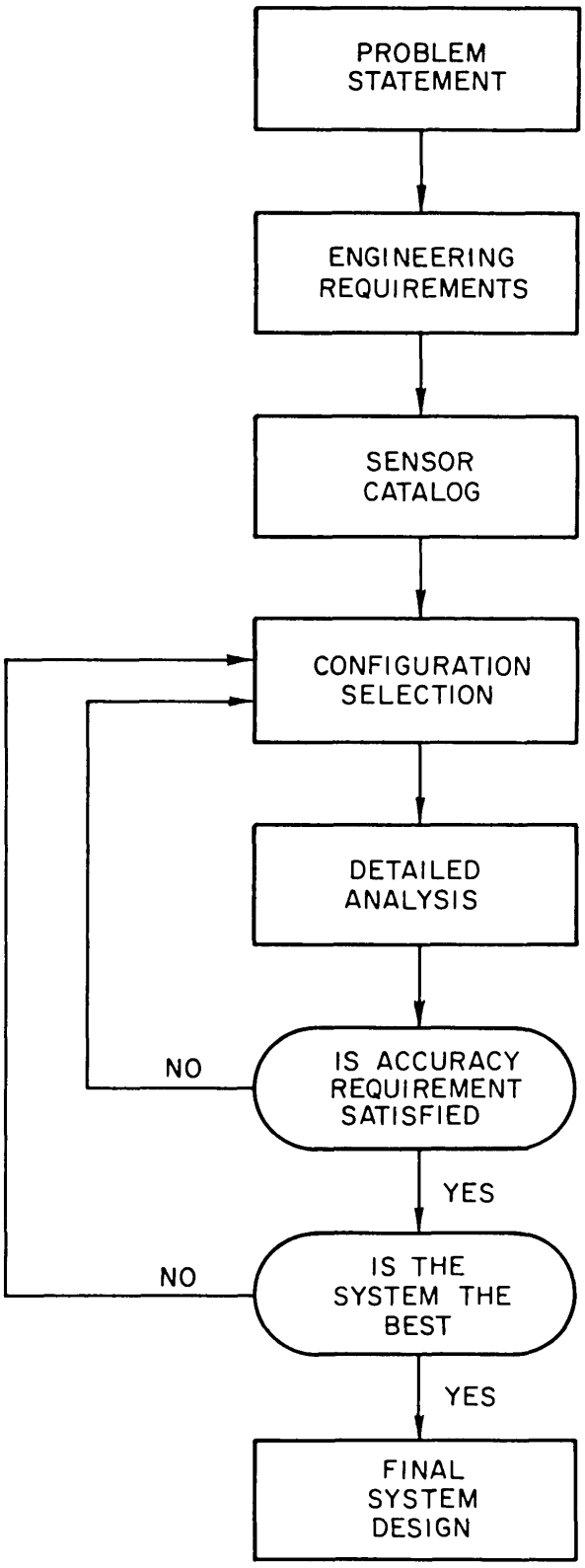


Figure 2.- Flow chart of design process

The remainder of the design process is iterative in nature. The designer must select the combination of sensors and computer that satisfies the system objectives for the prescribed mission. If the list of sensors and computers is long, the number of candidate system configurations may be very large. For n sensors and C computers, there are $(2^n - 1) \times C$ possible configurations. This expression is derived as follows. The number of combinations M of n sensors taken p at a time is given by

$$M = \frac{n!}{p!(n-p)!}$$

(ref. 2). The total number of possible sensor combinations is

$$\sum_{p=1}^{n} \frac{n!}{p!(n-p)!} = 2^n - 1.$$

Since each system is required to use one of the C computers, the total number of configurations is given by $(2^n - 1) \times C$. If n=6 and c=3, there are 189 possible configurations. To start the iterative process, one of the $(2^n - 1) \times C$ system configurations is selected. For this configuration, a detailed analysis is performed to determine its ability to satisfy the system objectives. On completion of this analysis the question is asked; "Can this configuration satisfy the performance requirements?" If the answer is "No", this configuration is eliminated and the process restarted with a new configuration. If the answer is "Yes", then a second question is asked; "Is this configuration the best of all those configurations which satisfy the performance requirements?" This question differs from the previous one due to the fact that there is no required value of "best" specified. It is, therefore, necessary to determine the efficiency of all systems which satisfy the performance requirement. The system which can answer "Yes" to this question will be the final design configuration.

2.3 ANALYTIC DESIGN PROCEDURE

The problem of determining the "best" system configuration as outlined above is a theoretical goal. To achieve this goal, it would be necessary to perform detailed analysis on all the $(2^n - 1) \times C$ possible system configurations. This approach is not feasible for problems which have large lists of candidate sensors or computers because of the large amount of analysis required. A second approach to the design of such a system is to have the designer select a small subset of the configurations based on

his past experience. The detailed analysis is performed on this subset and then the question is asked, "For the selected systems which is best and is this good enough?" This approach, although practical from a workload point of view, offers no assurance that a better configuration is not being overlooked. It is in the area between these two approaches that an analytic design procedure can be useful to the designer. The analytic design procedure provides additional data that fortifies and enhances the designers understanding of the design problem. With this additional information his selection of systems for detailed analysis can be made with greater confidence that the "best" system of the (2^n-1)xc systems is not being overlooked.

Several general concepts can now be stated which will provide guidelines in the development of an automatic design procedure. First it will be required that the procedure determine the capabilities of all configurations by applying analysis at some level. This produces a high confidence in the selected configurations. If the design procedure is to save work, it is necessary that the level of analysis be less than used to perform the detailed analysis. Simplifications are made in both the definition of "best" and in the models used to evaluate the navigation systems. The factors which determine the relative ranking of systems include among other things system accuracy, cost, equipment availability, reliability, and maintainability. Instead of trying to model and weigh all these factors to form a super cost function, only the two considerations of system performance (in terms of accuracy) and system cost (in terms of dollars) will be used to evaluate configurations. Left to the designer is the tasks of applying the other factors at the time of selection of those systems on which further analysis will be performed. The second area of simplification is in the model of the navigation system. Such factors are sensor compensation, computation errors, and software mechanization are not considered. The models will, however, include the major influences on system performance, including sensor errors, computation limits, and environmental disturbances.

A second desirable feature for the design procedure is that it provides a variety of information allowing the designer choices which reflect his preference and the particular application. This feature is provided by identifying three design options and certain auxiliary information useful in the design and utilization of systems.

The total design process, including the design procedure, is shown in Figure 3. The functions of problem statement, conversion to physical terms, and the development of a catalog of candidate sensors and computers are tasks which are performed by the designer. The design procedure performs the tasks of configuration selection and evaluation.

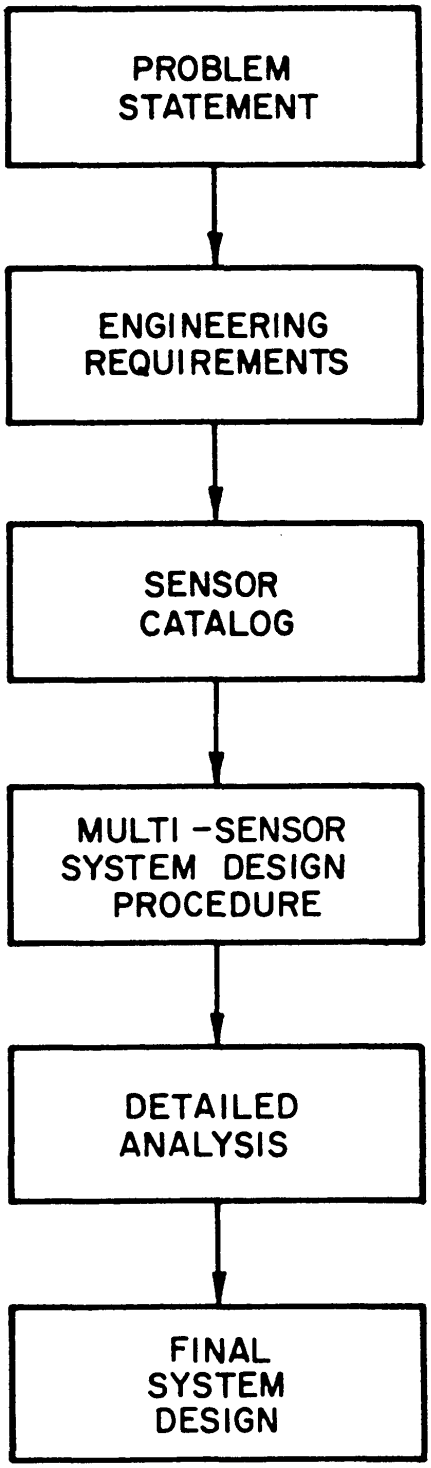


Figure 3.- Flow chart of design process including multi-sensor design procedure

The work remaining in the development of the design procedure are (1) the development of a mathematical model of a navigation system, and a specification of the design problem, (2) the development of a technique that allows the system's accuracy capabilities to be determined, and (3) a set of logic that allows the systematic analysis of all candidate configurations. The mathematical models of the navigation system and the design problem are given in Chapter 3. Chapter 4 presents the technique of determining the optimal schedule of navigation measurements used to evaluate systems. Chapter 5 presents the formulation of the design procedure including system evaluation and selection logic.

Chapter 3

FORMULATION OF THE DESIGN PROBLEM

3.1 INTRODUCTION

To apply automatic computation to the evaluation of navigation systems requires both models of the factors which influence a system's performance (accuracy) and cost and a general mathematical framework that can account for the interaction of these factors. The required models are developed by first identifying the important design parameters and then converting these into mathematical terms. A mathematical framework which incorporates these models is developed by assuming that the data will be processed in the on-board computer using a Least Square Estimator.

3.2 MODEL OF A NAVIGATION SYSTEM

The final configuration of a navigation system is influenced by many factors. In order to evaluate a navigation system configuration, it is necessary to identify these factors and to model them in sufficient detail that a realistic system performance evaluation can be accomplished. To obtain an understanding of the navigation system, consider the total system in which the navigation system operates. The total system shown in Figure 4 includes the vehicle with its guidance and control systems in addition to its navigation system. The motion of the vehicle is described by the vectors $\underline{X}$ and $\underline{\phi}$. $\underline{X}$ describes the linear state of the center of mass of the vehicle and $\underline{\phi}$ describes the orientation or rotational state of the vehicle. The motion of the vehicle is given by the set of nonlinear differential equations

$$\dot{\underline{X}} = \underline{G}(\underline{X},\underline{\phi},\underline{U},\underline{W}) \tag{3.1}$$

$$\dot{\underline{\phi}} = \underline{H}(\underline{\phi},\underline{X},\underline{U}_{\phi}) \tag{3.2}$$

where:

$\underline{U}$ = command force vector to control the vehicle's translational motion.

$\underline{U}_{\phi}$ = command moment vector to control the vehicle's orientation

$\underline{W}$ = external force vector acting on the vehicle

$\underline{V}$ = navigation system measurement error vector.

The definition of navigation presented in this work is the measurement and determination of the motion of the center of mass of the vehicle. It is possible to include the orientation vector as part of a larger navigation state vector $\underline{x}'$ where:

$$\underline{x}' = \begin{bmatrix} \underline{X} \\ \underline{\phi} \end{bmatrix}$$

It is possible to separate the translational and rotational motions when configuring a navigation system, due to the fact that the vehicle's attitude control system has a higher bandwidth than the navigation system. It is assumed, therefore, that the vehicles attitude will be held at its nominal value. Also, except for a few navigation sensors, e.g., inertial measuring unit, the rotational information is derived from a different set of sensors than those used to measure the motion of the center of mass.

From this starting point, it is possible to identify the important influences on the configuration of the navigation system. These factors are divided into mission related, system related, and mission objective related categories.

3.2.1 Mission Related Parameters

The parameters related to the mission are the vehicle, the trajectory, and the physical environment. Because only the function of navigation is of interest in this work, the vehicle can be modeled by its center of mass with its motion completely defined by Eq. (3.1).

For most applications, whether air, space, or marine navigation, the vehicle is constrained or controlled to be near a predetermined nominal trajectory. The nominal trajectory propagates according to the same dynamical equation as the vehicle model

$$\dot{\underline{X}}_{nom} = \underline{G}(\underline{X}_{nom}, \underline{\phi}_{nom}, \underline{U}_{nom}, \underline{W}_{nom}) \qquad (3.3)$$

The final mission related factor affecting system design is the physical environment. The vehicle will travel through some physical environment during the mission; e.g., atmosphere, ocean, or space. The interaction of this environment with the vehicle will perturb the vehicle's motion. The effects of these environmantal disturbances are of two basic types: (1) a deterministic component $\underline{W}_{nom}$ which can be included in the equation for the

nominal trajectory, and (2) a non-deterministic or random component. Examples of these are the structure of the wind fields in the atmosphere. These fields are made up of constant winds which are known plus random gusts. The determination of the effect of this type of disturbance on the vehicle's motion requires a knowledge of the vehicle. For example, the determination of the acceleration on an aircraft flying nominally straight and level due to a wind gust perpendicular to the velocity vector requires a knowledge of the aerodynamic characteristics of the vehicle; e.g., its side force coefficient as well as its mass and velocity. In some applications, the effects of these random disturbances are large enough to require modeling of their effects.

3.2.2 System Related Parameters

The system in question here is the navigation system. It is assumed that the guidance and control systems are already specified quantities. The attitude control system is not considered, since present interest is in only translational motion. It is necessary, however, that required navigation measurements be available without interruption. A violation of this requirement is illustrated by considering doppler radar. The doppler radar consists of several narrow beams which emit a series of pulses (Figure 5). These pulses are reflected from the ground and backscatter is received in the vehicle. The difference in frequency of the transmitted and received signals is measured and is proportional to velocity. The angle of incidence of the beam to the ground for Beam 1 is $(\beta + \phi)$, where β is the nominal angle, and ϕ is the aircraft roll angle. There is an angle ϕ^* for which the return signal is not sufficient to maintain the doppler's synchronization. If the roll control allowed a roll angle greater than ϕ^* to exist, the information from the doppler radar would be lost.

The navigation system shown in Figure 6 consists of a set of measurement sensors (subsystems) and a digital computer. The navigation sensors can measure a scalar quantity or virtually simultaneously measure several variables. Also, the sensor might measure information from a single source or from multiple sources. In all cases, the measurements are a function of the vehicle's state vector $\underline{x}$. For example, the vehicle's position and velocity can be inferred from a set of bearing measurements to two independent radio stations with known locations (Figure 7). To relate the navigation measurements to $\underline{x}$, it is necessary to consider the system geometry. This geometry is, in general, non-linear and time varying as the vehicle moves along it's trajectory. Associated with this geometry is a measurement sensitivity which can detract from or enhance the value of a particular measurement.

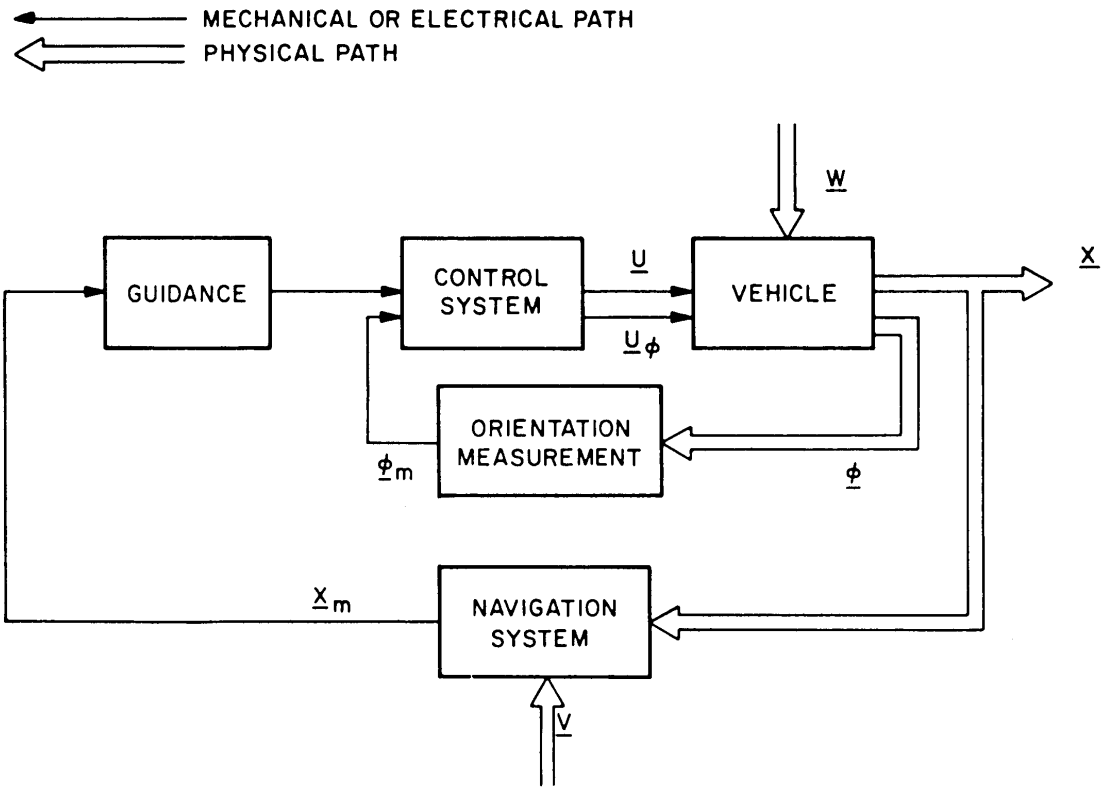


Figure 4.- Navigation, guidance, and control system

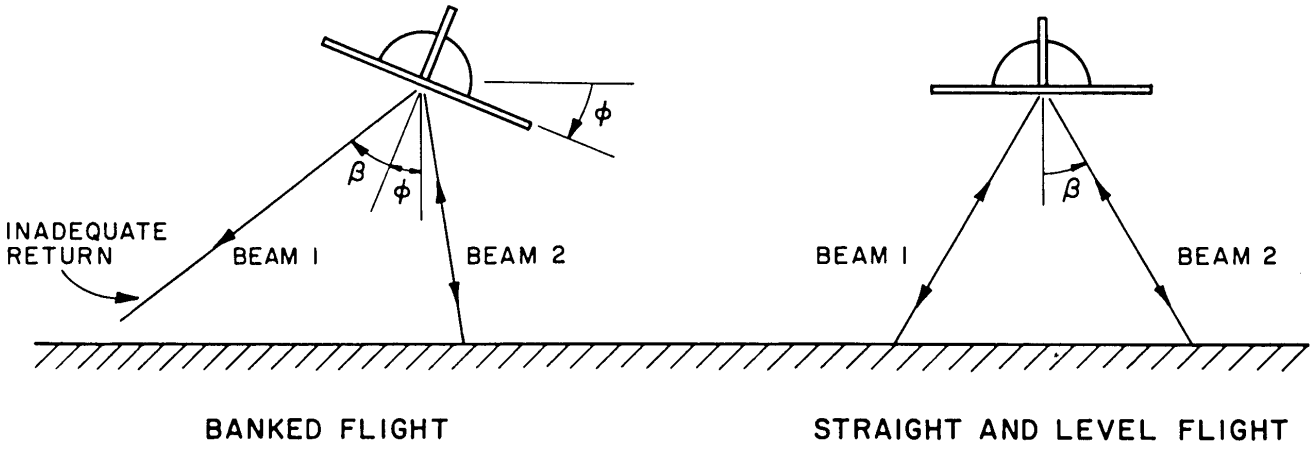


Figure 5.- Doppler radar geometry

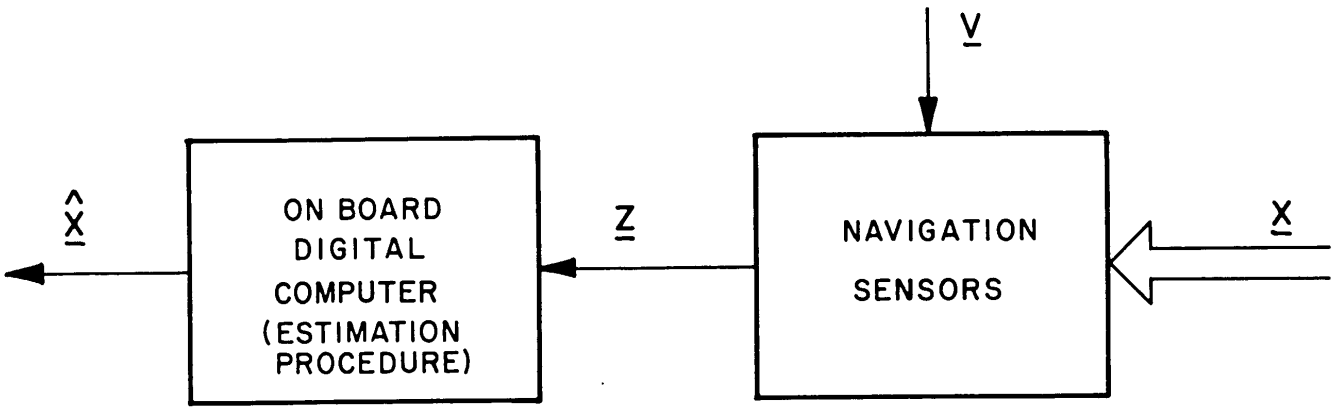


Figure 6.- Navigation system components

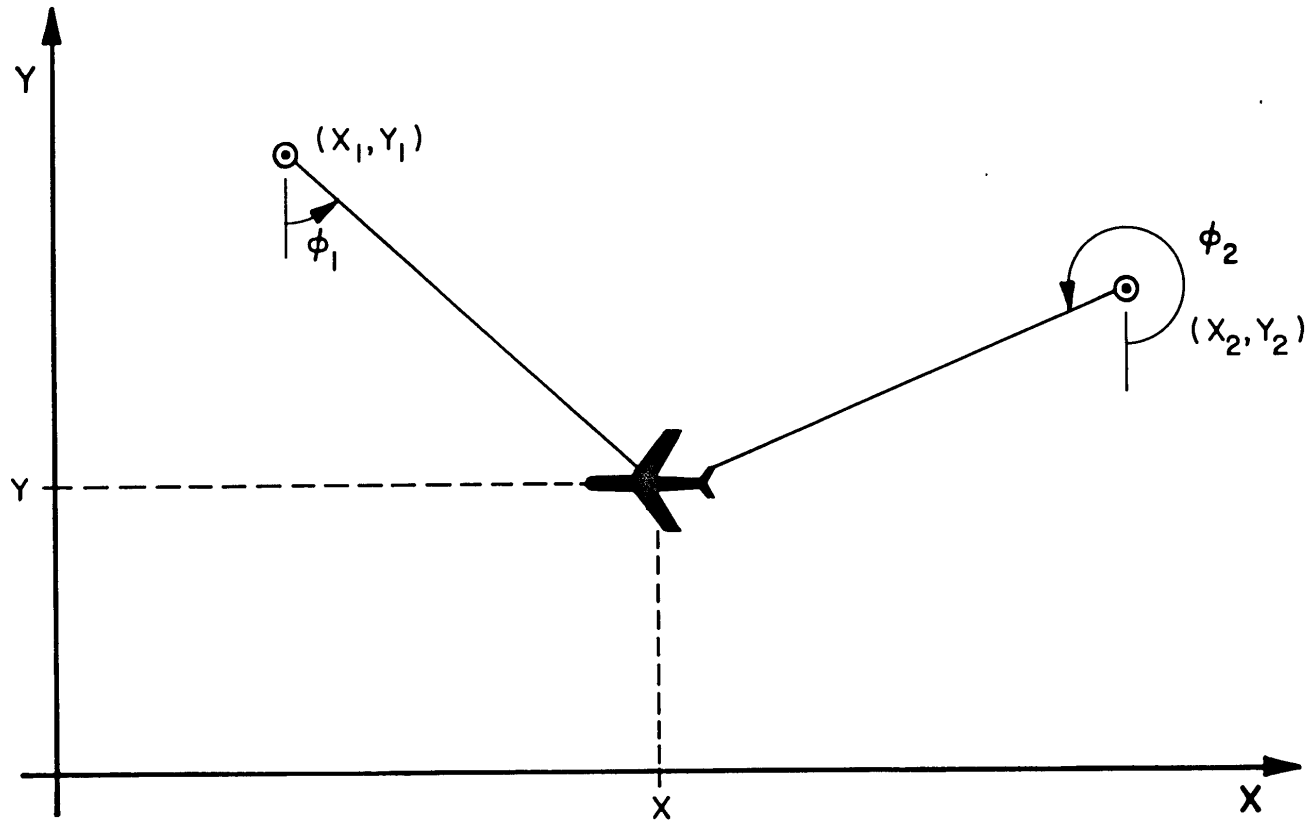


Figure 7.- Navigation in horizontal plane using bearing from two radio stations

Furthermore, a real sensor cannot make an exact measurement. There are two types of measurement errors. The first type is deterministic in nature and can be determined by preflight calibration. After calibration, it is possible to correct or compensate for these error sources. The second type of errors are those which are non-deterministic or random and by definition cannot be compensated. It will be assumed that the deterministic errors will be corrected and, therefore, will not be considered further.

The physical sources of the errors are of interest in developing realistic models. The information is, in general, corrupted by one or more of the following errors: receiver errors, information source errors, and errors associated with the propogation media. To account for these effects, sensor measurement accuracy is best modeled as the sum of a constant error plus an error dependent on the range to the source.

The final set of navigation sensor parameters are the maximum rates at which the sensors can be sampled. This limit can come from several physical sources; e.g., information is inherently in sampled form or if in continuous form, it must be sampled for use in the on-board digital computer. In any case there exists a set of constraints of the form:

$$DT_i \geq \hat{DT}_i \qquad i = 1, \ldots m \tag{3.4}$$

where

DT_i = time between successive samples of the i-th measurement subsystem

$\hat{DT}_i$ = smallest permitted time interval between successive samples of the i-th measurement subsystem

The measurements are processed in an onboard digital computer. The onboard computer is also responsible for performing the control and guidance computations and, therefore, only a certain portion of its total capacity will be assigned to the navigation computation. This assignment will be a percentage of the major cycle time of the computer. The amount of navigation data that can be processed in any given cycle is a function of two factors: (1) the amount of time assigned to navigation and, (2) the complexity of the required computations. The first factor is normally a design constraint, while the second factor is a design variable, i.e., the designer must make a trade-off of performance versus complexity of computation. To model relative computer requirements, a set of weighting factors must be derived which represent relative computer loading (relative to

total capacity). Then, it is possible to impose the constraint that the total weighted sum of the measurements to be processed must be less than or equal to the computer capacity. If N_i is the rate at which the i-th measurement is processed, this constraint takes the form:

$$\sum_{i=1}^{m} K_i N_i \leq CC \tag{3.5}$$

where:

K_i = computer loading weighting factors

CC = computer capacity

m = number of navigation sensors

Depending on the application, CC could be a constant or a function of time or vehicle position. When CC is not constant, this indicates that the amount of computation alloted to the processing of navigation data changes. An example where CC depends upon the flight regime is the V/STOL situation. During hover or transition, the computer loading of the vehicle attitude control system is much higher than during cruise. This combined with the higher priority for the control function would produce a reduced value of CC for this part of a flight.

3.2.3 Mission Objective Parameters

The major objective of a navigation system is the most accurate determination of navigation information at the lowest cost. The accuracy requirement is strongly mission dependent. For some applications, accurate navigation is required continuously throughout the mission. In other applications, accurate navigation is required only at a number of discrete times during the mission (perhaps only at the terminal time). The important point, common to all accuracy requirements, is that they are presented in the form of maximum allowable errors which cannot be exceeded. This type of specification is a constraint on the system design rather than a design parameter at the disposal of the designer. To define system accuracy, consider Figure 6 which shows the two main elements of the navigation system. The measurement subsystems form the measurement vector $\underline{Z}$. This vector is then used in the on-board computer to estimate the state vector. This estimate is denoted by $\hat{\underline{x}}$. The error in the knowledge of the state is given by the error vector $\underline{\varepsilon}(t)$.

$$\varepsilon(t) = \hat{\underline{x}} - \underline{x} \tag{3.6}$$

The system accuracy is specified as a given function of the error in the estimate or the statistics associated with that error.

The second design objective is the minimization of system cost. Two distinct types of costs are associated with the navigation system's sensors and with the computer. The first is referred to as the Cost of Ownership and is modeled as a constant dollar cost. The Cost of Ownership includes such factors as initial purchase cost, maintenance costs, costs for special training of crews and maintenance personnel, required spare parts inventory, and ground equipment. Depending on the application, this cost may be amortized over many missions, as would be the case for a commercial airlines navigation system, or for only one flight for a launch vehicle application.

A second type of cost is one that is incurred during a mission and is a function of the use of the navigation system. An example of this kind of cost is the attitude fuel required to orient a spacecraft so that a navigation measurement can be taken. This cost is directly proportional to the number of measurements. In applications where both the cost of ownership and measurement costs are incurred, the cost function that is minimized when selecting the design has the form

$$J = (IC)_{computer} + \sum_{i=1}^{m} IC_i + \int_o^T \sum_{i=1}^{m} C_i N_i \, dt \tag{3.7}$$

where

IC_i = cost of ownership per flight for the i-th component

N_i = rate at which the i-th sensor is being sampled

C_i = weighting factors with units dollars/measurement

m = number of sensors

This cost function is minimized in a design where the accuracy requirement is a constraint on the design.

Virtually all applications have some form of Cost of Ownership. Not all have costs associated with measurement; e.g., an aircraft navigation system. For applications which have no Measurement Cost, the best system from a cost standpoint is that which meets the system performance requirements and has the lowest Cost of Ownership.

In the design of a Navigation System, the only control that the designer has over the Cost of Ownership is at the system level where he may select from among the sensors and computers. At the component level, Cost of Ownership is given and is not a design parameter at the disposal of the designer. On the other hand, the designer does have some limited control over the Measurement Cost. By how he chooses to use the sensor, the Measurement Cost can be varied to minimize the Measurement or total Cost while achieving the required navigation accuracy.

3.3 MATHEMATICAL FORMULATION

Once the important design parameters are identified, mathematic models for these parameters and a mathematical framework connecting these models can be developed. To generate the models and the framework, assumptions concerning the specific nature of the design factors are required. These assumptions restrict the design procedure to a class of navigation systems. The class of systems for which the design procedure as developed in the following chapters is applicable is defined in the following paragraph.

The navigation system design is characterized by a vehicle trajectory given as $\underline{x}(t)$ which satisfies the nonlinear differential equation:

$$\dot{\underline{X}} = \underline{G}\ (\underline{X},\underline{U},\underline{\phi},\underline{W}) \tag{3.8}$$

This trajectory is close to a nominal trajectory $\underline{X}_{nom}$ which is a solution to

$$\dot{\underline{X}}_{nom} = \underline{G}\ \left(\underline{X}_{nom},\underline{U}_{nom},\underline{\phi}_{nom},\underline{W}_{nom}\right) \tag{3.9}$$

The on-board sensors take measurements which are related by the nonlinear equation:

$$\underline{Z} = \underline{Z}\ (\underline{X},\underline{V}) \tag{3.10}$$

The sampling rates of these sensors are constrained according to:

$$DT_i \geq \hat{DT}_i \tag{3.11}$$

These measurements are processed in the computer which has limitations on its processing capabilities given by:

$$\sum_{i=1}^{m} K_i N_i \leq CC \tag{3.12}$$

The result of the processing is an estimate $\hat{\underline{X}}$ of the state vector

$$\hat{\underline{X}} = \hat{\underline{X}}\ (\underline{X},\underline{Z},t) \tag{3.13}$$

The system cost is the Cost of Ownership. Mission accuracy constraints are imposed only at the terminal time. The related problems which include Measurement costs and/or internal state constraints are discussed as recommendations in Chapter 7.

The first step in developing the mathematical framework is the use of the nominal trajectory to simplify the description of the problem. This simplification is accomplished by linearizing the state and measurement equations about the nominal trajectory. The linearized state equation is:

$$\dot{\underline{x}} = F(t)\underline{x} + G(t)\underline{\omega} \tag{3.14}$$

where:

$$F(t) = \frac{\partial G}{\partial \underline{X}}\bigg|_{nom} + \left(\frac{\partial G}{\partial \underline{U}}\,\frac{\partial U}{\partial \underline{x}}\right)\bigg|_{nom}$$

$$G(t) = \frac{\partial G}{\partial \underline{W}}\bigg|_{nom}$$

$$\underline{W} = \underline{W} - \underline{W}_{nom}$$

$$\phi = \phi_{nom}$$

Similarly a linearized form of the measurement vector is given:

$$\underline{z} = H_1(t)\underline{x} + H_2(t)\underline{v} \tag{3.15}$$

$$\underline{z} = \underline{Z} - \underline{Z}_{nom}$$

$$H_1(t) = \frac{\partial \underline{Z}}{\partial \underline{X}}\bigg|_{nom} \quad ; \quad H_2(t) = \frac{\partial \underline{Z}}{\partial \underline{V}}\bigg|_{nom}$$

There are two areas that require a more detailed development: (1) the accuracy specification, and (2) the techniques used to derive the estimate of the state from the measurements. The accuracy specification is chosen as:

$$J - \text{tr}\,[A\,P(T)] \tag{3.16}$$

where

$P(t)$ = convariance matrix of the errors in the estimate

T = prescribed terminal time

A = weighting matrix

If A is a diagonal matrix, J is the weighted sum of the variances of the estimation errors of the components of the state vector. The estimation procedure is chosen to be a linear estimator which minimizes the mean-squared error in the estimate for a given set of measurements. It is further assumed that the measurement errors, the system disturbances, and the initial uncertainty in the state vector are Guassian - White Noise random process, i.e.:

$$\begin{aligned} E\left(\underline{v}(t)\right) &= 0 \qquad E\left(\underline{v}(t)\underline{v}^T(\tau)\right) = R\delta(t-\tau) \\ E\left(\underline{\omega}(t)\right) &= 0 \qquad E\left(\underline{\omega}(t)\underline{\omega}^T(\tau)\right) = Q\delta(t-\tau) \end{aligned} \tag{3.17}$$

where $\delta(t)$ is the Dirac Delta function. Using these assumptions, it can be shown (ref. 3) that the least mean-square error estimate $\hat{\underline{x}}$ of the state vector for times between measurements is given by:

$$\hat{\underline{x}}^- = \Phi_{i-1}\,\hat{\underline{x}}_{i-1} \tag{3.18}$$

where Φ is the state transition matrix and satisfies the differential equation

$$\dot{\Phi}(t,t_o) = F(t)\;\Phi\;(t,t_o) \tag{3.19}$$

with $$\Phi(t_o,t_o) = I$$

When a measurement is taken, the estimate is updated according to:

$$\underline{\hat{x}}_i^+ = \hat{x}_i^- + P_i^- H_i^T R^{-1} \left[\underline{Z} - H_i \underline{\hat{X}}_i^- \right] \tag{3.20}$$

The covariance of the errors in the estimate propogates between measurements as:

$$P_i^- = \Phi_{i-1} P_{i-1}^+ \Phi_{i-1}^T + G_{i-1} Q_{i-1} G_{i-1}^T \tag{3.21}$$

with $P(t_o) = P_o$

and P(t) is changed after a measurement as:

$$P_i^+ = P_i^- - P_i^- H_i^T (H_i P_i^- H_i^T + R_i)^{-1} H_i P_i^- \tag{3.22}$$

A few words are in order at this point concerning the model assumed for the measurement errors and the system disturbances. Although White Noise does not exist in the physical world, the use of it in the mathematics does not introduce significant errors. The applications where this is true are those that have broad-band noise acting through a dynamic system. If the bandwidth of the noise is larger than the bandwidth of the system, then using White Noise models of the noise is an accurate assumption. For applications where this relation between the system and noise bandwidths does not exist, techniques exist (ref. 4) which give an estimation error propogation of the same form as Eqs. (3.21 and 3.22). These techniques use shaping filters to process the White Noise and then they expand the state vector by the inclusion of the correlated noise variables. This then is a system which has a larger state but is then considered to be driven with white noise.

The elements of the covariance matrix of the estimate errors are functions of the nominal trajectory, measurement errors statistics, measurement sequence, system disturbance statistics, and measurement geometry. For a configured system and a prescribed mission, the only one of these parameters available to the designer is the sequence of navigation measurements. There exists a particular history of navigation measurements that gives the minimum value of the accuracy measure $\underline{A}$ (P(t)). To determine this optimal measurement schedule requires the solution of an optimal control problem. A statement of this problem is, "Find the sequence of measurements, subject to the sampling and processing constraints (Eqs. 3.12, 3.13), such that the value of A)P(t)) is minimized where P(t) propogates according to (Eqs. 3.22 and 3.23)." In the next chapter, an interative optimization procedure is developed which determines the optimal schedules.

Chapter 4

OPTIMAL SCHEDULING OF NAVIGATION MEASUREMENTS

4.1 INTRODUCTION

The optimal scheduling of navigation measurements has been of interest in the last few years (refs. 1, 2, 3, and 4). The procedures appearing in the technical literature have used the general optimization techniques of calculus of variations and dynamic programming to solve for the measurement schedules for navigation in earth orbit, translunar, and interplanetary missions. The present work differs from the above work by the inclusion of constraints on the minimum sampling interval of the sensors and the constraint on the maximum processing rate.

The optimization process is presented in three sections. First the theoretical development of the optimality conditions is presented. These include the first-order necessary conditions and optimal control logic, both given in terms of an approximate continuous formulation. Next, a computer algorithm is developed which mechanizes the required optimality conditions. Finally, an example problem is given which illustrates the basic characteristics of the optimal solution and the optimization procedure.

4.2 THEORETICAL DEVELOPMENT

The theoretical development consists of a reformulation of the discrete measurement problem, that had as control variables the times at which the various measurements were taken, into a continuous measurement process with the rates at which measurements are taken as control variables. An application of the Maximum Principle determines the necessary conditions for optimality. From these conditions the optimal sensor sampling logic is developed for (a) single scalar measurement sensors, (b) sensors which can sample several sources of information, and (c) sensors that simultaneously measure several scalar quantities. The optimal control is shown to have a Bang-Bang form and it requires that the computer be used to its full capacity at all times.

4.2.1 Continuous Measurement Formulation

The discrete form of the estimation error covariance, Eqs. (3.22) and (3.23), is derived for the problem of estimating the state vector which has continuous dynamics, using discrete measurements. The determination of the optimal sequence of discrete measurements subject to the sampling and computer constraints (Eqs. 3.12 and 3.13) is difficult. The difficulty arises partly

due to the form of the constraints. To alleviate this difficulty, the discrete measurement process is reformulated as a continuous measurement process. It can be argued (ref. 5) that if the interval between discrete measurements is small compared to system characteristic times and if the change in system measurement geometry is small, then the sequence of discrete measurements, with mean squared measurement error σ^2, can be approximated by a continuous measurement process with

$$\text{cov } [v] = \sigma^2 \, DT \, \delta(t - \tau) \tag{4.1}$$

For the estimation of a continuous state using continuous measurements, the estimation error covariance matrix P(t) can be shown (ref. 6) to satisfy

$$\dot{P} = FP + PF^T - PH^T NR^{-1} HP + Q \tag{4.2}$$

where

$$N_{ij} = \begin{cases} \dfrac{1}{DT_i} & i = j \\ 0 & i \neq j \end{cases}$$

and

$$R_{ij} = \begin{cases} \sigma_i^2 & i = j \\ 0 & i \neq j \end{cases}$$

The control variables are the elements of N_i each of which is the rate at which its corresponding sensor is sampled. Also, the measurement constraints given by Eqs. (3.12) and (3.13) take the natural form:

$$N_{ii} \leq NM_i \quad i = 1, \cdots, m \tag{4.3}$$

$$\sum_{i=1}^{m} K_i N_{ii} \leq CC \tag{4.4}$$

where NM_i is the inverse of the minimum sampling interval for the i^{-th} sensor. As mentioned in Chapter 3, the value of NM is limited by the physical availability of the measurement. The use of the continuous formulation imposes another restriction on the sample rate. The value of NM_i is also affected by the finite bandwidth of the physical measurement noise. This limit occurs because in the development of the relation between the discrete measurement error and the approximate continuous formulation, it was assumed that the discrete measurements contained statistically independent noise.

4.2.2 Necessary Conditions

Using the continuous form of the measurement process and covariance propagation, the optimal measurement schedules are defined as the control histories N(t) which minimize the cost function:

$$J = tr[AP]_{t=T} \tag{4.5}$$

This minimization must be done subject to the equality differential constraint Eq. (4.2) and the two sets of control inequality constraints Eqs. (4.3) and (4.4). The first step in the determination of the necessary conditions for the optimal N(t) is the formation of the system's Hamiltonian. From Eqs. (4.2) and (4.5) and the introduction of the nxn costate matrix $\Lambda(t)$,

$$\mathscr{H} = tr[\Lambda\{FP + PF^T - PH^T NR^{-1} HP + Q\}] \tag{4.6}$$

Rearranging terms and using the properties of the trace operation, this can be written as:

$$\mathscr{H} = tr[-(R^{-1} HP\Lambda PH^T)N + \Lambda(FP + PF^T + Q)]$$

Finally writing the term involving N in series form

$$\mathscr{H} = \sum_{i=1}^{m} (-R^{-1}HP\Lambda PH^T)_{ii} N_{ii} + tr\Lambda(FP + PF^T + Q) \qquad (4.7)$$

An examination of the Hamiltonian and the inequality constraints shows that all three are linear in the control variables. This indicates that this problem is a linear optimization problem and the necessary conditions for optimality can be determined by applying Pontryagin's Maximum Principle (ref. 7). For the problem defined by Eqs. (4.2), (4.3), (4.4), (4.5), and (4.7), the Maximum Principle states; as follows.

If the costate matrix satisfies:

$$\dot{\Lambda} = -\Lambda F - F^T\Lambda + H^T NR^{-1}HP\Lambda + \Lambda PH^T NR^{-1}H \qquad (4.8)$$

$$\Lambda(T) = A$$

then the optimal N(t) is that value of N(t) which satisfies the control constraints (Eqs. (4.3) and (4.4)) and minimizes the system Hamiltonian for all $0 \leq t \leq T$.

To see what form the control takes, consider first the case without the computer constraint. Upon examination of the Hamiltonian, it can be seen that the controls which minimize Eq. (4.7) are given by:

$$\left(N_{OPT}\right)_{ii} = \begin{cases} 0 \quad , & SW_{ii} > 0 \\ NM_{ii}, & SW_{ii} < 0 \end{cases} \qquad (4.9)$$

where SW_{ii} are known as the switching functions and are given by:

$$SW_{ii} = -(R^{-1}HP\Lambda PH^T)_{ii} \qquad (4.10)$$

The logic defined by Eqs. (4.3) and (4.4) defines the admissible control region which for m measurements is an m dimensional hypercube. The case m = 2, is shown in Figure 8. The control defined by Eq. (4.9) is known as Bang-Bang control because it is

characterized by rapid shifts from one boundry of its admissible region to another. There is one condition for which the application of the Maximum Principle does not determine the optimal control. This kind of control is known as Singular control. A discussion of this case will follow the introduction of the computer constraint.

The computer constraint of Eq. (4.4) imposes a restriction on the admissible control region. Geometrically, this constraint is an (m - 1)-th degree hyperplane which intersects the hypercube. For m = 2, this corresponds to a line as shown in Figure 9. Again the optimal control is on the boundry and, in particular, at the vertices of the control region. The particular vertex depends on two factors which determine the ability of a measurement to reduce the Hamiltonian. The more negative the switching function the larger the reduction; the larger the amount of computation, indicated by K_i, required to process a particular measurement, the smaller the reduction. The quantity of interest in determining the relative efficiency of the measurements is the weighted switching function, SW_{ii}/K_i.

Return now to the question of Singular Controls. There exist necessary conditions (Refs. 10, 11) that determine if Singular Controls are optimal. Application of these to the present problem indicates that the existence of singular controls can not be ignored. Further analysis however was performed which settled this question. In Appendix A, two theorems relating to singular controls are proved. The first theorem states that for $\Lambda(T)$ positive semidefinite, the switching functions given in Eq. (4.10) are always less than or equal to zero. This condition on $\Lambda(T)$ is true if, for example, the cost J were:

$$J = P_{11}(T) + P_{22}(T)$$

The second part of Appendix A proves that under no circumstances will a measurement increase the value of $J = tr[AP(T)]$. This, and the fact that no cost is directly associated with the number of measurements indicates that a singular control, e.g., a control value not on the boundary of the admissible region, is not optimal.

It is interesting to note that, for this logic, the optimal control history in the case of no computer constraint is obvious — use all sensors at their maximum rate. It is only the inclusion of the processing restriction that makes the optimization non-trivial. The optimal strategy then calls for using all the computer capacity all the time provided that the processing requirements of all sensors sampled at their maximum rates would

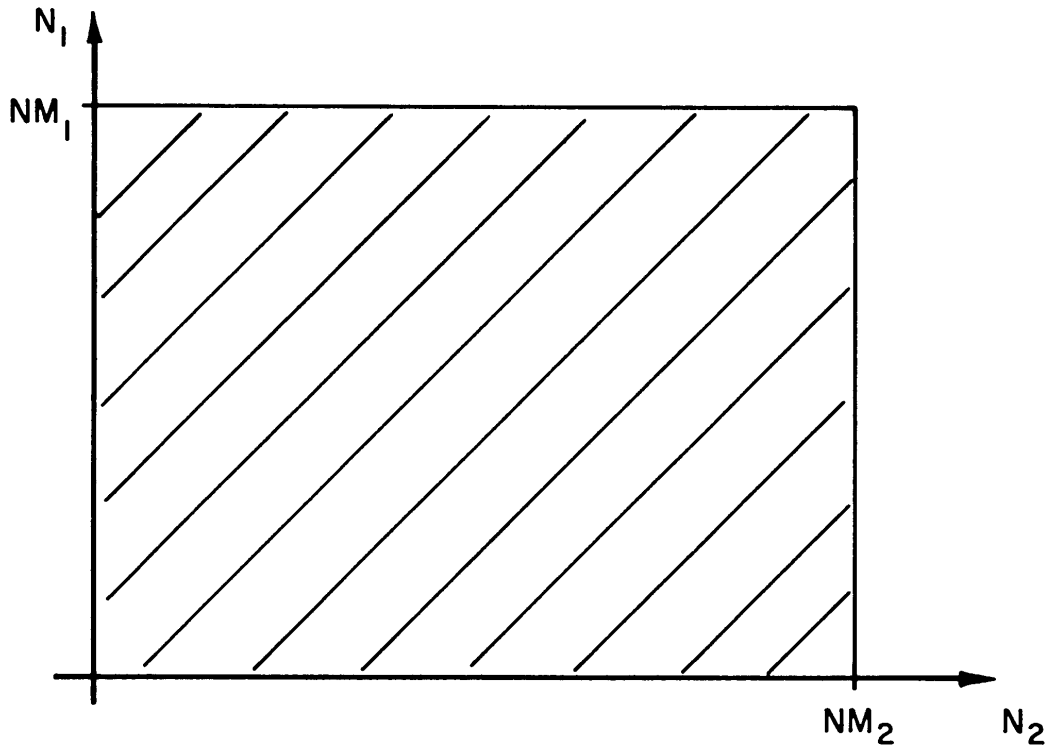


Figure 8.- Admissible control region with magnitude limiting

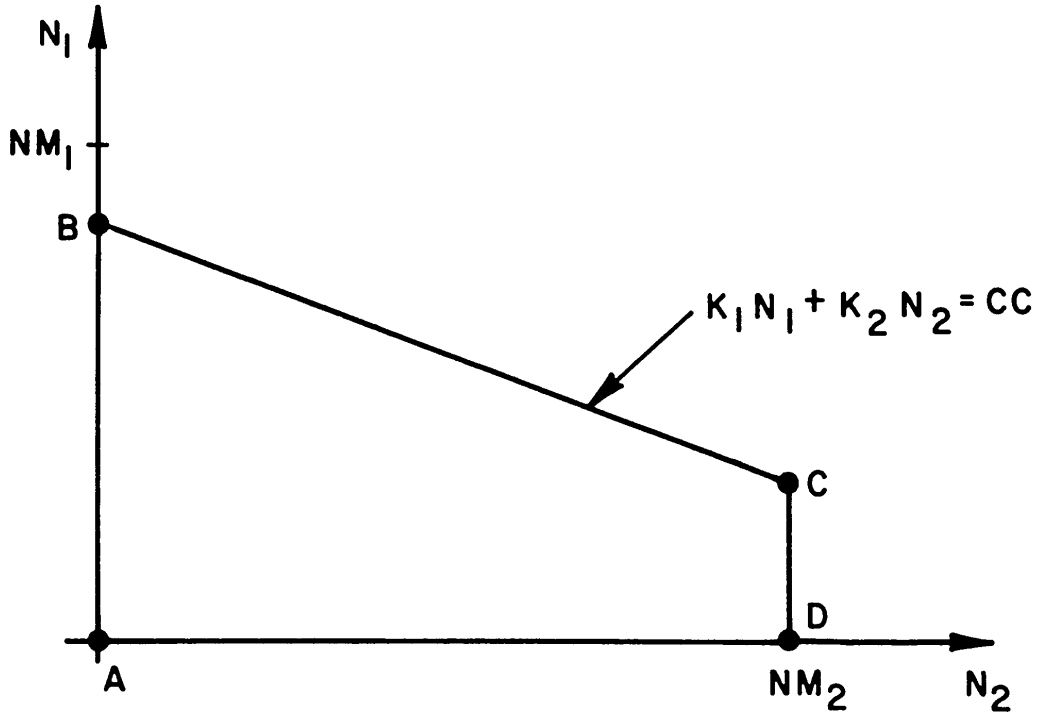


Figure 9.- Admissible control region with magnitude and computer limiting

require more than the computation capacity. The optimal control strategy is known in Figure 10. The weighted switching functions are first ordered from most negative to least negative. Starting with the most negative, the corresponding sensor is sampled at its maximum value provided this does not violate the computer constraint. If there is still computation time left, the next measurement in the ordering is used until either all sensors are being sampled at their maximum rates or the computer is full. If the latter condition is true, all the rest of the sensors are not sampled. It can be seen that with this logic there will be at most one sensor sampled at a rate not on the boundry, i.e., different from its maximum rate or zero. As an example of the connection between conditions on the weighted switching function and optimal controls, consider Figure 9. The vertices of the allowable control region correspond to the following combination of the weighted switching functions.

Point A

$$\frac{SW_1}{K_1} > 0 \quad \text{(Does not occur)}$$

$$\frac{SW_2}{K_2} > 0$$

Point B

$$\frac{SW_2}{K_2} > \frac{SW_1}{K_1}$$

$$\frac{SW_1}{K_1} \leq 0 \quad \text{and} \quad K_1NM_1 > CC$$

Point C

$$0 > \frac{SW_1}{K_1} > \frac{SW_2}{K_2}$$

$$K_2NM_2 < CC$$

$$K_1NM_1 + K_2NM_2 > CC$$

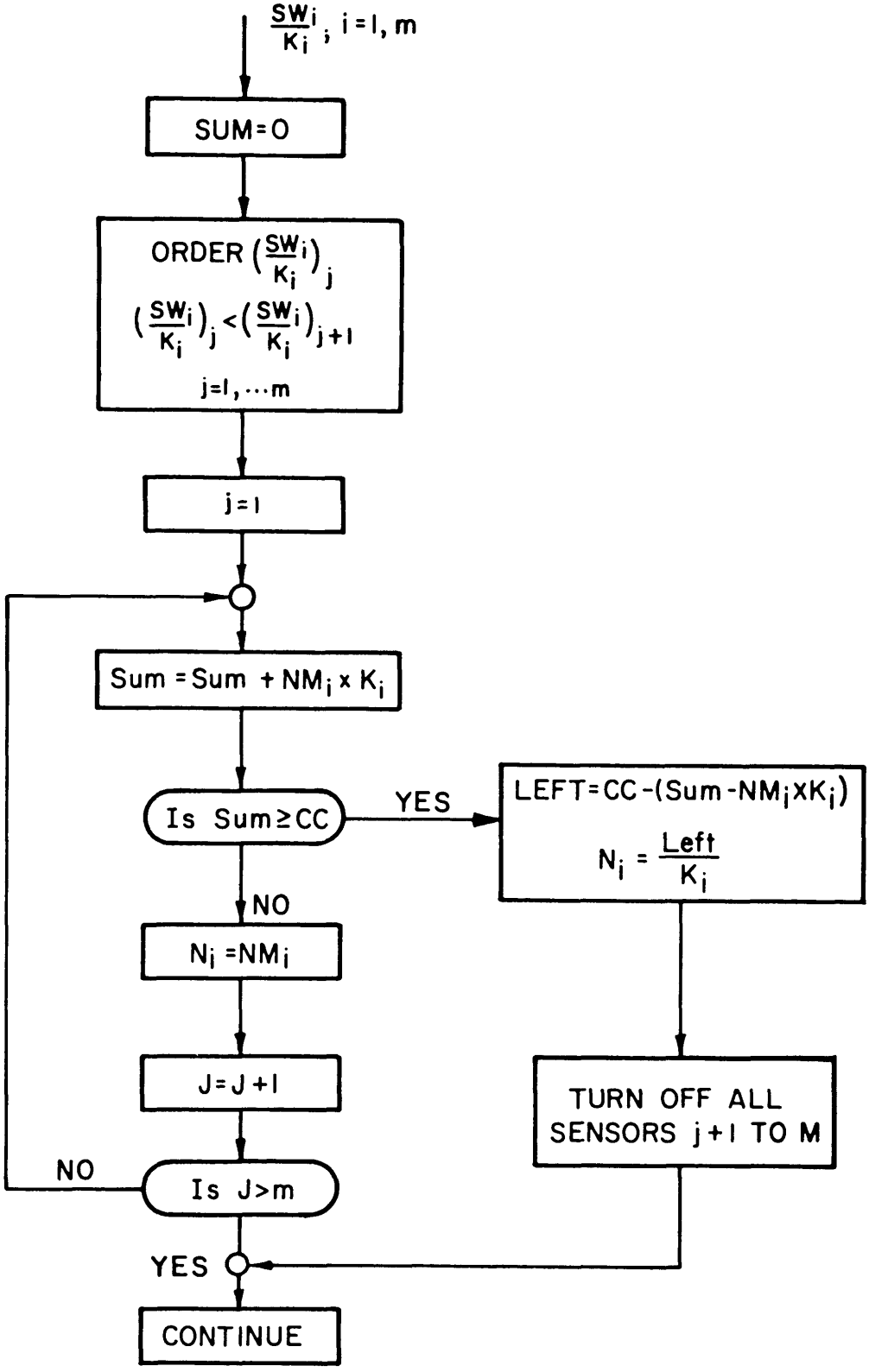


Figure 10.- Computer constrained optimal control strategy

Point D

$$\frac{SW_1}{K_1} > 0$$

$$\frac{SW_2}{K_2} < 0 \qquad \text{(Does not occur)}$$

$$K_2 NM_2 < CC$$

An interesting fact can be seen if the expression for the switching functions is examined:

$$SW_{ii} = -(R^{-1}HP\Lambda PH^T)_{ii}$$

In the switching function matrix, SW, the particular combination $P\Lambda P$ of the state and costate matrix is of interest since if the matrix Z is defined by:

$$Z = P\Lambda P \qquad (4.11)$$

Then, using Eqs. (4.2) and (4.8) it is possible to derive the differential equation:

$$\dot{Z} = (F + QP^{-1})Z + Z(F^T + P^{-1}Q) \qquad (4.12)$$

This is a simpler equation than the differential equation in $\Lambda(t)$, Eq. (4.8). Since the only reason $\Lambda(t)$ is required in the problem is to determine SW_{ii}, it is possible to use Eq. (4.12) instead of Eq. (4.8) as a costate equation. The physical significance and the advantage of using $Z(t)$ as the costate are discussed in Appendix B in connection with the special problem of $Q = 0$, e.g., navigation in a benign environment.

The necessary conditions for optimal $N(t)$ are the control logic shown in Figure 10, and the costate equations which can be either Eq. (4.8) when $\Lambda(t)$ is used or Eq. (4.12) when $Z(t)$ is calculated directly.

4.2.3 Formulation of Special Measurement Processes

Thus far, the formulation of the measurement scheduling problem has been in terms of m independent sensors. Each sensor has associated with it a scalar measurement with measurement error R_{ii}. This measurement is related to the state variable through the 1 x n geometry matrix H_i. In the modelling of the navigation sensors of Section 3.2.2, two types of sensors which do not directly fit into the above description were identified. These two cases are the multi-source sensors and the multi-measurement sensors. In both cases a slight modification to the optimal switching criteria must be developed. This development follows.

Multi-Source Sensors.- There exists a group of sensors which are capable of deriving information from several external sources. An example of this type of sensor is a Distance Measuring Equipment (DME) (used by aircraft). The DME measures the range from the sensor to known ground stations. Referring to Figure 11, it can be seen that the geometry and measurement accuracy which are modeled as functions of range depends on the source being sampled. Another characteristic of this type of Multi-Source Sensor is that only one source can be sampled at any time. This limitation is due to the fact that each ground station operates at a different frequency as a means of identification. A similar limitation is true for the class of startrackers that can track only one star at a time, e.g., a Canopus tracker. With this class of sensor, the switching matrix must be partitioned and an additional logic step included. First, associated with each source is its geometry and measurement error covariance. The switching matrix will be M x M, where M is the total number of measureables, i.e., the number of sources of information. Those diagonal elements corresponding to a particular sensor are collected and the source whose information is most efficient is identified. This weighted switching function will then be the one used for that sensor in the logic given in Figure 10.

Multi-Measurement Sensors.- Another class of sensors which requires special consideration is that in which the sensors simultaneously measure several independent scalar quantities. An example of such a sensor is a doppler radar used on aircraft. As shown in Figure 12, there are four radar beams which are sampled simultaneously. It does not take significantly more computation to process the information from four beams than from one beam and, therefore, it does not make sense to disregard the information from any of the beams. Each beam has a different geometry matrix $H_i(t)$ and, therefore, each beam will have a switching function. The total efficiency of the doppler radar is the sum of the corresponding switching functions. The switching function used in the optimal control logic Figure 10 is:

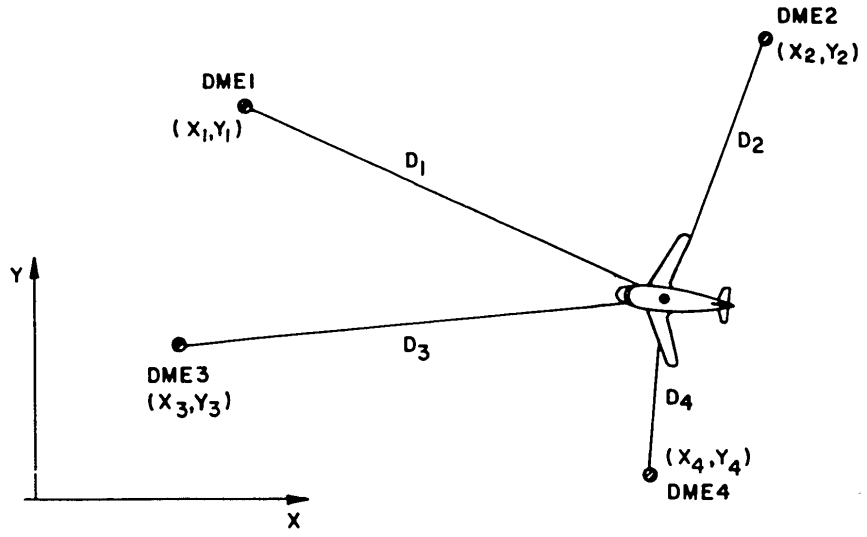


Figure 11.- DME source geometry

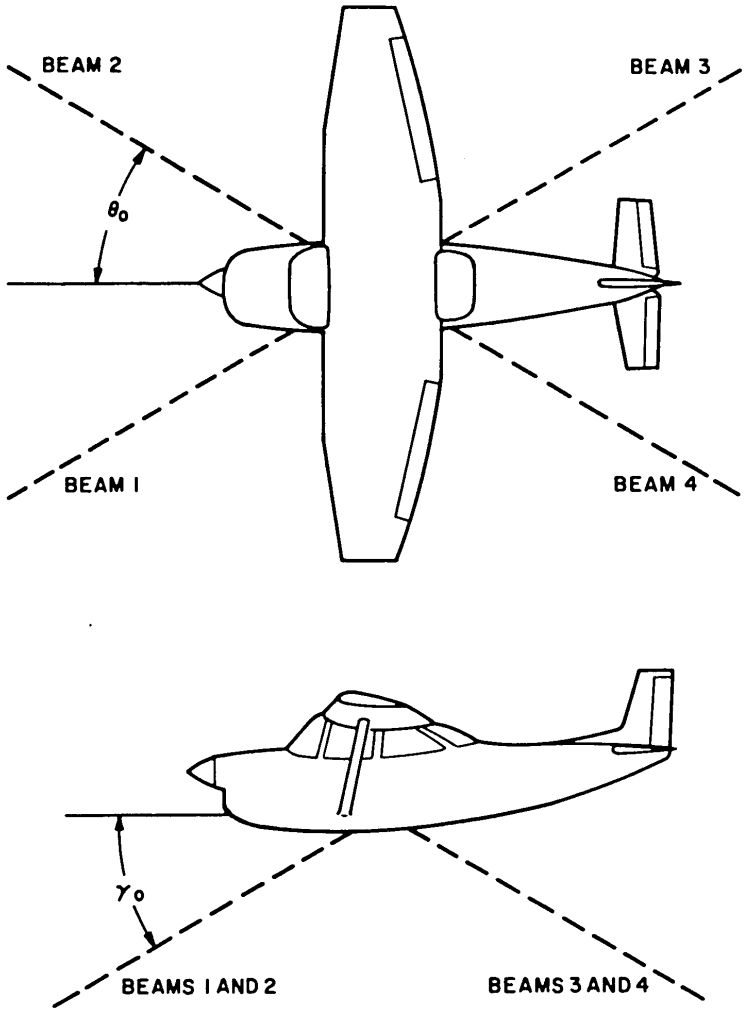


Figure 12.- Four-beam Doppler radar

$$\left(\frac{SW}{K}\right)_{Doppler} = \frac{SW_{Beam\ 1} + \cdots + SW_{Beam\ 4}}{K_{Doppler}} \qquad (4.13)$$

4.3 COMPUTATION ALGORITHM

The development of an algorithm to solve the optimization of the measurement schedule involes the determination of which necessary conditions are to be satisfied on any iteration and which conditions are to be iterated. Having made this selection, it is necessary to determine the scheme that will be used to mechanize these equations on a digital computer. This involves the selection of numerical integration schemes, time step and iteration controls. A brief description of the computer program and the digital machine on which it was used is given in Appendix C.

4.3.1 Algorithm Selection

An optimization procedure based only on first-order information was selected for this problem. This procedure was found to converge in a reasonable number of iterations and avoided the complexities that would have resulted from the large number of Bang-Bang controls in a higher order scheme. The particular optimization technique employed was the procedure known as the "Approximation to the Solution" (ref. 7). The procedure is not a simple gradient method; in fact, gradient information is never calculated. Rather this procedure, shown in Figure 13, performs an iteration on the control history by integrating the state equation:

$$\dot{P} = FP + PF^T - PH^T NR^{-1} HP + Q \qquad (4.14)$$

from $t = 0$ to $t = T$, using the known initial condition P_o, terminal time T and an assumed control history $\bar{N}(t)$. The values of $P(t)$ are stored during the forward integration and used to integrate the costate equations:

$$\dot{Z} = (F + P^{-1}Q)Z + Z(F^T + QP^{-1}) \qquad (4.15)$$

backward from $t = T$ to $t = 0$, starting with $Z(t) = P(t)\Lambda(t)P(t)$. At each point in the backward integration, the optimal control logic given in Figure 10 is applied to determine the control $N^*(t)$.

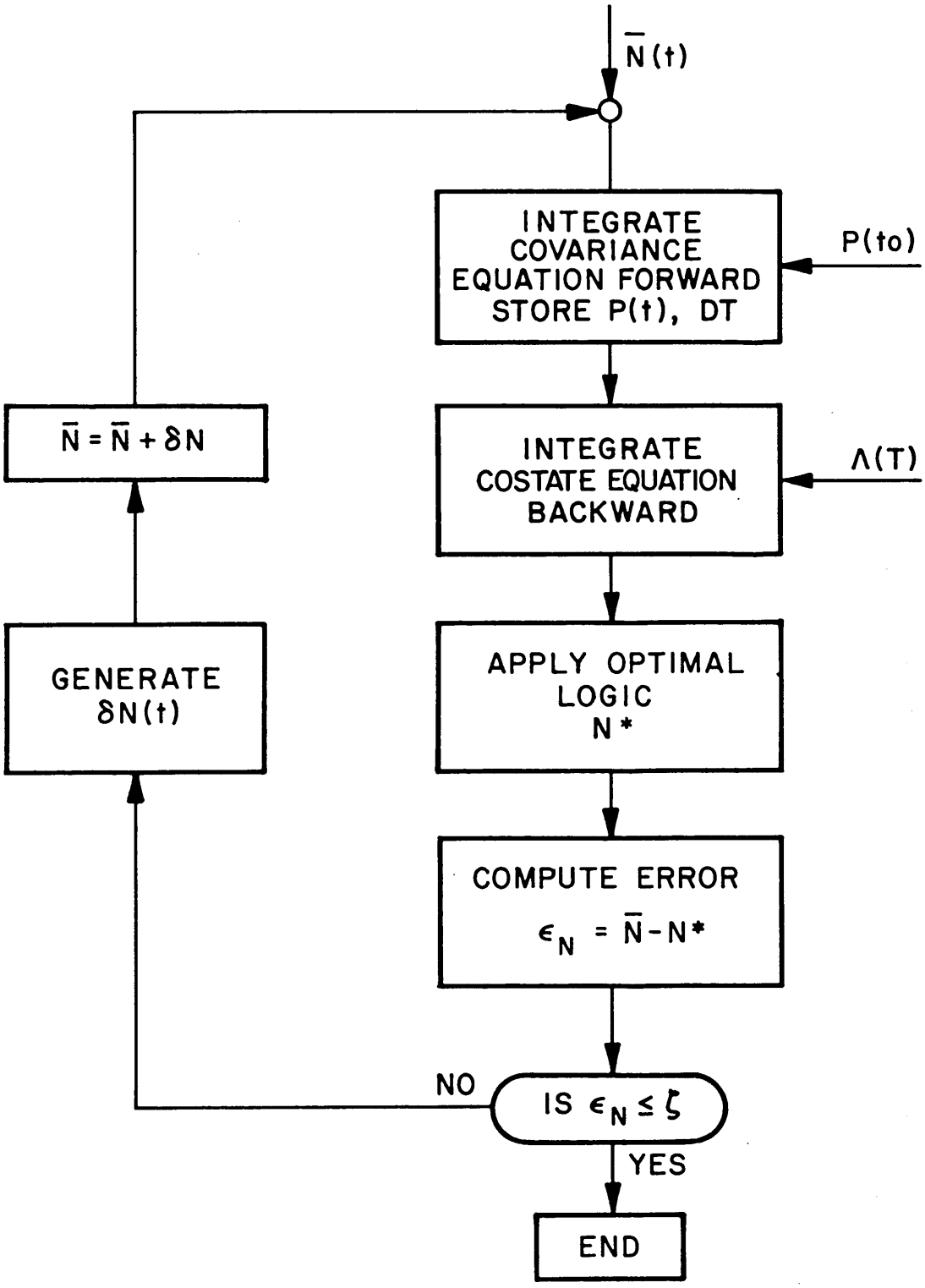


Figure 13.- "Approximation to the solution" optimization procedure

Since $N^*(t)$ is based upon a $P(t)$ derived from $\bar{N}(t)$, the two control histories will not agree. The error is then used to update $\bar{N}(t)$ for the next iteration.

The advantage of this procedure is that both the state and the costate equations are integrated in their stable direction from known boundary conditions. This eliminates the problems associated with the numerical integration of an unstable equation. The main disadvantage is the requirement that $P(t)$ be stored at each time step in the forward integration. The storage required for an n dimensional state with N_{DT} integration steps is $1/2\ n\ (n + 1)\ N_{DT}$ which can be substantial for large dimensioned state equations.

4.3.2 Computer Mechanization

The optimization procedure shown in Figure 13 has three parts; the integration of the state and costate equations, the application of the optimal switching logic, and the generation of the increment in the control variables. The mechanization of the optimal switching logic follows from straight forward programming of Figure 10, and will not be discussed here.

Integration Scheme.- To integrate the state equation forward in time, a fourth-order Runge-Kutta integration scheme was selected. For the backward integration of the costate equation, a second-order Runge-Kutta scheme was used. These schemes (refer to Table I) were selected because of their simplicity and accuracy.* The use of a Second-Order Runge-Kutta Scheme for the backward integration is compatible with the forward integration scheme in that the required values of $P(t)$ at the beginning and end of each time step are available. Unlike some other schemes that numerically integrate differential equations, as for example in the predictor corrector class of integration schemes (ref. 8), Runge-Kutta techniques do not have a built-in variable time step control. Such control is required because the covariance equations can have several time intervals where large derivations occur. These intervals depend on the control history and will shift when changes in control are made. A time step control was developed which controls the error between a predicted value of the $P(t)$ and the value generated by the fourth-order Runge-Kutta integration by adjusting the time step. This procedure starts with the value of the derivative $\dot{P}_{i-1}$ at time t_{i-1}, and the time step DT_i as shown in Figure 14. Using the value of $P(t_i)$ and

*The error in the fourth order is proportional to $(DT)^5$ and the second order to $(DT)^3$ (ref. 8).

TABLE I.- SECOND AND FOURTH ORDER RUNGE-KUTTA INTEGRATION ALGORITHMS

For the differential equation $\dot{y} = g\ (y, t)$, the second- and fourth-order Runge-Kutta Numerical Integration Algorithms give $y(t + \Delta T)$ as follows:

FOURTH-ORDER RUNGE-KUTTA

$$y(t + \Delta t) = y(t) + 1/6\ K_1 + 1/3\ K_2 + 1/3\ K_3 + 1/6\ K_4$$

where

$$K_1 = \Delta t\ g(y, t)$$

$$K_2 = \Delta t\ g(y + 1/2\ K_1, t + 1/2\ \Delta t)$$

$$K_3 = \Delta t\ g(y + 1/2\ K_2, t + 1/2\ \Delta t)$$

$$K_4 = \Delta t\ g(y + K_3, t + \Delta t)$$

SECOND-ORDER RUNGE-KUTTA

$$y(t + \Delta t) = y(t) + 1/2\ (K_1 + K_2)$$

where

$$K_1 = \Delta t\ g(y, t)$$

$$K_2 = \Delta t\ g(y + K_1, t + \Delta t)$$

Eq. (4.14), the derivative $\dot{P}(t_i)$ is calculated. For a guess at DT_{i+1}, say $\overline{DT}$, a linearly predicted value of $\dot{P}(t_{i+1})$, $\bar{\dot{P}}(t_{i+1})$ is calculated. Using $\bar{P}(t_i)$, $\bar{\dot{P}}(t_i)$, and $P(t_{i+1})$, calculate:

$$\bar{P}(t_{i+1}) = P(t_i) + (\dot{P}_i + \bar{\dot{P}}_{i+1}) \frac{DT_{i+1}}{2} \tag{4.16}$$

Using $\overline{DT}$ and the corresponding values of P_i and t_i the fourth-order algorithm computes $P(t_{i+1})$. If the values of $P(t_{i+1})$ and $\bar{P}(t_{i+1})$ agree to within a prescribed accuracy ε_1 the step is accepted. If the error is too large, the time step $\overline{DT}$ is halved and the process repeated. This procedure is the first loop shown in Figure 15. It can be seen that if $\overline{DT}$ is much too large, several cycles are required and a large amount of computer time is required. Also, after a region in which very small time steps are required is passed, it would be inefficient to retain this small value of DT. The second loop in Figure 15 indicates the logic used to increase the time step. Again, the error in the prediction is used as the guide to the time step. Two limits are introduced, ε_2 and $(DT)_{max}$. If the error is less than ε_1 but greater than ε_2 the latest acceptable time step is again tried. If the error is less than ε_2, the time step is doubled for the next pass. Finally, since the time step history cannot be generated solely on the behavior of the forward integration (these same time steps are used in the backward integration) a limit is put on the maximum value of DT. A satisfactory set of limits ε_1, ε_2, and DT_{max} depend on the application and may require some experimentation.

Control Iteration.- To perform the forward integration of the covariance equation, it is necessary to assume a control history $\bar{N}(t)$. Once having $P(t)$ it is possible to perform the backward integration of $Z(t)$ and, by applying the logic given in Figure 11, to calculate the control history $N^*(t)$. The minimum cost is the cost corresponding to the situation where $\bar{N}(t) = N^*(t)$.

To arrive at this condition a procedure must be developed which uses the error quantity $\bar{N} - N^*$ to develop an increment in control $\delta N(t)$. Then, letting $\bar{N}^{(i)} = \bar{N}^{(i-1)} + \delta N^{(i)}$, the procedure is repeated until the error is reduced to an acceptable level.

Because of the bang-bang nature of the control functions, care must be taken in developing a procedure for determining $\delta N(t)$. This is required so that the N^* is well behaved. The procedure developed in this work is a modification of Jacobson's first order Differential Dynamic Programming technique (ref. 9).

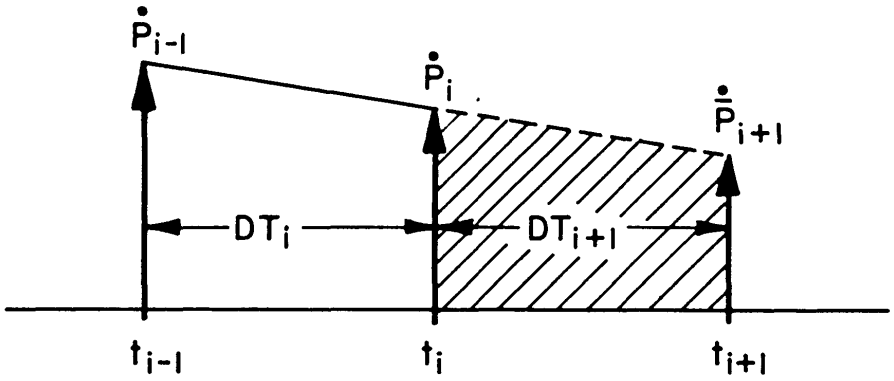


Figure 14.- Predicted increment in P(t)

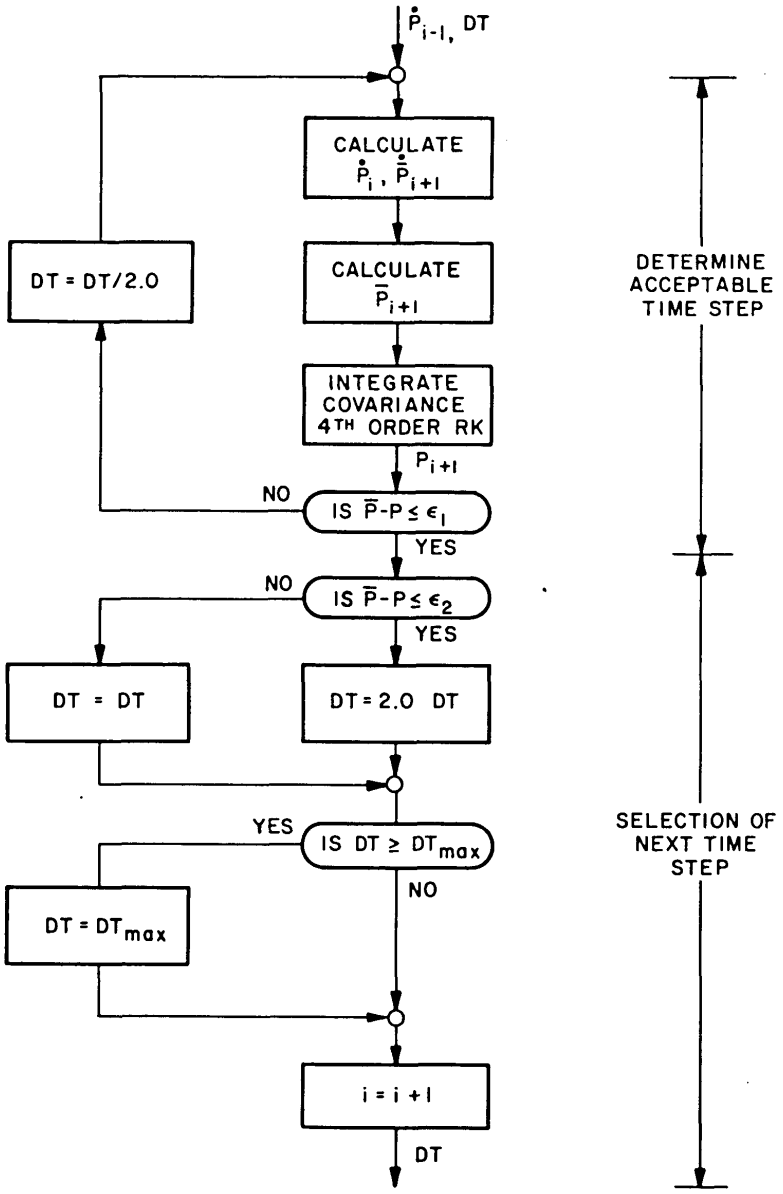


Figure 15.- Time step control routine

It is characterized by the fact that only a portion of the control history is interpolated on each pass. Although apparently this type of iteration requires more passes through the equations than a scheme which interpolates between the full $\bar{N}$ and N^* histories, this is not true in general. The reason is that interpolation can cause large δP and $\delta \Lambda$ and thus produce N^* which are less representative of the true optimal.

To illustrate the procedure, consider the set of forward and backward control histories given in Figure 16. These controls correspond to a contrived situation in that for the system with one sensor there are three measurement rates 60, 30 and 0 M/H. This situation could never exist, since by the logic given previously, a single sensor can only have one level whose value is either on the computer constraint or the sampling constraint boundary. It is convenient, however, to use only a single control variable to develop the control iteration scheme. Also for convenience the control histories are converted into tabular form. This form includes a number and time for each switch in a control; i.e., each time a control variable changes magnitude. Also associated with each switch is the value of all controls just prior to the switch. The tabular representation of the control histories shown in Figure 16 is listed in Table II, starting with switch 1, the values of $\bar{N}$ and N^* are compared. If they are equal (as in the case) switch 2 is considered. The case where $\bar{N}$ and N^* are not equal will be considered shortly. At switch 2, the controls $\bar{N}$ and N^* just to the left of the switches are again equal and, therefore, the Number 2 switches differ only in the time at which the switches occur. As an increment in the next assumed control, the second switch point is updated using the algorithm

$$t_2^{(1)} = t_2^{(0)} + \varepsilon_4 \left(t_2^{*(0)} - t_2^{(0)} \right) \tag{4.17}$$

where $0 \leq \varepsilon_4 \leq 1$. The value of ε_4 depends on the particular application and requires some experimentation. Too large a value produces oscillations which can diverge and too small a value converges too slowly. A value of 0.5 was found to work well for the example problem presented in Section 4.4 while values of 0.1 - 0.3 were used in the applications given in Chapter 6. Using Eq. (4.17), the control history assumed for the next pass is shown in Table III. Provided ε_4 is properly chosen, the results of the first iteration will not produce large changes in the controls and the error in the Number 2 switch $t_2^{*(1)} - t_2^{(1)}$ will be smaller than after the initial pass. This procedure of iteration on only switch 2 is continued until the error in this switch is below a specified level ε_3. The

control histories which exist at this point are given in Figure 17 where it is assumed that m iterations were required. Since the t_2's are sufficiently close, the Number 3 switches will be considered. It can be seen that, in this case, the control levels to the left of the t_3's are not compatible (i.e., are not equal). This requires the addition of a new switch time to the next assumed control. This new switch is added at a time between $t_3^{(m)}$ and $t_3^{*(m)}$ $\bar{N}^{(m+1)}$ then has the values presented in Table IV. It can be seen that t_2 is still being iterated. This allows the correction of changes in t_2 that will occur when t_3 is changed. This procedure is continued, switch points iterated and switches added or subtracted when necessary until the total histories agree as to number of switches and the controls are compatible at each switch. It only remains to reduce the errors in the switch times. Since the controls at each switch time are within the set tolerance ε_3, the control N^* should be very close to the true optimal. To make use of this fact, the step size should be increased so that the new $\bar{N}$ is close to the last N^*. Also, since iterations are being made on the total control history, it is possible to use logic based upon the system cost function to select the step to be taken. These are incorporated by taking a step corresponding to $\varepsilon_4 = 0.9$ and then checking the cost ($J = tr[AP(t)]$) resulting from the forward integration of the covariance equations. If the cost is less than or equal to its value on the last iteration, the step is accepted and a new N^* is calculated. If the cost increases, the step is cut in half and the forward integration repeated. The whole process is said to have converged when the error between t_i and t_i^* at each switch point is less than a prescribed level ε_5, where in general $\varepsilon_5 < \varepsilon_4$. A flow chart of the control iteration process is given in Figure 18. This procedure was used to develop the optimal measurement schedules for the navigation system discussed in Chapter 6. Values of the control limits for T = 1 hr were $\varepsilon_4 = 0.005$ hr and $\varepsilon_5 = 0.001$ hr.

4.4 NUMERICAL EXAMPLE: OPTIMAL SCHEDULING OF DME MEASUREMENTS

The problem of optimally scheduling DME measurements is considered. Using this example, the nature of the optimal measurement schedules, the switching functions, and the time history of the RMS estimation errors are examined. Also, typical values for the optimization procedure parameters (ε_1, ε_2, DT_{max}, ε_3, ε_4, and ε_5) are presented. Finally, the factors affecting the efficiency of the optimization procedure are presented and discussed.

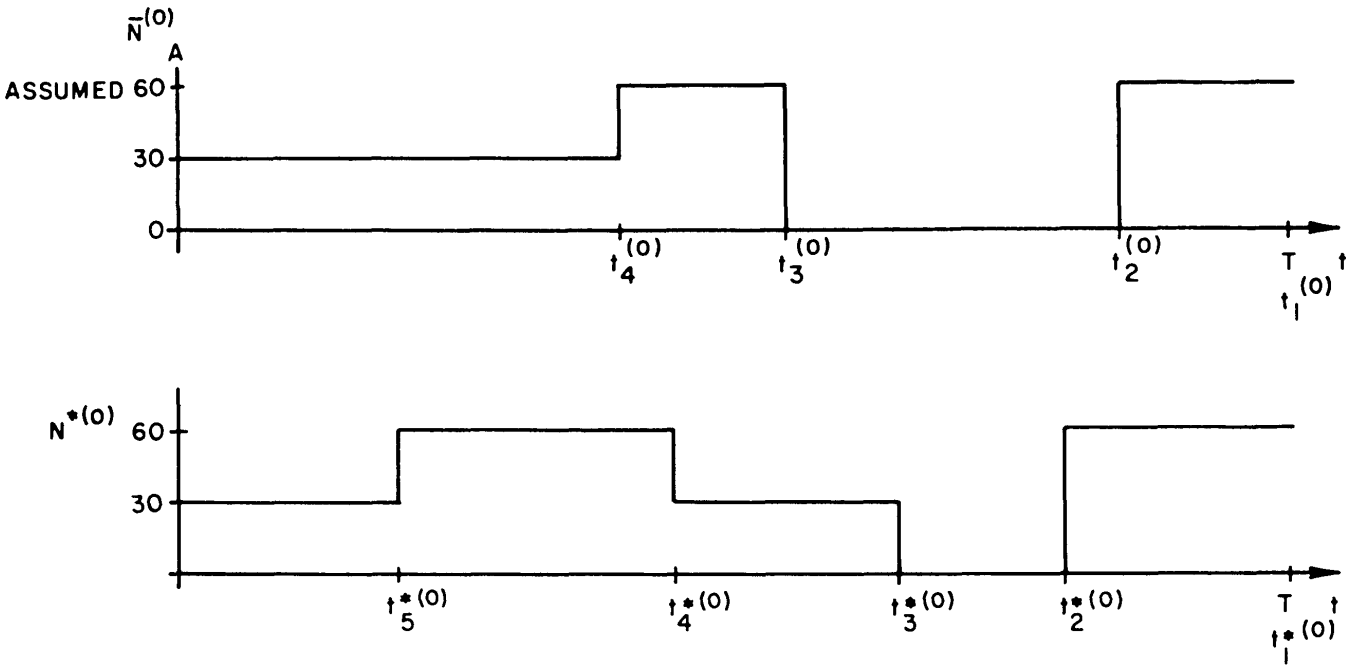


Figure 16.- Initial control histories

TABLE III.- ITERATION 1 ASSUMED CONTROL $\bar{N}^{(1)}$

SWITCH NUMBER	SWITCH TIME	$\bar{N}^{(1)}$
1	$t_1^{(1)} = T$	60
2	$t_2^{(1)} = t_2^{(0)} + \varepsilon_4 \left(t_2^{*(0)} - t_2^{(0)} \right)$	0
3	$t_3^{(1)} = t_3^{(0)}$	60
4	$t_4^{(1)} = t_4^{(0)}$	30

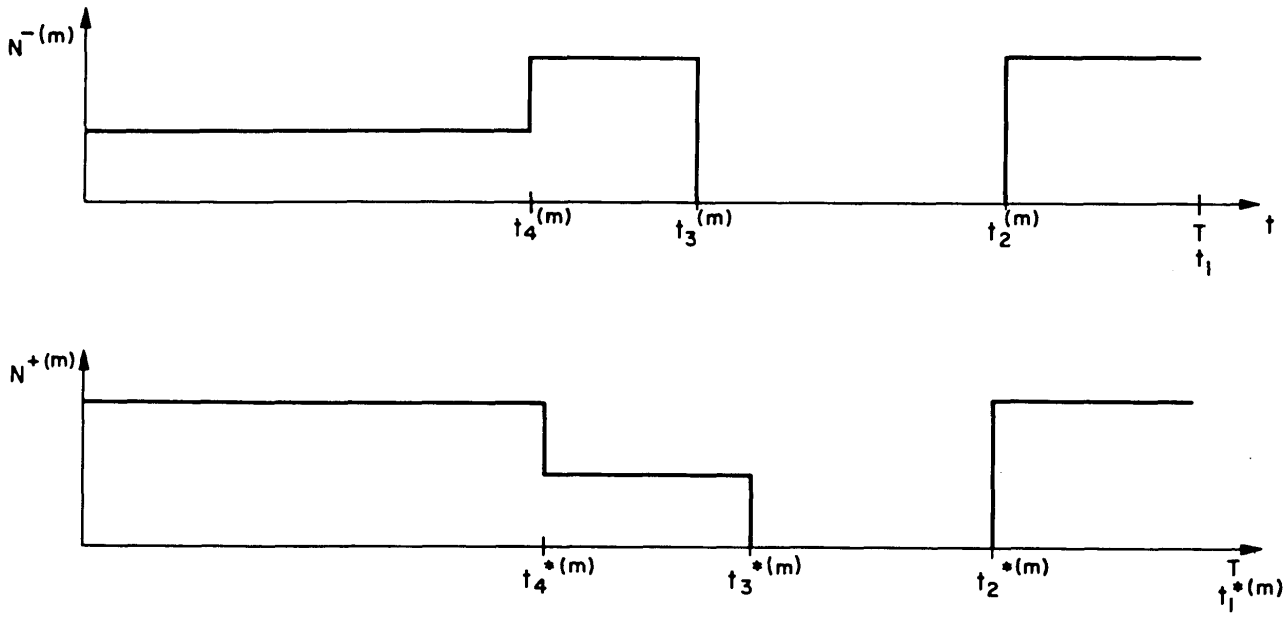


Figure 17.- m^{th} iteration control histories

TABLE IV.- $(m+1)^{th}$ ASSUMED CONTROL HISTORY

SWITCH NUMBER	SWITCH TIME	$\overline{N}^{(m+1)}$
1	T	60
2	$t_2^{(m+1)} = t_2^{(m)} + \varepsilon_4 (t_2^{*(m)} - t_2^{(m)})$	0
3	$t_3^{(m+1)} = t_3^{(m)} + \varepsilon_4 (t_3^{*(m)} - t_3^{(m)})$	30
4	$t_4^{(m+1)} = t_3^{(m)}$	60
5	$t_5^{(m+1)} = t_5^{(m)}$	30

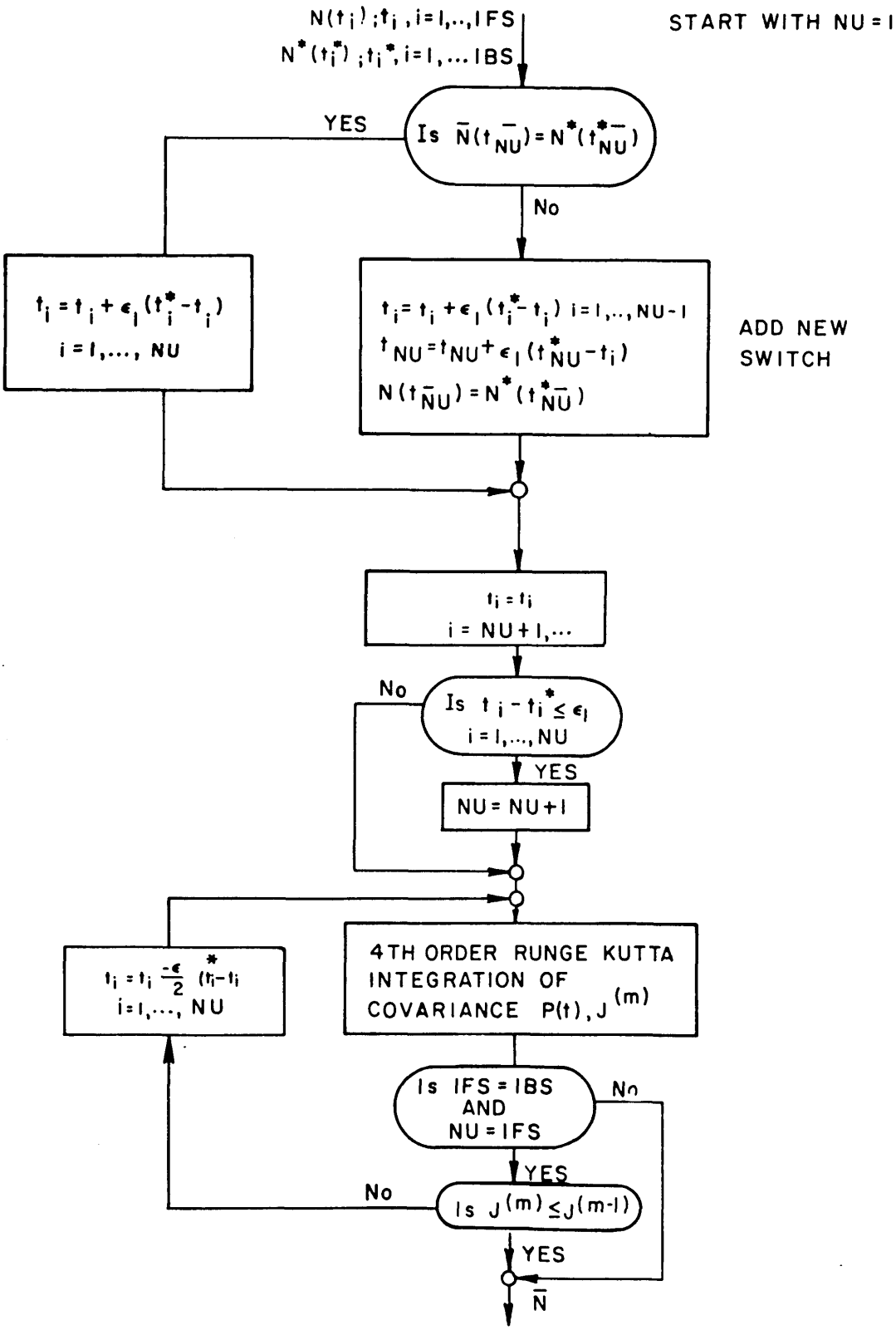


Figure 18.- Control iteration scheme

4.4.1 Problem Statement

Consider a vehicle moving from x = 0 to x = 360 nm along the nominal trajectory

$$\left.\begin{aligned} \dot{X}_{nom} &= 360 \text{ nm/hr} \\ \dot{Y}_{nom} &= 0 \\ X_{nom} &= 360\ t \text{ nm} \\ Y_{nom} &= 0 \end{aligned}\right\} \qquad (4.18)$$

A DME receiver is carried on-board the vehicle and receives range information from two ground transmitters. The location of the transmitter relative to the nominal trajectory is shown in Figure 19. The measurement schedule that minimizes mean-squared position uncertainty at the terminal time is to be determined.

Using the formulation presented earlier in this chapter, the covariance of the errors in the estimate is given by:

$$\dot{P} = FP + PF^T - PH^T NR^{-1} HP + Q$$

$$\text{with } P(T_o) = \begin{bmatrix} 1\ \text{nm}^2 & 0 & 0 & 0 \\ 0 & 1\ \text{nm}^2 & 0 & 0 \\ 0 & 0 & 2\ \frac{\text{nm}^2}{\text{Hr}^2} & 0 \\ 0 & 0 & 0 & 2\ \frac{\text{nm}^2}{\text{Hr}^2} \end{bmatrix}$$

The linearized system dynamics F is:

$$F = \begin{bmatrix} 0 & 0 & 1 & 0 \\ 0 & 0 & 0 & 1 \\ 0 & 0 & 0 & 0 \\ 0 & 0 & 0 & 0 \end{bmatrix}$$

For the DME transmitters located at (90 nm, 20 nm) and (270 nm, -20 nm), the geometric sensitivity H is:

$$H = \begin{bmatrix} \frac{90-x}{D_1} & \frac{20-y}{D_1} & 0 & 0 \\ \frac{270-x}{D_2} & \frac{-20-y}{D_2} & 0 & 0 \end{bmatrix}_{NOM}$$

where D_1 and D_2 are the nominal ranges between the vehicle and the DME 1 and DME 2 transmitters.

The measurement errors are modeled (ref. 13) as:

$$R = \begin{bmatrix} (0.1 + 0.01\ D_1)^2\ nm^2 & 0 \\ 0 & (0.1 + 0.01\ D_2)^2\ nm^2 \end{bmatrix}$$

The environmental disturbances, as modeled in Appendix D:

$$Q = \begin{bmatrix} 0 & 0 & 0 & 0 \\ 0 & 0 & 0 & 0 \\ 0 & 0 & 0.0895\ \frac{nm^2}{hr^3} & 0 \\ 0 & 0 & 0 & 32.0\ \frac{nm^2}{hr^3} \end{bmatrix}$$

This corresponds to an isotropic gust field with root-mean-squared value σ_V = 2fps and correlation time τ = 0.4285 sec. The sampling limit for the DME is NM = 60 M/H, and the computer constraint is $N_1 + N_2 \leq 60$ M/H.

4.4.2 Optimization Results

Application of the Optimization technique provides the optimal measurement histories. Also produced are the corresponding time histories of the 1-sigma values of position and velocity uncertainties and the switching functions. These results are the products of interactions of the sensor characteristics (R and H), the environmental disturbances (Q), the system performance index (J), and the time history of the estimation uncertainty (P).

Consider first the optimal measurement schedule shown in Figure 20. The sampling histories have the expected form, i.e., the majority of the time the source nearest the vehicle is used. The exception to this rule occurs for $0.205 \leq t \leq 0.242$.

To explain this behavior, consider the following. In this interval, source 1 has high accuracy (due to the short range) but senses almost no x information. Source 2 which has a lower accuracy, senses almost no y information but has an x geometric sensitivity of almost unity. This combined with the fact that, due to the large y disturbance accelerations, y information taken early in the flight has little effect on the performance index ($J = P_{11}(T) + P_{22}(T)$) produces the measurement history shown in Figure 20. Referring to the switching curves presented in Figure 21, it can be seen that in the interval $0.205 \leq t \leq 0.242$ the switching curves are almost equal. This indicates that J, using the optimal control histories or sampling only source 1 for $0 \leq t \leq 0.644$ should be similar. In fact, the optimal performance index is 0.50491 nm^2, where as this suboptimal control history gives 0.5050 nm^2.

In examining the position and velocity uncertainties time histories shown in Figure 22, it can be seen that the y position uncertainty tends to grow except in regions where there is sensitive y information. This is due to the localized nature of valid y information and the large y disturbance accelerations. If the y velocity uncertainty $\sqrt{P_{44}}$ is examined for $0.32 \leq t \leq 0.62$, it is almost linear with slope of 5.25 nm/hr^2. The value of the acceleration due to the y acceleration disturbance with no y information is $\sqrt{Q_{44}}$ = 5.65 nm/hr^2. Comparing these two numbers shows that for $0.32 \leq t \leq 0.62$, the y uncertainty is primarily the result of the acceleration disturbances. A similar result is true for $t \geq 0.80$. By contrast, both the x position and

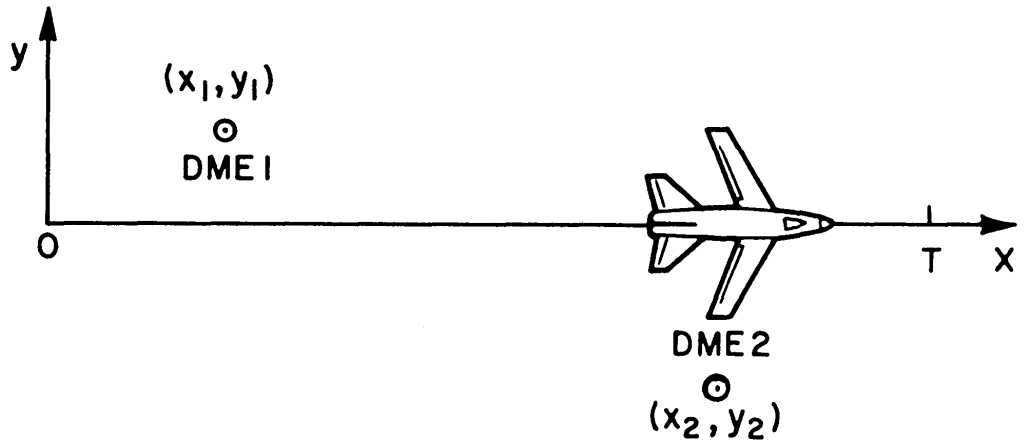


Figure 19.- System geometry

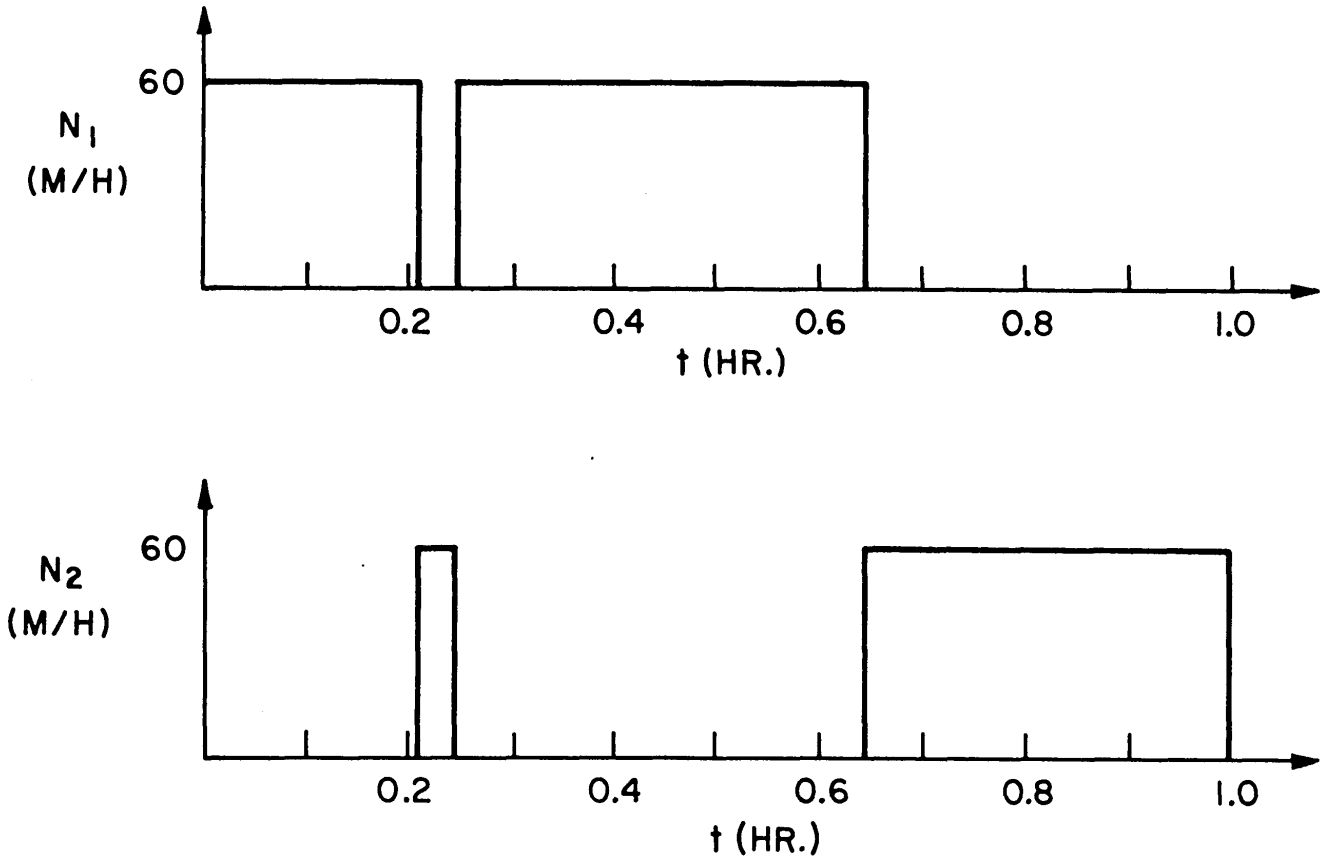


Figure 20.- Optimal measurement history

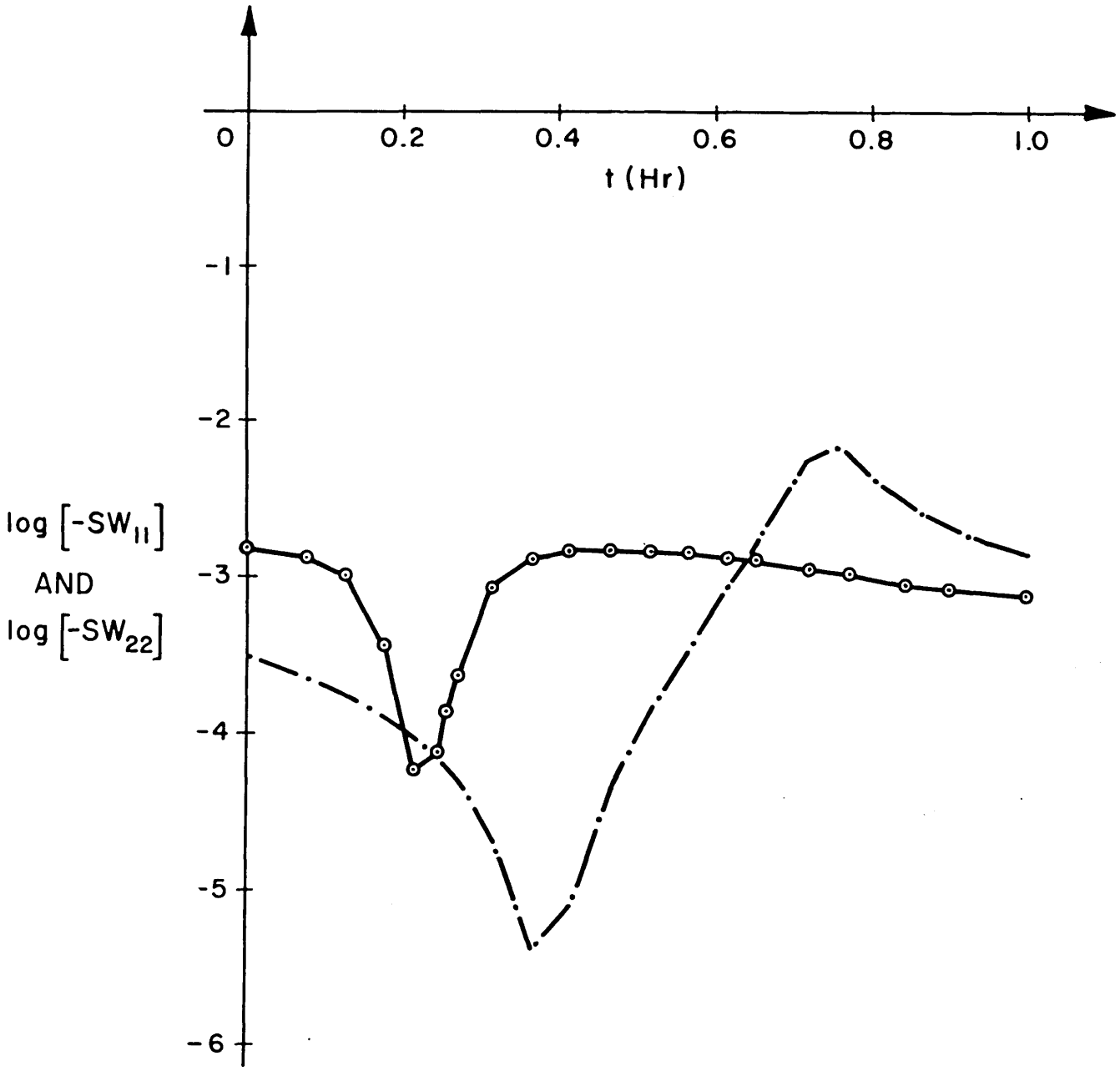


Figure 21.- Switching function for optimal control

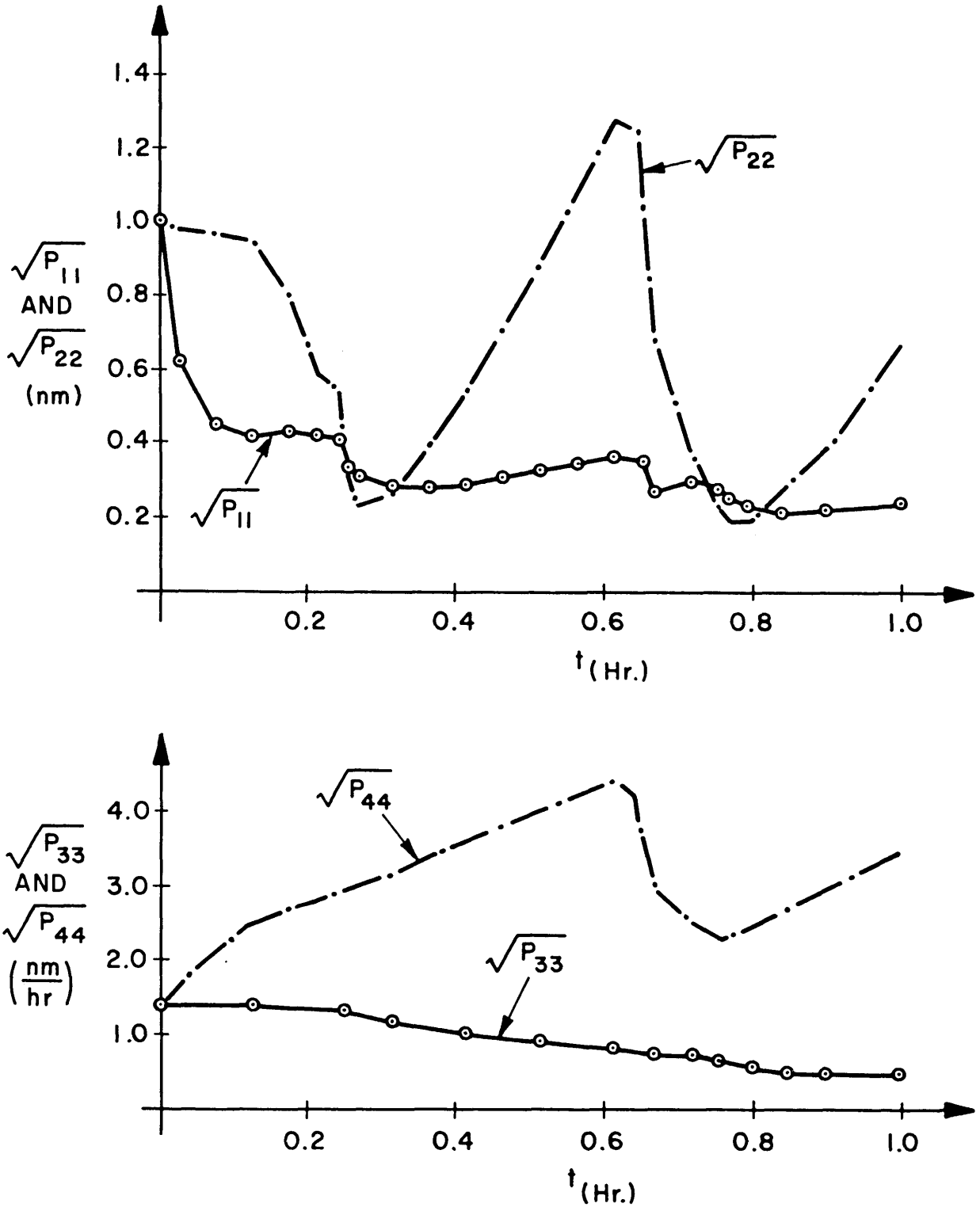


Figure 22.- RMS position and velocity estimation errors

velocity uncertainties have a general decaying form throughout the flight. This is due to the availability of x information throughout the flight and the relatively low disturbance acceleration.

4.4.3 Optimization Procedure Characteristics

The main characteristic of an optimization procedure is the computation time required to converge on the optimal solution. The computation time is a function of the number of control iterations required to arrive at a solution and the computation time per iteration. Consider first the computation time for each iteration.

The number of time-steps required per iteration and the speed of the computer are the prime influences of the time per iteration. The effect of computer speed is obvious and, since it does not reflect on the algorithm's efficiency, it will not be discussed further. The number of time-steps is a function of the time-step control parameters (ε_1, ε_2, and DT_{max}) and the behavior of the equations. A set of parameters used for the example problem is given in Table V. Using these parameter values 300 - 400 time-steps were required for a one hour flight.

TABLE V.- TIME STEP CONTROL PARAMETERS

$\varepsilon_1 = 0.01$
$\varepsilon_2 = 0.005$
$DT_{max} = 0.005$ hr

The number of iterations required to arrive at a solution is a function of the number of switch points in the solution, the initial assumed control history, the iteration controls ε_3, ε_4, and ε_5 and the sensitivity of the solution. The influence of the number of switch times in the solution is a direct result of the technique used of only iterating on a few switch times on each iteration.

The starting solution or the initial assumed control histories used in the forward integration plays an important role. A poor choice produces a very slow convergence or a divergent situation. A procedure that was found useful in many cases was to let the optimality conditions determine the starting

solution. An assumed control was selected that ignored the computer constraint. This shall be referred to as the Limiting Case Solution, and will be discussed in Chapter 5. For this case, all sources are sampled at their maximum rates. For the example in this section, N_1 = 60 M/H and N_2 = 60 M/H. Integrating forward and backward produces a N^*. For the next iteration, N^* is used for the forward integration, i.e., $\bar{N}^{(1)} = N^{*(0)}$. From this point on, the techniques of Section 4.3 are used to iterate on the individual switch times. This procedure was found very useful especially in cases where the regions in which the sensors produced good information have little overlap.

The effects of the iteration control parameters ε_3, ε_4, and ε_5 and the sensitivity of the solution are inter-dependent. The set of parameters used in the example problem are given in Table VI. ε_3 determines how well a t_i and t_i^* must match before t_{i+1} can be iterated. ε_4 is the fraction of the error $(\bar{N} - N^*)$ used to update $\bar{N}$. ε_5 is the limit that defines convergence; i.e., if $|t_i - t_i^*| < \varepsilon_5$ for all i, then convergence is declared. There are two types of solution sensitivity. The first type is when the parameters of the application (sensor accuracies, environmental disturbances, and geometry) are such that the optimal switching functions have regions where the switching functions for two or more sensors are almost equal. In such cases, the optimization procedure will oscillate between two control histories which have a different number of switch points. An example of this behavior is shown in Figure 23 (Mode B). This corresponds to the example given in this section with environmental disturbances σ_v = 2.5 fps. The optimal control logic states that if the switching functions are equal then either sensor can be used. For the optimization procedure to converge to a solution for such cases, the step size, ε_4, should be reduced and the convergence limit, ε_5, relaxed. When ε_4 = 0.3 and ε_5 = 0.002 hr were used, the procedure produced solution (A). The form of the optimal measurement histories appears to be dependent on the values of the ε's. This is not disturbing because the value of the performance index (which is the important quantity) using either switching Mode (A) or (B) is the same to five decimal places.

TABLE VI.- CONTROL ITERATION PARAMETERS

ε_3 = 0.005 hr
ε_4 = 0.5 (Nondimensional)
ε_5 = 0.001 hr

A second type of sensitivity occurs when the driving noise, Q, is large compared with the available information. In such cases, the uncertainties are allowed to build up to large values. Under such conditions, a small change in the control history can produce large changes in P(t). This can result in unstable control iterations. For this situation, the step size ε_4 must be reduced. This results in slower convergence but is unavoidable.

The optimal measurement schedule (Figure 20) for the sample problem was generated on a Scientific Data Systems (SDS) 9300 digital computer. Characteristics of this machine are given in Appendix C. Using the time-step parameters (Table V) and the iteration control parameters (Table VI), the optimization procedure converged in four iterations. Each iteration used 300-400 time-steps and required 4 to 5 minutes of computer time for a total computer requirement of 18 minutes.

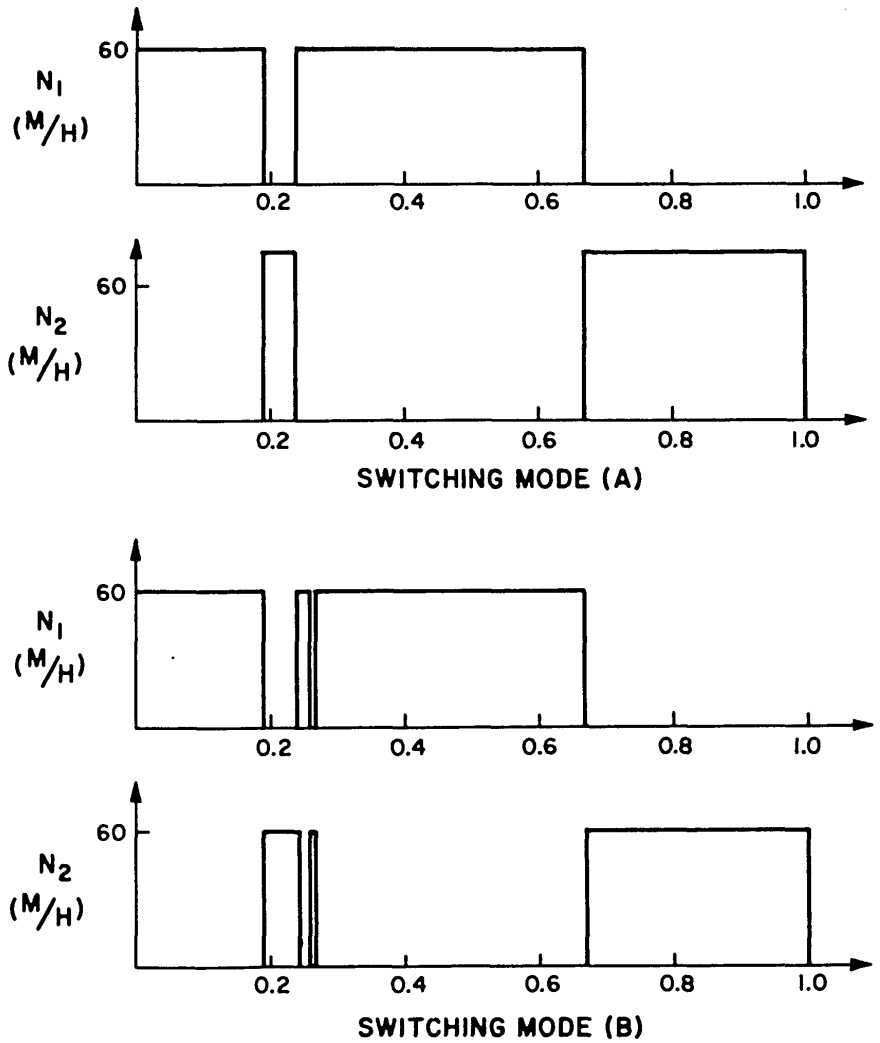


Figure 23.- Two near optimal switching histories for σ_V = 2.5 fps

Chapter 5

DESIGN PROCEDURE

5.1 INTRODUCTION

The object of this section is the detailed development of an efficient and flexible set of logic to provide the system designer with system design and utilization data. This logic is called the design procedure. The data generated by the design procedure will be utilized by the designer to select the "best" navigation system. The design procedure, shown in Figure 24, starts with the list of candidate sensors and computers and with the system performance requirements. This data is operated on by one of three design options. Each option (Figure 25) contains a selection logic which determines the order in thich the candidate systems are evaluated and a set of techniques for evaluating the systems. The output of this procedure includes the results of the selected design option plus auxiliary data selected by the designer. The emphasis in this development is on the generation of efficient logic as opposed to the presentation of an efficient computer program. For this reason no computer program listing is included. Detailed logic flow charts are included in sufficient detail so that an interested reader can write a program using these flow charts.

The techniques used to evaluate a system are essentially the same for each of the three design options and will be presented first. Next, the design options and the selection logic for each option are discussed. Finally, a discussion is given of the auxiliary data available to the designer. The combination of selection and avaluation logic plus the auxiliary data forms an efficient and flexible design tool.

5.2 EVALUATION TECHNIQUES

Before discussing the system evaluation logic it is useful to define two terms. First, candidate systems refers throughout the discussion to the set of $(2^n - 1) \times C$ possible systems, corresponding to the n candidate sensors and the C candidate computers. Also, the Optimization Technique refers to the technique developed in Chapter 4 for the determination of the optimal measurement schedule and the minimum value of the system performance index.

To evaluate the candidate systems, it is possible to apply the Optimization Technique to all systems. It is recognized, however, that this requires a good deal of computation, and thus to improve the efficiency of the design procedure, a second level of evaluation analysis, the Limiting Case Analysis, is introduced

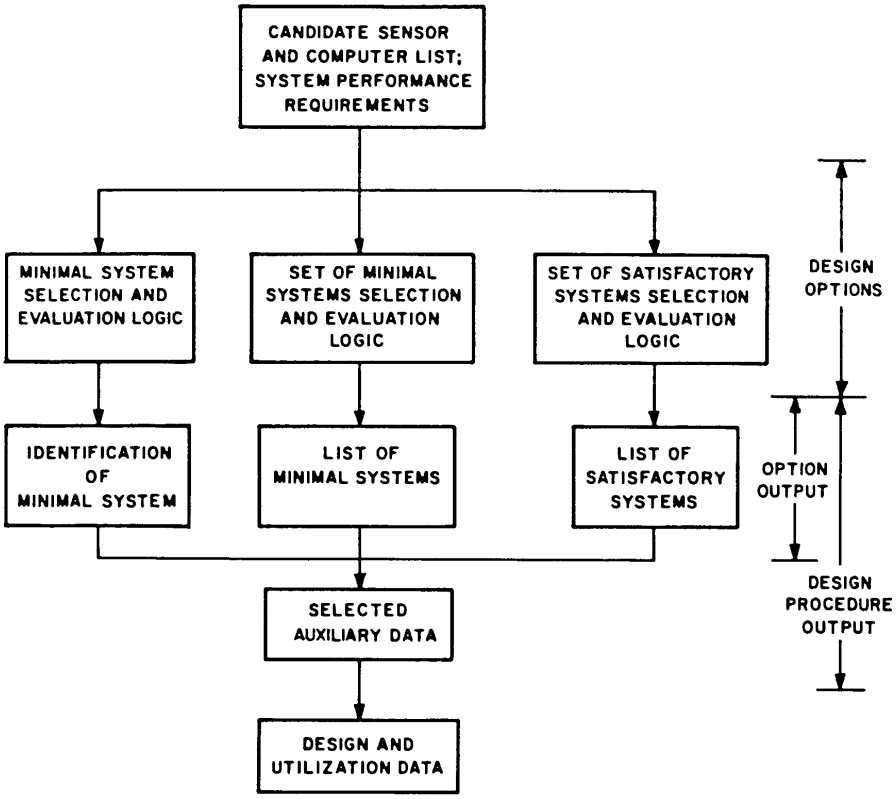


Figure 24.- Design procedure block diagram

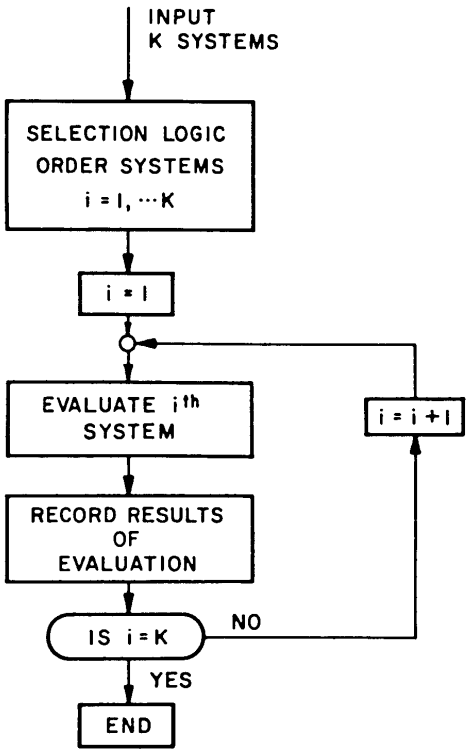


Figure 25.- Flow chart of typical design option

(Figure 26). This analysis makes use of an open loop integration of the covariance matrix equation

$$\dot{P} = FP + PF^T - PH^T N R^{-1} HP + Q \qquad (5.1)$$

using selected measurement histories N(t).

To illustrate the techniques used to select the N(t) and to investigate the physical meaning of these control histories, consider a simple example.

Table VII presents the characteristics of the two candidate sensors and the three candidate computers considered in this example. (Assume that these sensors are single-source type sensors). The total number of configurations to be analyzed is $(2^2 - 1) \times 3 = 9$. On examination of the data in Table VII, it can be recognized that the optimal measurement schedule for seven of the nine configurations can be determined by inspection. These configurations and their optimal measurement schedules are given in Table VIII. The optimal schedule can be determined by inspection for two reasons. First, for a single sensor configuration the optimal switching law requires that the use of that sensor be limited by either the computation limit or physical sampling limit. In the present example, the optimal schedules for the single-sensor systems, S1-C1 and S2-C1, are determined by the processing constraint while the schedules for systems S1-C2, S2-C2, S1-C3, and S2-C3 are determined by the sensor sampling constraints. The second situation arises when the limiting factor for multi-sensor systems such as S1-S2-C3 is the sensor sampling constraints. In this situation, the computer does not limit the sampling rates. Both types of limitations usually occur for systems with a small number of sensors. To evaluate the performance of such systems, the optimal N(t) given in Table VIII are used to integrate Eq. 5.1 from t = 0 to t = T. Then the optimal value of the system performance J = tr [AP(T)] is computed.

Of the original nine configurations, only two systems, S1-S2-C1 and S1-S2-C2, require further investigation. Consider the system S1-S2-C2. The admissible control region for this system is shown in Figure 27. The optimal measurement schedule does not correspond to any one point on this figure but rather to a switching between points A and B. To determine the times at which these switches occur would require the application of the Optimization Technique. It can be seen, however, that although point C is not an admissible control point due to the violation of the computer constraint, the following relation is true

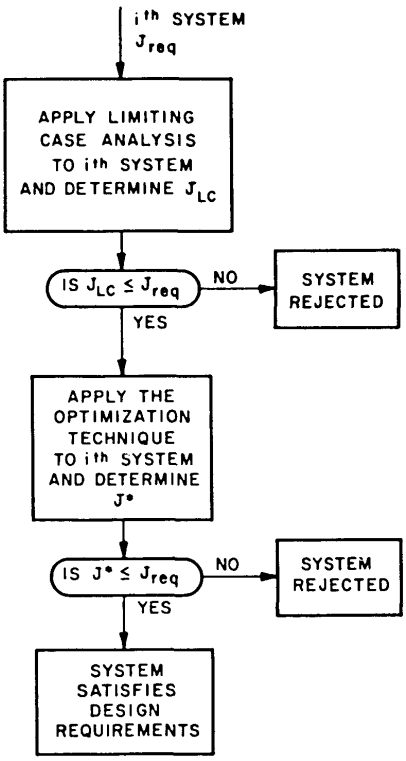


Figure 26.- Evaluation technique

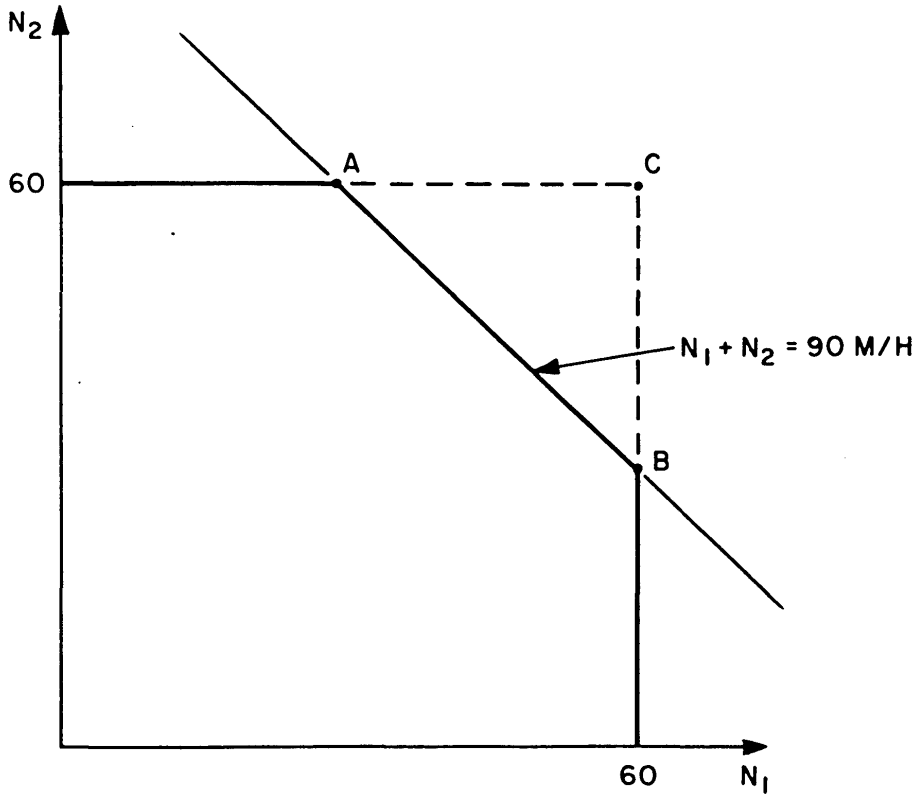


Figure 27.- Admissible control region

TABLE VII

CANDIDATE SENSORS

Sensor Number	Maximum Sampling Rate (M/H)*	Relative Computer Loading
S1	60	1
S2	60	1

CANDIDATE COMPUTERS

Computer Number	Computer Capacity (M/H)*
C1	50
C2	90
C3	150

*M/H = Measurements/hour

TABLE VIII

OPTIMAL SCHEDULE OF MEASUREMENTS

SYSTEM CONFIGURATION	OPTIMAL MEASUREMENT SCHEDULE (MPH)
1. S1 - C1	$N_1 = 50$
2. S1 - C2	$N_1 = 60$
3. S1 - C3	$N_1 = 60$
4. S2 - C1	$N_2 = 50$
5. S2 - C2	$N_2 = 60$
6. S2 - C3	$N_2 = 60$
7. S1 - S2 - C3	$N_1 = 60$; $N_2 = 60$

$$J_C \leq J^* \tag{5.2}$$

where J_C is the value of the system performance index tr[AP(t)] of the inadmissible measurement schedule corresponding to point C in Figure 27 and J* is the optimal value of tr[AP(t)]. The result given in Eq. (5.2) can be used to evaluate this configuration by comparing the value J_C with the value J_{Req} specified in the System requirements. If $J_C > J_{Req}$ then $J^* > J_{Req}$ and this configuration can be eliminated from further consideration. If $J_C < J_{Req}$, then the Limiting Case Analysis yields no definite statement regarding the relationship of J* to J_{Req}. It is then necessary to use the Optimization Technique to evaluate this system.

A situation similar to the foregoing case (not an option in this example problem) is shown in Figure 28. Here it can be seen that the interaction of the sensors and computer is such that for sensor 2, the factor which limits its use is the computer. For this case, the approximate control used in the Limiting Case Analysis is point D rather than point C since:

$$J^* \geq J_D \geq J_C \tag{5.3}$$

Point D is better approximation to the optimal behavior of this configuration.

It was assumed at the start of this example that the sensors were of the single-source type; i.e., they receive information which is being generated at a single source. This restriction is necessary because special techniques are needed to perform the Limiting Case Analysis on systems which include multi-source sensors. To illustrate, consider a system with two sensors. Sensor 1 is a single source type sensor with NM_1 = 60 M/H; sensor 2 is a multiple source sensor with three ground stations located as shown in Figure 29 and with NM_2 = 60 M/H. The system computer is assumed to have CC = 90 M/H. The admissible control region is equivalent to that shown in Figure 27 and the value of the Limiting Case sampling rates is N_1 = 60 M/H and N_2 = 60 M/H. The difficulty arises when the following question is asked, "For Sensor 2 which source is being sampled at 60 measurements/hour?" The correct answer, since there is a physical limitation that makes it impossible to sample more than one source at a time, is that there is switching from one source to another as the vehicle traverses the flight path. It is, necessary therefore, to determine the switching history for sensor 2. There is only one switch history for sensor 2 that permits an evaluation of the system. This history is the one derived using the Optimization

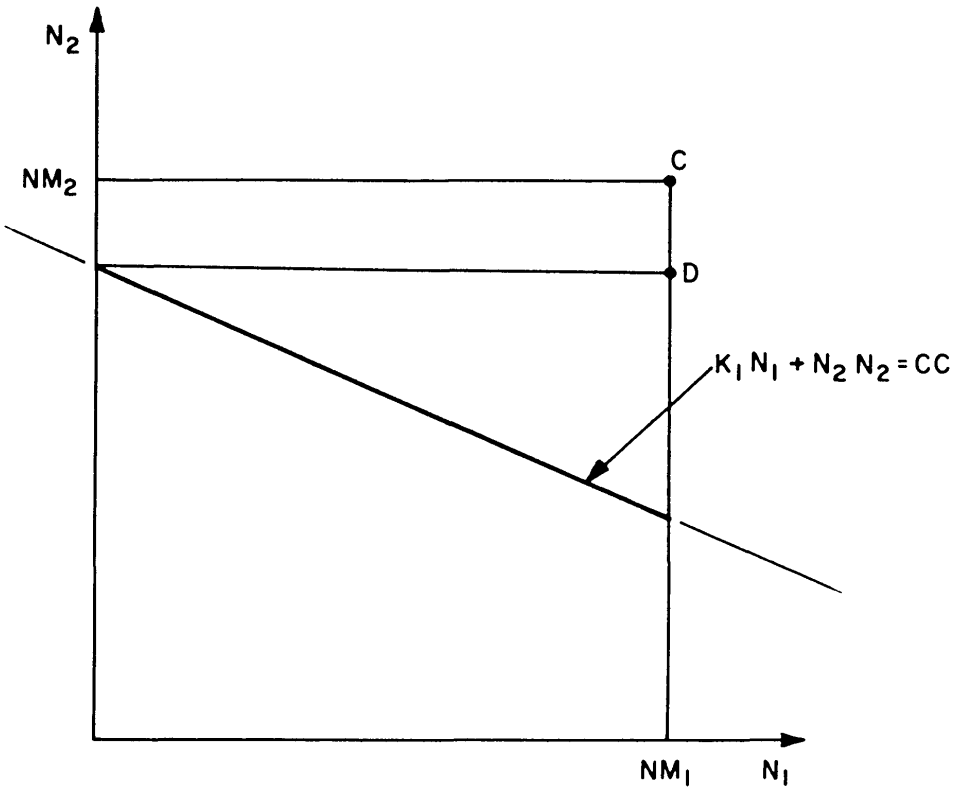


Figure 28.- Admissible control region

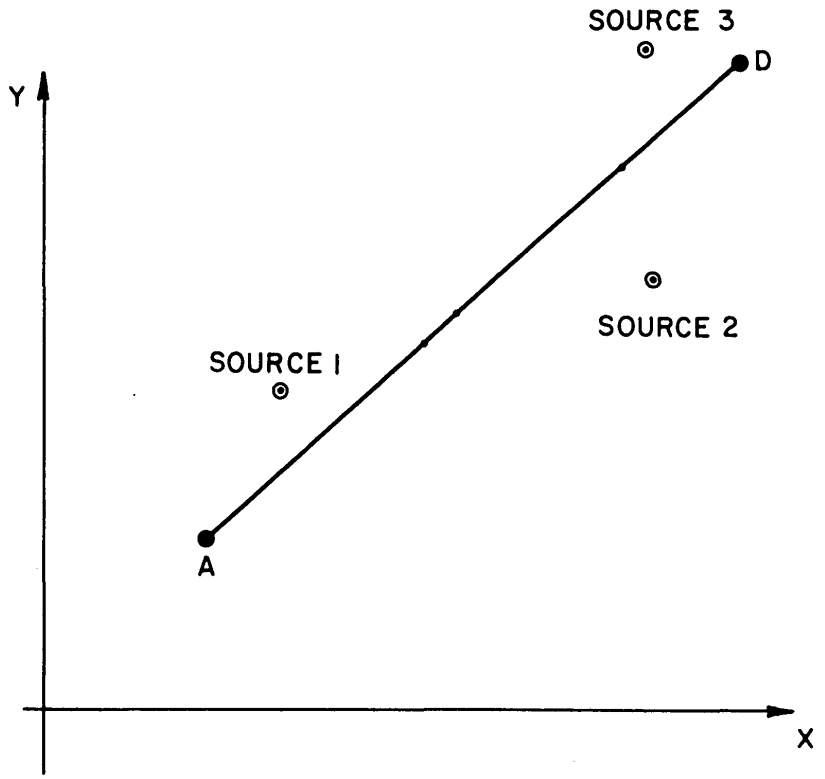


Figure 29.- Multiple source geometry for sensor 2

Technique. This is true because of the interaction of the effects of eliminating the computer constraint and using non-optimal switching for sensor 2. The first of these two effects gives a value of J less than the true optimal value. The second effect, using non-optimal N_2, gives a value of J greater than J^*. Since no information is available concerning the relative magnitudes of these effects nothing can be concluded. If, however, N_2 is the optimal measurement history when N_1 = 60 M/H, then the Limiting Case does produce $J \leq J^*$.

Having applied the limiting case analysis to the Candidate configurations, some of the systems can be eliminated because of failure to meet the system performance requirements. If no system satisfies the requirements, new candidate sensors or computers can be considered or the requirements relaxed. The remaining systems must then be evaluated using the Optimization Technique.

5.3 DESIGN OPTIONS

To be of most use, design procedures should contain alternative approaches. The designer can then select the procedure to fit the application. Flexibility is achieved here by developing three design problems that provide the designer with a choice of approaches. These problems differ slightly in the kind and amount of information generated and the form of the logic used to arrive at the solution. They are discussed in the following sections.

5.3.1 Minimal System

The first design problem is the determination of the Minimal System from among the candidate systems. The Minimal system is defined as the system that satisfies the system accuracy requirements and has the smallest system cost. Employing this option, the designer relies heavily on the design procedure since only the single "best" system, from an accuracy and cost point of view, is presented. This option is most applicable where accuracy and cost are of prime importance. This option requires the least computation of the three options and therefore it is chosen when a quick answer is required.

The cost of a system is the sum of the sensor costs and the computer cost. An example of this cost information is shown in Table IX. The logic used to determine the Minimal system is shown in Figure 30. The first step involves the ordering of the systems according to total system cost. Starting with the system with the lowest cost, the system is evaluated using the

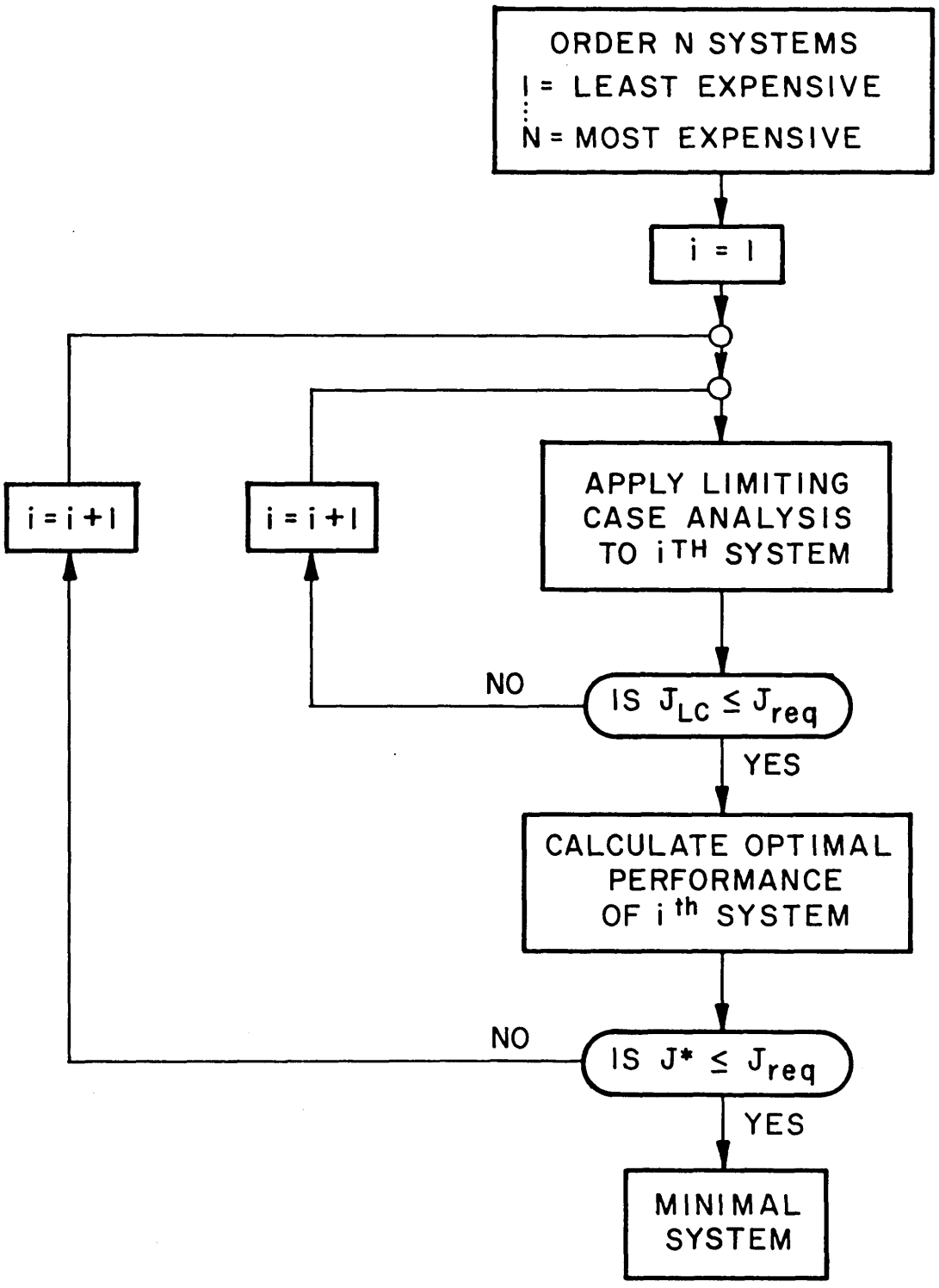


Figure 30.- Minimal system selection and evaluation logic

TABLE IX

SENSOR COST DATA

Sensor	Cost (dollars x 10^3)
DME Receiver	6
Doppler Radar	40

COMPUTER COST DATA

Computer	Cost (dollars x 10^3)
C1	10
C2	40

SYSTEM COST DATA

Configuration	Total Cost (dollars x 10^3)
1. DME - C1	16
2. DME - C2	46
3. Doppler - C1	50
4. Doppler - C2	80
5. DME - Doppler - C1	56
6. DME - Doppler - C2	86

Limiting Case Analysis. If the result shows that this system cannot satisfy the system accuracy requirements, then this system is eliminated and the Limiting Case Analysis is applied to the next configuration in the list. If the results of the Limiting Case Analysis indicate that the system may be capable of satisfying the requirements, the optimal measurement schedule is determined. The optimal value of the performance index J^* is compared with the required values J_{Req}. If $J^* \leq J_{Req}$, then this is the minimal system and the process is terminated. If $J^* > J_{Req}$ this system is eliminated and Limiting Case Analysis is applied to the

to the next system in the order. The first system which has a $J^* \leq J_{Req}$ is the Minimal system.

This logic is efficient, not only due to the use of Limiting Case Analysis, but also due to the order of selection from least expensive to most expensive. At each stage, the process has the possibility of eliminating all systems which occur further down in the order.

5.3.2 Set of Minimal Systems

The second design problem, which is more complicated than the Minimal System design option, is the determination of the set of Minimal Systems. To explain this option, it is necessary to define some terms. A sensor chain is defined as the list of all configurations that include a particular sensor. A Computer chain is defined in an analogous fashion. For n sensors and c computers each sensor chain has $2^{n-1} \times C$ systems and each computer chain has $(2^n - 1)$ systems. Table X shows the 4 chains corresponding to 2 candidate sensors and 2 candidate computers. For each chain, there may be a Minimal System. The set of Minimal Systems is the list of those local minimals. The overall Minimum System is seen to be a subset of this list. The information provided by this option is useful if, for reasons other than system accuracy or cost, it is desireable to either use or eliminate a particular sensor or computer from the list of candidate elements. An example of this would be if the designer lacks confidence in the ability of a vendor to deliver a particular sensor according to schedule, he may decide not to choose any configuration which uses that sensor. To insure a comparison

TABLE X

Candidate Sensors - S1, S2

Candidate Computers - C1, C2

S1 Chain	S2 Chain	C1 Chain	C2 Chain
S1-C1	S2-C1	S1-C1	S1-C2
S1-C2	S2-C2	S2-C1	S2-C2
S1-S2-C1	S1-S2-C1	S1-S2-C1	S1-S2-C2
S1-S2-C2	S1-S2-C2		

between systems with and without that sensor, he can require the determination of the system which is the minimum of all systems in each chain which do not include that sensor. He does not want to eliminate this sensor before the analysis, however, since a system containing this sensor might prove sufficiently superior to the others to warrant the risk.

The logic used to find the set of Minimal Systems is similar to that presented in the previous section but requires some additional steps. This logic makes use of the properties of Augmented Systems. An Augmented System is defined as having either more sensors or more computer capacity than the system being evaluated. For example, if system 1 is made up of a DME receiver and a doppler radar plus computer C1, then system 2 is an Augmented System of system 1. The usefulness of this concept is due to a result of Chapter 4. There it was proven that if more measurements are used, which is also the case if the computer is expanded, then the system performance index cannot increase. This can be extended to the case where yet more sensors are used. Since the Optimization Technique selects the most efficient measurements at every point in time, the inclusion of a new sensor cannot increase the performance index. Using this idea, if a system is found to satisfy the performance requirements, then all augmented versions of this system also satisfy the requirements.

Figure 31 presents a flow chart of the logic that determines the Set of Minimal Systems. The first step is to form both a system cost list, ordered according to total system cost, and a set of sensor and computer chains also ordered within each chain according to total system cost. The least expensive system in the system cost list is evaluated using the Limiting Case Analysis, and the Optimization Technique if required: to determine if this system satisfies the performance requirements. If this system does not satisfy the requirements, it is eliminated and the next system in the cost list is selected and the process repeated.

The first system which satisfies the performance requirement will be a Minimal System for one sensor chain and one computer chain. For this satisfactory system, its augmented systems are identified and the remaining sensor and computer chains are examined to determine if any of these augmented systems is the Minimal System for any other chain. If this is not the Minimal System for all the chains, a new system is chosen for evaluation. This new system will be the next system on the cost list which is not an augmented system of the systems already evaluated. This process is stopped when a Minimal System has been determined for all chains. To illustrate this logic, consider the situation of finding the Set of Minimal Systems for two candidate

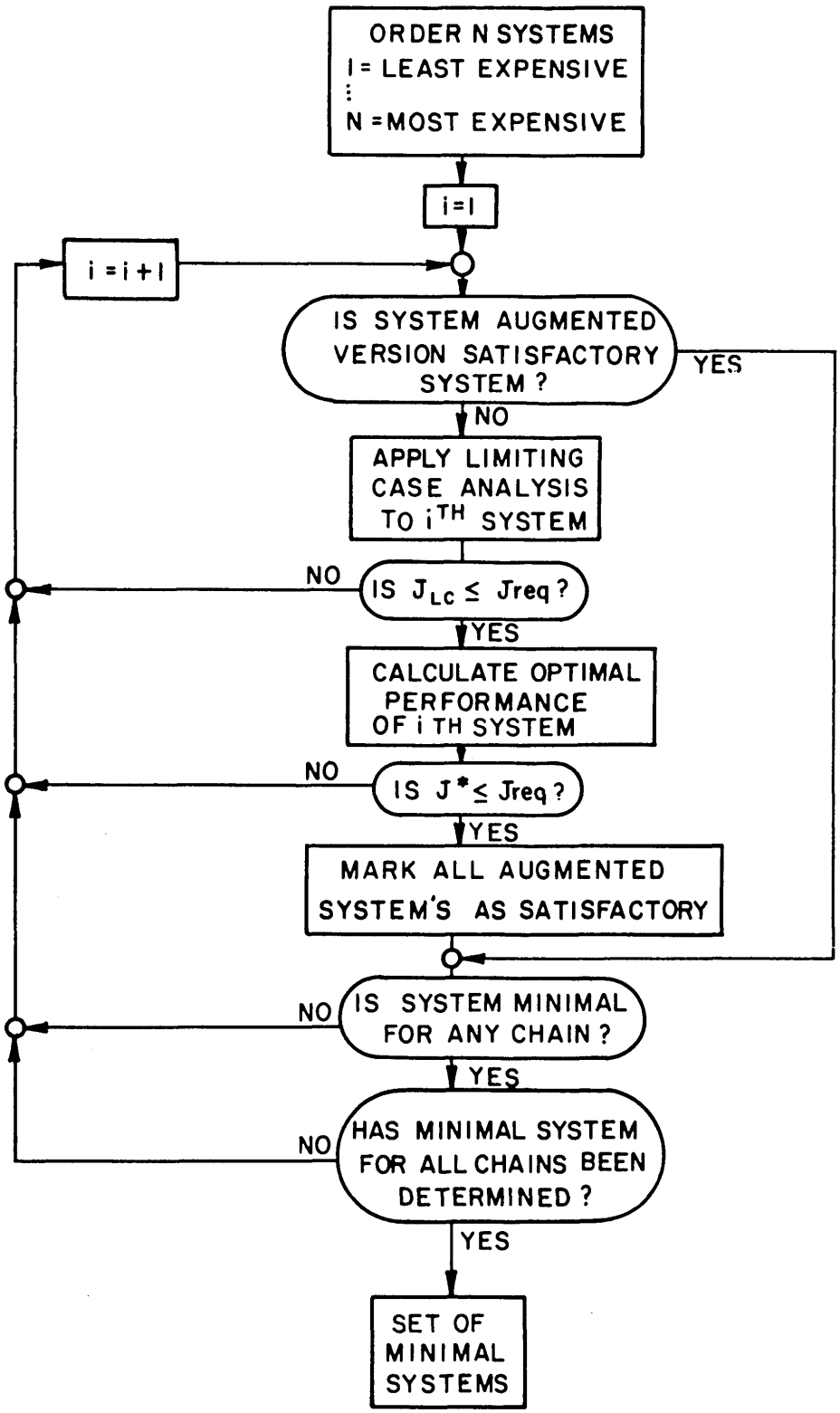


Figure 31.- Set of minimal systems selection and evaluation logic

sensors (DME and Doppler) and two candidate computers (C1 and C2 with $CC_1 < CC_2$). The two cost listings are given in Table XI. The process is started with an evaluation of the DME-C1 configuration. Assuming this system meets the system performance requirements, it is the Minimal System for the DME-chain and the C1-chain. The set of augmented systems includes the DME-C2 system which is the Minimal System for the C2-chain. It only remains to determine the Minimal System for the Doppler-chain. This involves the evaluation of only the Doppler-C1 configuration. This is due to the fact that the second system in the Doppler-chain is an augmented system of the DME-C1 configuration and is known to satisfy the requirements. Assuming the Doppler-C1 system cannot meet the performance requirement, the resulting set of Minimal System would be:

DME-Chain	:	DME-C1
Doppler-Chain	:	DME-Doppler-C1
C1-Chain	:	DME-C1
C2-Chain	:	DME-C2

5.3.3 Satisfactory Systems

The third design problem determines all the Satisfactory Systems where a Satisfactory System is defined as a system which can satisfy the system accuracy specifications. This option requires the most computation but provides the most information of the three options. In fact, the Minimal System and the Set of Minimal Systems can be selected from the output.

The logic used to generate the list of Satisfactory Systems is influenced by the lack of information regarding the relative accuracy performance of the configurations. For example, no information exists which allows the ordering according to performance of two systems which have the same number of sensors but of different types. This lack of information requires that all configurations be evaluated using either Limiting Case Analysis or the Optimization Technique or the Augmented System concept. This limitation also dictates that the selection logic be such that a system is always evaluated before augmented versions are evaluated.

The logic to be used starts by ordering the candidate systems into levels which correspond to the number of sensors. Within each level, the systems with the same computer are grouped into sublevels. These sublevels are ordered based on computer capacity CC from the smallest capacity to the largest. An example of this type of listing for the case of two candidate sensors and two

TABLE XI

ORDER SYSTEM AND CHAIN COST LISTINGS

ORDERED SYSTEM COST LIST	
1. DME-C1	(16)*
2. DME-C2	(46)
3. Doppler-C1	(50)
4. DME-Doppler-C1	(56)
5. Doppler-C2	(80)
6. DME-Doppler-C2	(86)

ORDERED SENSOR AND COMPUTER CHAINS COST LISTS

DME-Chain	Doppler-Chain	C1-Chain	C2-Chain
1. DME-C1 (16)*	1. Doppler-C1 (50)	1. DME-C1 (16)	1. DME-C2 (46)
2. DME-C2 (46)	2. DME-Doppler-C1 (56)	2. Doppler-C1 (50)	2. Doppler-C2 (80)
3. DME-Doppler-C1 (56)	3. Doppler-C2 (80)	3. DME-Doppler-C1 (56)	3. DME-Doppler-C2 (86)
4. DME-Doppler-C2 (86)	4. DME-Doppler-C2 (86)		

* System Cost in dollars x 10^3

candidata computers is shown in Table XII. The ordering at any level and for a particular computer is arbitrary. In this ordering, the systems are numbered consecutively.

TABLE XII

EXAMPLES OF ORDERING OF SYSTEMS FOR SATISFACTORY SYSTEM DETERMINATION

Candidate Sensors : DME, Doppler Radar Candidate Computers : C1 (60)*, C2 (150)			
Level	Sublevel	System Number	Configuration
1	1	1	DME-C1
		2	Doppler-C1
	2	3	DME-C2
		4	Doppler-C2
2	1	5	DME-Doppler-C1
	2	6	DME-Doppler-C2

*Computer Capacity in measurements/hour

The selection and evaluation logic which was chosen proceeds from the lowest level to the highest. The reason for this choice was the observation that the systems in the high levels most likely will meet the system specifications. Since the Limiting Case Analysis determines only if a system does not satisfy.the requirements, it will not be of use in analyzing the high level systems. The analysis of the high-level systems will require application of the Optimization Technique. To take advantage of the lower computation required by the Limiting Case Analysis, it was decided to evaluate from low to high levels.

The evaluation logic is shown in Figure 32. After ordering the Systems, the first system in the first sublevel of level 1 is evaluated using Limiting Case Analysis and then, if needed, the Optimization Technique. If this System does not satisfy the requirements, the next system in that sublevel is evaluated. If the system satisfies the requirements, then all its augmented systems are noted as being satisfactory. The reason for proceeding through these various levels is to evaluate (directly or by

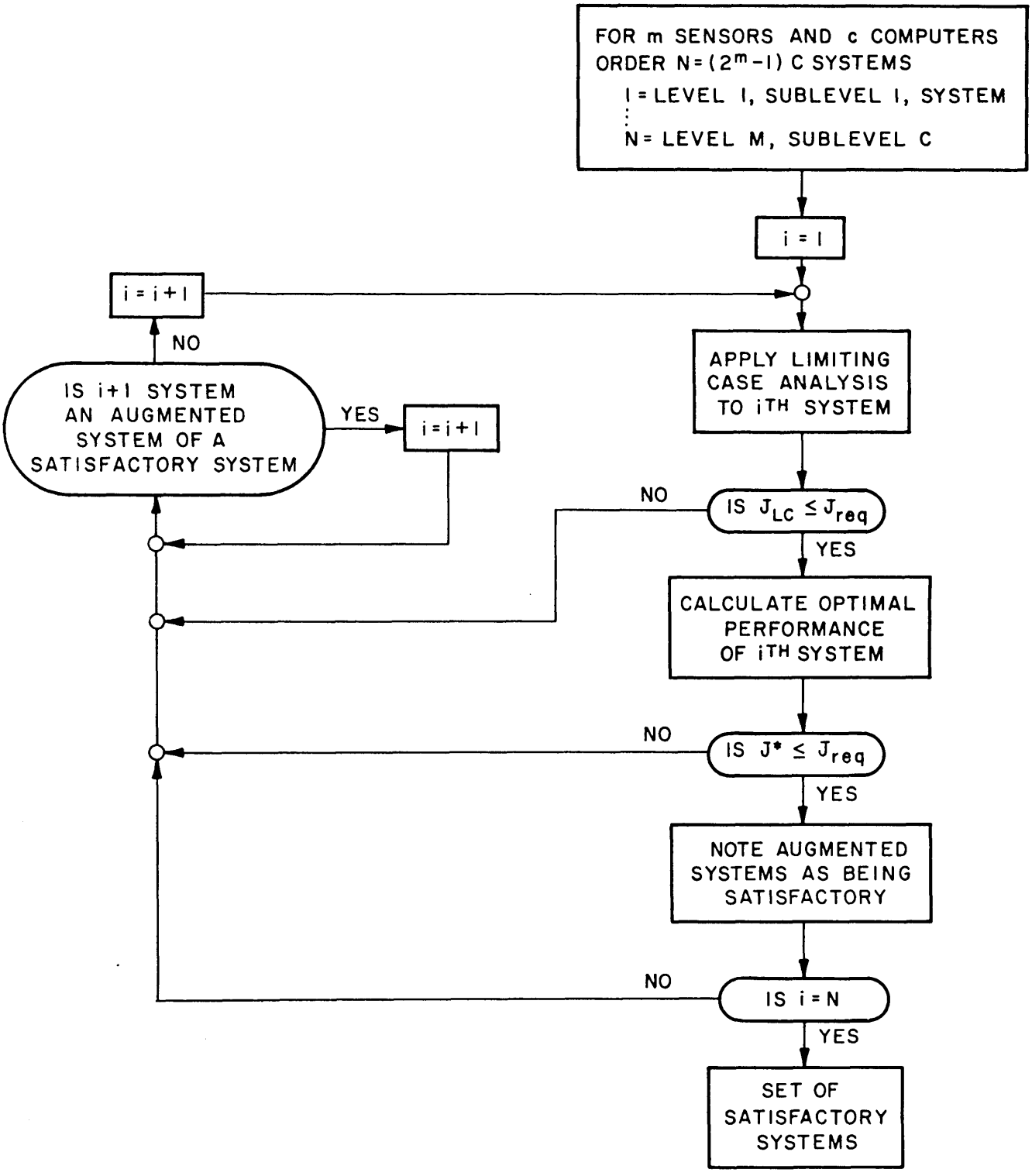


Figure 32.- Selection and evaluation logic for determination of satisfactory systems

application of the augmentation concept) all systems in a sublevel and then to proceed to the next sublevel in this level. When all systems at one level are evaluated, the process goes to the first sublevel in the next level and so on until all systems have been evaluated, and the list of satisfactory systems determined. If a satisfactory system which was analyzed using the Augmented System concept is selected as the system to be used, the optimal measurement schedule will have to be determined by applying the Optimization Technique.

5.3.4 Suboptions

All three options involved the determination of the list of systems that satisfied some criteria. There was no mention of the level of analysis used in the determination of these lists. The level of analysis can thus be chosen by the designer. As an example, consider the case of finding the Set of Minimal Systems. Would the designer be satisfied with the set determined by using only Limiting Case Analysis or would he want the optimal performance determined for this list. These decisions are available to the designer as suboptions to the design options. In all cases, more information requires more work. Other suboptions that the designer could select would be the determination of the two or three least expensive systems. The techniques used to generate this additional information are straight forward extensions of the logic used for the three design options.

5.4 AUXILIARY DATA

To determine the list of systems which constitutes the solution to one of the three design problems, much analysis is required. In the process, a great deal of useful information is generated. Much of this information is directly useful to the designer in his task of designing the "best" system for the specified application. In addition, some of this data is directly applicable to the related problem of how the selected sensors and computer should be utilized. The auxiliary information will now be discussed.

5.4.1 Design Data

A major tool used to evaluate the candidate systems efficiently is the Limiting Case Analysis. Part of the Limiting Case Analysis is the determination of the accuracy performance using assumed non-optimal measurement schedules. The particular technique used to select these measurement schedules was that of ignoring the computer constraint except as it applies to an

individual sensor. The resulting performance index was a measure of the basic capabilities of the sensors in the configuration. A comparison of this result with the results of using the Optimization Technique is a direct indication of the impact of the computer on the effectiveness of the system. For example, consider the case of a system made up of a DME sensor (which measures range from a DME transmitter) and a very High Frequency Omnidirectional Radio Range (VOR) sensor (which measures magnetic bearing of the receiver from the VOR transmitter) and a computer which allows only one sensor to operate at a time. This system is used in an aircraft whose flight path is as shown in Figure 33. The results of the Limiting Case Analysis were $J = P_{11}(T) = 0.3982 nm^2$ and the optimal performance was $J = 0.4108\ nm^2$. This indicates that a doubling in computer capacity produces virtually no improvement in the system performance index. Physically speaking, the sensors and not the computer are the limiting factors. For this simple case, this is anticipated since the regions in which each sensor produces good information have virtually no overlap. For more complicated systems, this same line of reasoning can be applied even though system complexity may rule out a correct intuitive guess.

A second class of data which is available from the application of the Optimization Technique consists of the time histories of the estimation error covariance matrix. Although only the values of this covariance at the terminal time are included in the performance index, the behavior of the elements of P (t) at times between t = 0 and t = T may be used in the design selection. As an example, consider the time histories of the root mean squared (RMS) position uncertainty for two systems shown in Figure 34. Although they both have approximately the same RMS value at t = T, System 1 goes through a region where little information is received and therefore, the uncertainty builds up in this region. Based on the application at hand, this may or may not be important. With such data, however, the designer can make his decision.

A third set of data is sensitivity data. This kind of data is developed only for the computer because this is the only part of the system in which changes in characteristics are meaningful. For example, a ten-percent change in the measurement accuracy of a sensor would most likely require the development of a new sensor which would not be available in time to be used. Also a small change in the location of a ground transmitter does not make sense. It does make sense in some cases to consider a ten-percent change in computer capacity. This might correspond to a slight adjustment of the computer budget. There are two forms of computer sensitivity: one which is analytic in nature and applies only for a small change in computer capacity CC, and one which is developed by repeated application of the Optimization

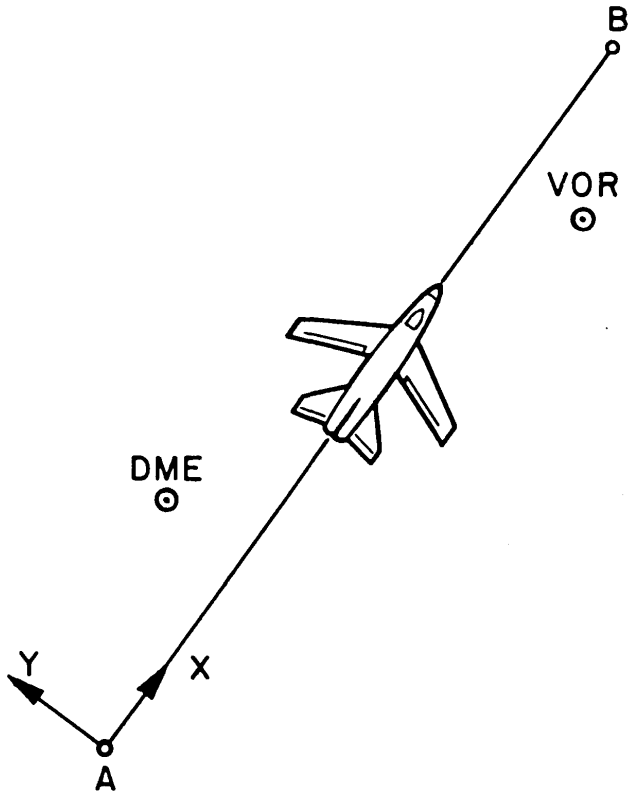


Figure 33.- Nominal flight path

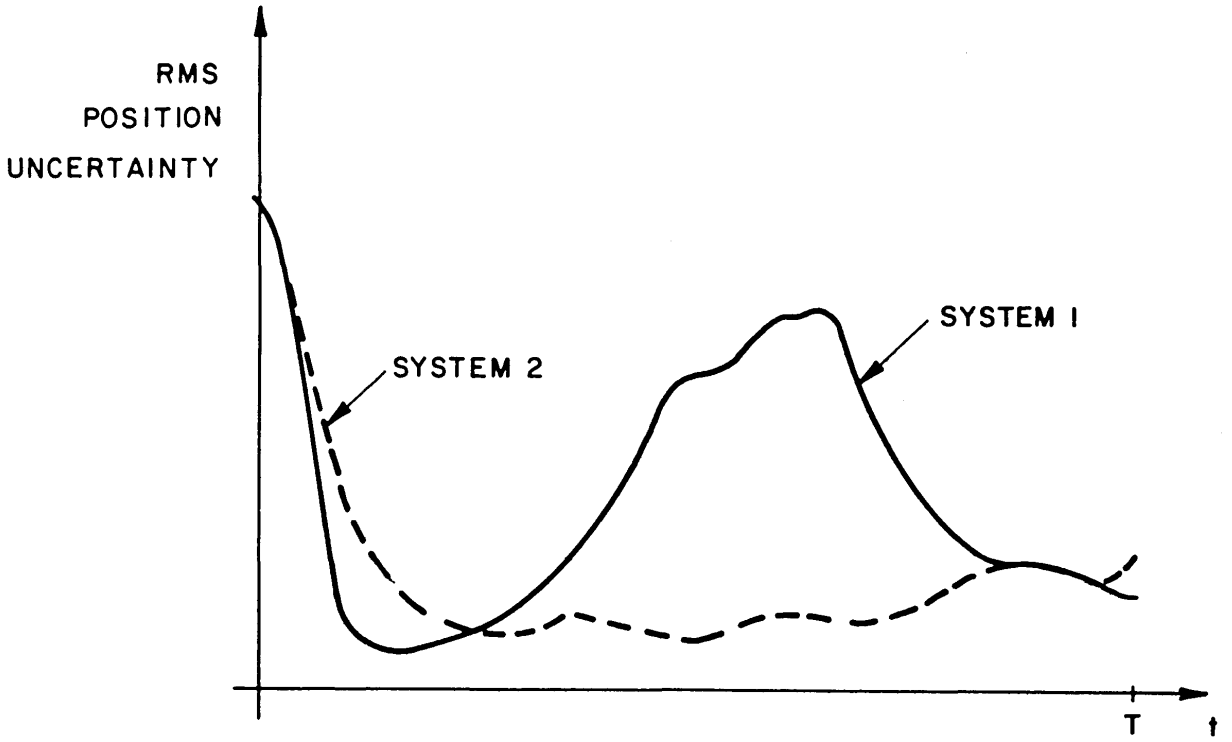


Figure 34.- Comparison of time behavior of the RMS position uncertainty for two different systems

Technique. Consider first the analytic sensitivity. Figure 35 shows the flight path and source geometry for a system which has two DME receivers. DME1 is tuned to receive information only from source 1 and DME2 can receive information only from source 2. Also shown are the optimal measurement schedules for two computers cc = 60 M/H and CC = 90 M/H. Two effects of the increase in computation capacity on the control histories can be seen. First the level of the sensor not on its boundaries has changed from zero to thirty M/H as would be expected. The second difference is that the time of the switch in measurement rates has changed. This change is relatively small considering that the computer capacity has been increased by 50 percent. For smaller changes in CC, it is anticipated that this difference would be still smaller. Therefore, it is assumed that for small changes in computer capacity Δ CC the change in the control history is approximated by leaving all switch times unchanged and using $\Delta N_i = \Delta CC$ for the sensor not on its limit. Applying this logic to Case A in Figure 35 the change in the control is given by:

$$\begin{aligned} 0 < t \leq t_1 \qquad & \Delta N_1 = 0 \quad ; \quad \Delta N_2 = \Delta CC \\ t_1 < t \leq T \qquad & \Delta N_1 = \Delta CC \quad ; \quad \Delta N_2 = 0 \end{aligned} \tag{5.4}$$

In Appendix F, the expression for the first-order variation is system performance index δJ due to a first order variation in the control histories δN is given by:

$$\delta J = -\left[\int_o^T \sum_{i=1}^{m} \left(R^{-1} H P \phi^T A \phi P H^T\right)_{ii}\right]_{cc_o} \delta N_{ii} \, dt \tag{5.5}$$

where the time histories of P, ϕ, H, and R correspond to the optimal N(t) which had a computer constraint of CC_o. ϕ is the transition matrix which satisfies the equation:

$$\dot{\phi} = \phi\left(F - P H^T N R^{-1} H\right) \tag{5.6}$$

with

$$\phi\left(T, T\right) = I$$

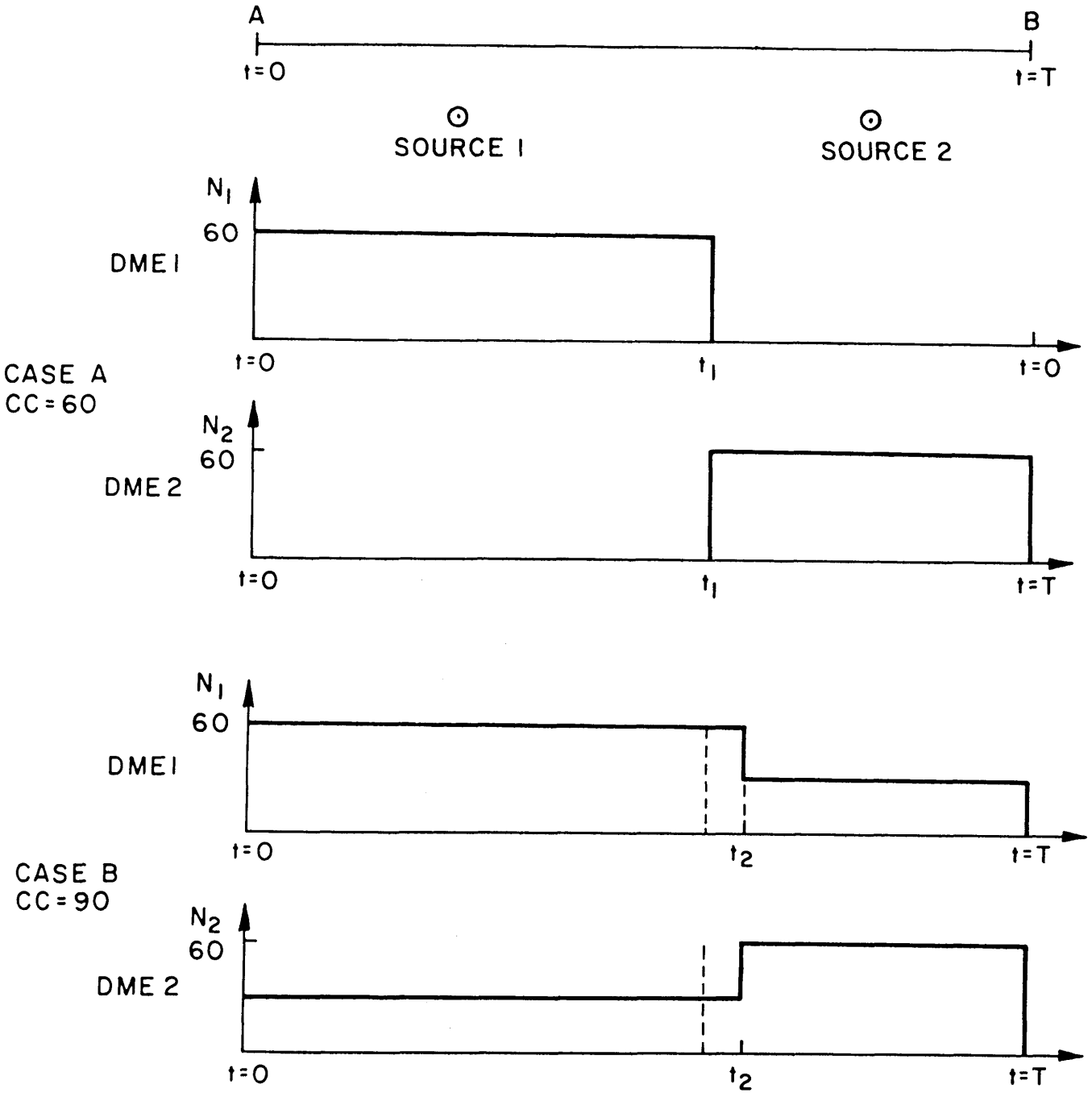


Figure 35.- Optimal control histories for system with two DME receivers and two computation capacities; CC = 60 and CC = 90

Assuming that $\delta N = \Delta N$ as given by Eq. 5.4 the change in J for small change ΔCC about CC_o is given by

$$\delta J = \left[-\int_o^{t_1} \left(R^{-1} HP\phi A\phi^T PH^T \right)_{22} \Delta CC \, dt \right. \tag{5.7}$$

$$\left. -\int_{t_1}^{T} \left(R^{-1} HP\phi A\phi^T PH^T \right)_{11} \Delta CC \, dt \right]_{CC_o}$$

Therefore:

$$\frac{\delta J}{\Delta CC} = -\left[\int_o^{t_1} \left(R^{-1} HP\phi A\phi^T PH^T \right)_{22} dt \right. \tag{5.8}$$

$$\left. +\int_{t_1}^{T} \left(R^{-1} HP\phi A\phi^T PH^T \right)_{11} dt \right]_{CC_o}$$

Equation 5.8 provides the designer with a measure of the effect of increased computer capacity. If this were to indicate a large return for a small increase in CC, it would be beneficial to adjust the computer budget slightly to accommodate this change.

A second form of the sensitivity of the system performance index J for various computer capacities can be generated by repeated applications of the Optimization Technique. The results of this analysis would be a curve similar to that shown in Figure 36. Point A corresponds to the situation in which no measurements are taken. The value of J for this case can be determined by direct integration of

$$\dot{P} = FP + PF^T + Q \tag{519}$$

with $$P(t_o) = P_o$$

The value of J corresponding to point B can also be calculated without using the iterative optimization techniques. This condition corresponds to the limiting case when

$$CC = \sum_{i=1}^{m} NM_i ,$$

i.e., when using all sensors at their maximum sampling rates just fills the computer. Values of CC larger than this do not change J and are not shown. To calculate a point between A and B requires the use of the Optimization Technique for a specific value of CC. It can be seen that the computer sensitivity presented in the format shown in Figure 36 contains more information than derived from Eq. 5.8 which only measures the slope of this curve at some nominal value of CC. This additional information is paid for by the optimizations required to generate Figure 5.13.

5.4.2 Utilization Data

There are two pieces of information useful in determining how a selected system configuration should be used in practice. These are the optimal measurement schedules and the corresponding switching functions. A typical set are shown in Figure 37. The use of the optimal measurement schedules is obvious but the usefulness of the switching functions requires some explanation. The switching function given by

$$\frac{-\left(R^{-1}HP\Lambda PH^T\right)_{ii}}{K_i}$$

for i = 1, ..., m indicates the efficiency of a sensor. The optimization procedure automatically determines the switching history which uses the most efficient measurements at all times. When a system is mechanized, however, other factors may dictate that for overall system efficiency a suboptimal measurement schedule is best. The switching functions allow the designer to make decisions of this type more easily. For example, consider the set of switching curves and the corresponding optimal measurement schedules shown in Figure 37. The optimal schedule requires switches at the times t_1, t_2, t_3 and t_4. The amount of trouble required to switch from one sensor to another depends on the type of sensor. For some systems, it is rather difficult. For example, in earth orbit the switch between a star tracker and a horizon sensor would, in some cases, require a change in vehicle orientation. In such cases, it would be useful to know what effect the use of a suboptimal measurement history would have on system performance.

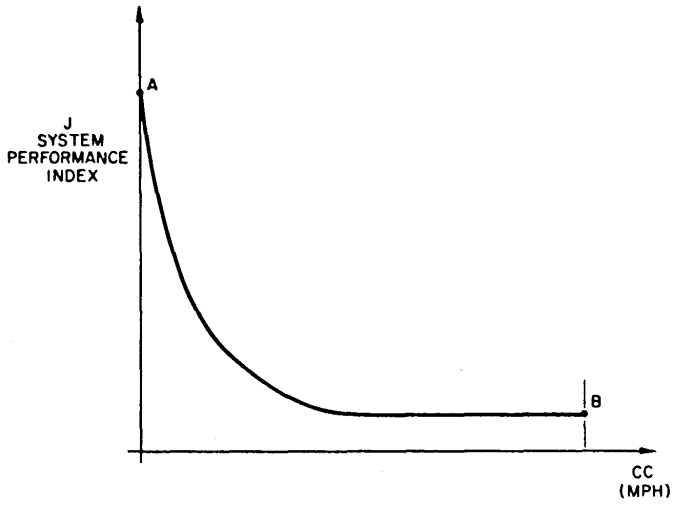


Figure 36.- Sensitivity of the performance index J

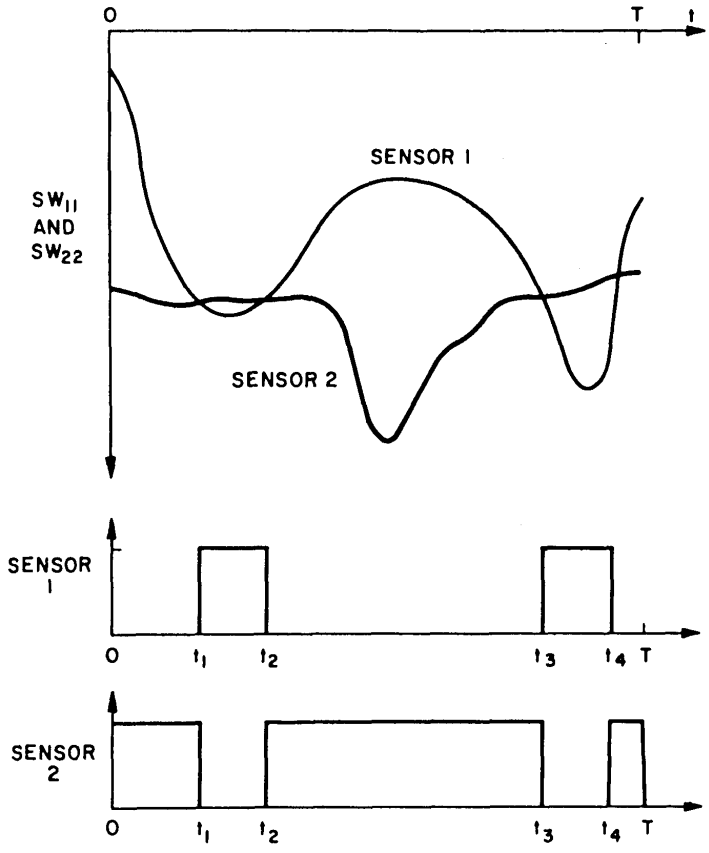


Figure 37.- Typical switching functions and corresponding measurements histories

It would also be useful to be able to select a good suboptimal measurement history. This type of information can be inferred from the switching functions. Referring to Figure 37, it can be seen that the optimal measurement schedule requires switches at t_1 and t_2. In this region, however, the efficiencies of the two sensors are almost equal. Therefore, it can be inferred that using sensor 2 for $t_1 \leq t \leq t_2$ will not substantially alter the system performance. The condition between the times t_3 and t_4 presents a slightly different problem. For this time interval, it appears that sensor 2 is definitely more efficient. The decision on which sensor should be sampled in this interval requires further analysis. Independent of the outcome of this analysis, the switching functions have given the designer information useful in determining the feasibility of using a suboptimal measurement schedule. Where feasible, they also help in determining the mechanization of these schedules.

5.3 SUMMARY

At the outset of this report, it was proposed that it is possible to formulate the design of a class of multi-sensor navigation systems in such a way as to allow a major portion of the total design process to be accomplished by automatic computation. The proof of this proposition required the development of analytic techniques which permit efficient evaluation and selection of candidate systems. The design procedure presented in this chapter fulfills these requirements. In addition, by using this procedure the designer can easily tailor it to the specific design application by choosing the best design option and by selecting the outputs generated. An example problem is presented in Chapter 6 to demonstrate the procedure and its use in the total design process.

Chapter 6

AVIONICS SYSTEM DESIGN

6.1 INTRODUCTION

To illustrate the characteristics of the Design Procedure, an example problem is now presented. This example considers the design of an aircraft cruise navigation system. Starting with a given problem statement, the engineering formulation is developed and the candidate components selected. All three design options are then applied to the design and the results of each option are presented and discussed. Also presented is a summary of the analysis used in generating the output of all three options. A list of all 45 candidate systems arranged in order of cost is given in Appendix G. Included in this appendix is a summary of the analysis and performance for all systems evaluated.

6.2 PROBLEM STATEMENT AND CONVERSION TO ENGINEERING TERMS

The designer is presented with the following assignment. "Design the best cruise navigation system for a V/STOL Airbus type operation between Boston and Washington, D.C. This system should arrive at its destination with position uncertainties no greater than 0.25 nm."

Converting this problem into engineering terms results in the following data.

6.2.1 Mission Data

The nominal trajectory was chosen as a straight line path between Boston and Washington, D.C. (Figure 38). The cruise altitude was selected as 20,000 ft, and the vehicle chosen was a modification of the XC-142 experimental tilt wing V/STOL aircraft. The characteristics of this vehicle (ref. 19) are given in Table XIII. The flight environment was taken as a random isotropic gust field with root-mean-squared gust of 2 fps (ref. 18) and a correlation time of 0.471 sec (ref. 20). Using the vehicle characteristics, the resulting acceleration perturbations were derived using the analysis given in Appendix E. They are:

$$Q_{33} = 0.358 \text{ nm}^2/\text{hr}^3$$

$$Q_{44} = 128.0 \text{ nm}^2/\text{hr}^3$$

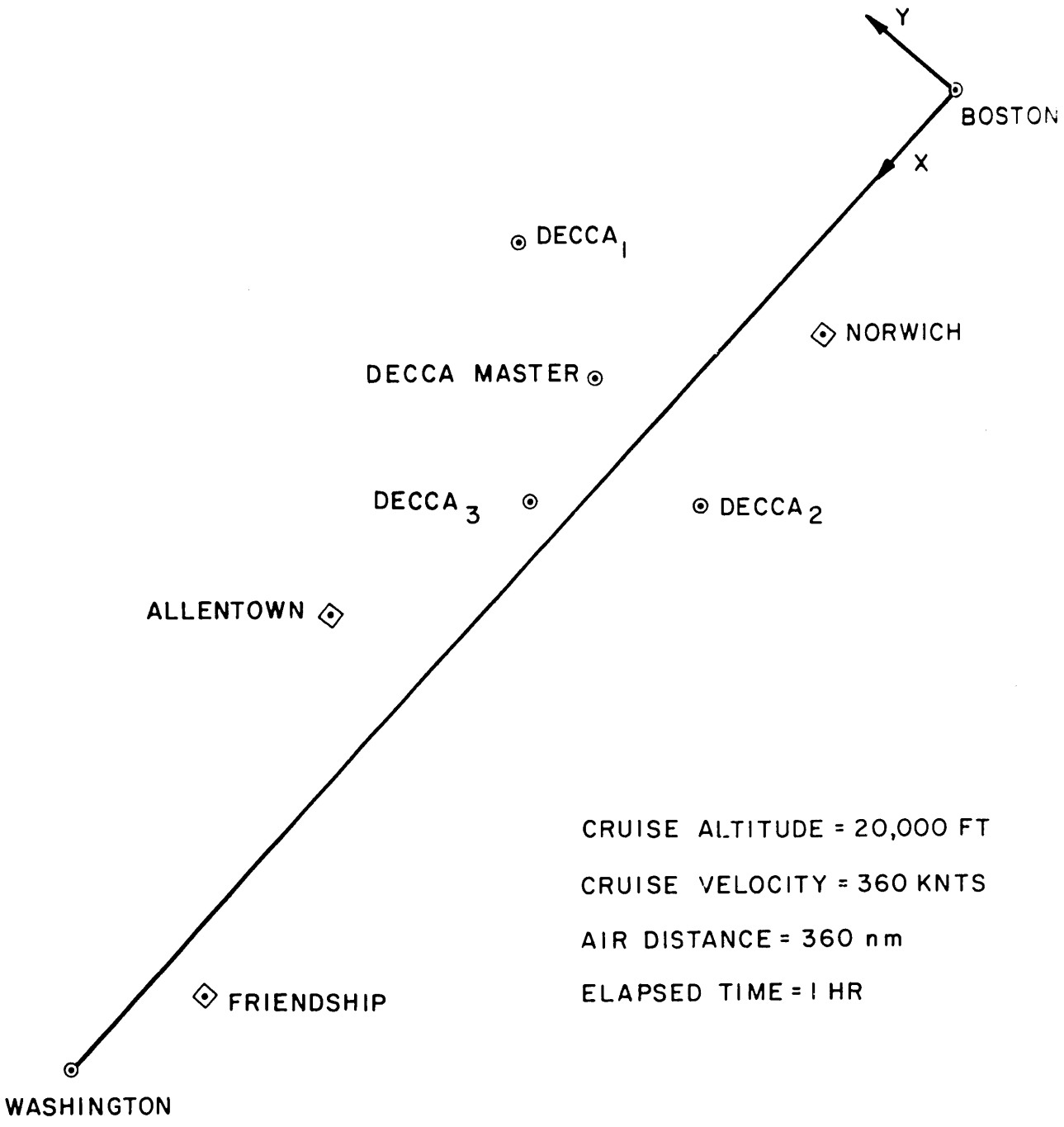


Figure 38.- Nominal trajectory and information sources

TABLE XIII.- VEHICLE CHARACTERISTICS

Cruise Velocity = 360 nm/hr
Wing Area = 535 ft^2
Side Area = 830 ft^2
Gross Weight = 38,000 lbs
Cruise L/D = 7.3
C_{y_β} = 1.03

6.2.2 Mission Objective

The mission objective is arrival at the terminal point with an uncertainty in position no greater than 0.25 nm. Considering this, the performance index was chosen as:

$$J = P_{11}(T) + P_{22}(T)$$

where P_{11} is the mean-squared uncertainty in the x (along track) direction, and P_{22} is the mean-squared uncertainty in the y (cross-track) direction.

6.2.3 System Data

The characteristics of candidate sensors and computers are given in Table XIV. Costs are given for the on-board equipment (refs. 13, 15). These 4 sensors were selected because of the general availability of this information in the Northeast Corridor. The ground network of information transmitters was taken to be three VORTAC stations which transmit both VOR bearing and DME range information from each site, and a Decca chain made up of one master and three slave transmitters. The locations of the ground transmitters are given in Table XV. The sensor sampling limits NM_i are taken as the availability of the transmitted data. The computers used do not correspond to any specific existing machines but represent a range of available computers.

An interesting fact that can be seen upon examination of the sensor and computer data given in Table XIV is that the rates at which the sensors will be sampled in the system are limited

by the processing constraint. This indicates that only one sensor will be sampled at a time. Having established the engineering model of the problem, it is possible to apply the Design Procedure.

TABLE XIV.- SENSOR AND COMPUTER CHARACTERISTICS

SENSOR	COST (Dollars x 10^3)	RMS MEASUREMENT ACCURACY	NM (M/H)	K_i
1. DME	5	2% of range	9,000	1.0
2. VOR	4	2 degrees	10,800	1.0
3. Doppler	28	4 knts	∞ (continuous)	2.0
4. Decca	14	0.5 nm	∞ (continuous)	3.0

COMPUTER	COST (Dollars x 10^3)	CC (M/Hr)
C1	20	180
C2	40	360
C3	60	720

TABLE XV.- INFORMATION NETWORK LOCATIONS

GROUND TRANSMITTER	DESIGNATION OR LOCATION	X (NM)	Y (NM)
DME 1 – VOR 1	Norwich	73.0	-18.0
DME 2 – VOR 2	Allentown	220.0	30.0
DME 3 – VOR 3	Friendship	319.0	-14.0
Decca – Master	Peekskill, N.Y.	145.5	19.0
Decca – Slave 1	Hudson, N.Y.	109.0	60.0
Decca – Slave 2	Bayshore, N.Y.	131.0	25.5
Decca – Slave 3	Dove, N.J.	160.5	10.0

6.3 DESIGN PROCEDURE RESULTS

The results of exercising all three design options of the Design Procedure are presented for the problem defined in Section 6.2. The desired output from each option, plus a summary of the analysis performed are given for each option. In addition, auxillary design data is presented for the Minimal System Option. In the analysis summaries, the following abbreviations are used.

L.C. = Limiting Case Analysis

O.T. = Optimization Technique

A.S. = Augmented System Concept

Also, when the Augmented System Concept is applied, the system performance is only bounded. This is indicated by the less than inequality symbol (<).

6.3.1 Minimal System

To determine the Minimal System, the two analysis techniques (Limiting Case and Optimization) were applied to the candidate systems, starting with the least expensive system and working down the cost listing. The first system which satisfies the performance requirement is the Minimal System.

The Minimal System for the present design problem was the VOR-DME-C3 system which has the following characteristics.

Minimal Configuration: VOR-DME-C3

Optimal Terminal Position Uncertainity: 0.2265 nm

Limiting Case Terminal Position Uncertainity: 0.1921

Systems Cost: $69,000

Determining this Minimal System required 25 applications of the Limiting Case Analysis and 9 applications of the Optimization Technique. A summary of this analysis is given in Table XVI.

An examination of the data in Table XVI shows a second system that misses satisfying the performance requirement by a small amount but has a smaller cost. This system (DME-Doppler-C1) warrents further examination. Two other system (Nos. 15 and 23) also show a terminal uncertainity only slightly larger than that which is required. These systems are, however, augmented versions of the DME-Doppler-C1 system, and show very small reductions

TABLE XVI

ANALYSIS SUMMARY FOR MINIMAL SYSTEM OPTION

SYSTEM NO.	CONFIGURATION	COST $ x 10^3	PERFORMANCE (nm)	ANALYSIS	ADDITIONAL DATA
1	VOR-C1	24	0.4153	L.C.	
2	DME-C1	25	0.4097	L.C.	
3	VOR-DME-C1	29	0.2980	L.C.	
4	Decca-C1	34	0.9308	L.C.	This is also optimal value
5	VOR-Decca-C1	38	0.3727	L.C.	
6	DME-Decca-C1	39	0.3204	L.C.	
7	DME-VOR-Decca-C1	43	0.2919	L.C.	
8	VOR-C2	44	0.3216	L.C.	
9	DME-C2	45	0.3610	L.C.	
10	Doppler-C1	48	1.5183	L.C.	This is also optimal value
11	DME-VOR-C2	49	0.2828	O.T.	Limiting Case 0.2405 nm.
12	VOR-Doppler-C1	52	0.3405	O.T.	Limiting Case 0.2493 nm.
13	DME-Doppler-C1	53	0.2509	O.T.	Limiting Case 0.1959 nm.

TABLE XVI (Continued)

SYSTEM NO.	CONFIGURATION	COST $ x 10^3	PERFORMANCE (nm)	ANALYSIS	ADDITIONAL DATA
14	Decca-C2	54	0.8616	L.C.	This is also optimal value
15	DME-VOR-Doppler-C1	57	0.2505	O.T.	Limiting Case 0.1761 nm.
16	VOR-Decca-C2	58	0.3068	L.C.	
17	DME-Decca-C2	59	0.3360	L.C.	
18	Doppler-Decca-C1	62	0.3763	L.C.	
19	DME-VOR-Decca-C2	63	0.2827	O.T.	Limiting Case 0.2349 nm.
20	VOR-C3	64	0.2585	O.T.	Limiting Case 0.2499 nm.
21	DME-C3	65	0.3176	L.C.	
22	VOR-Doppler-Decca-C1	66	0.3377	O.T.	Limiting Case 0.2402 nm.
23	DME-Doppler-Decca-C1	67	0.2506	O.T.	Limiting Case 0.1941 nm.
24.	Doppler-C2	68	1.4679	L.C.	This is also optimal value
25	DME-VOR-C3	69	0.2265	O.T.	Limiting Case 0.1921 nm.

TABLE XVI (Continued

SYSTEM NO.	CONFIGURATION	COST $ x 10^3	PERFORMANCE (nm)	ANALYSIS	ADDITIONAL DATA
26	DME-VOR-Doppler-Decca C-1	71			
27	VOR-Doppler-C2	72			
28	DME-Doppler-C2	73			
29	Decca-C3	74			
30	DME-VOR-Doppler-C2	77			
31	VOR-Decca-C3	78			
32	DME-Decca-C3	79			
33	Doppler-Decca-C2	82			
34	DME-VOR-Decca-C3	83			
35	VOR-Doppler-Decca-C2	86			
36	DME-Doppler-Decca-C2	87			

in terminal uncertainity while having higher cost than the DME-Doppler-C1 system. For these reasons, only the DME-Doppler-C1 system will be examined further. The characteristics of this system are as follows.

Configuration: DME-Doppler-C1

Optimal Terminal Position Uncertainity: 0.2509 nm

Limiting Case Terminal Position Uncertainity: 0.1921 nm

System Cost: $53,000

This system could be an acceptable design if either the design specifications were relaxed or if a small increase in computer capacity (a change in computer budget not a change of machines) gave a terminal uncertainity less than or equal to 0.25 nm. To investigate the latter possibility, a trade off of Mean-Squared Terminal Position Uncertainity versus computer capacity (CC) was performed. This tradeoff (Figure 39) was generated by application of the Optimization Technique for DME-Doppler systems with CC = 120, 180, 240, and 360 (M/H). This curve shows that an increase of only 3 percent in CC is required.

To aid the designer in his selection of which of these two systems (VOR-DME-C3 and DME-Doppler-C1) he should investigate in more detail, additional data were generated for both systems. These data are the time histories of the optimal control and RMS position and velocity estimation errors. These curves are shown in Figures 40 and 41 for the VOR-DME-C3 systems and in Figures 42 and 43 for the DME-Doppler-C1 system.

6.3.2 Set of Minimal Systems

The set of Minimal Systems and their characteristics are given in Table XVII. To arrive at this list required the use of the Limiting Case Analysis 31 times; the application of the Optimization Technique to 12 systems, and the use of the Augmented System concept once. A summary of this analysis is shown in Table XVIII. An examination of this data shows, as discussed in Section 6.3.1, that if C1 is enlarged slightly the DME-Doppler-C1 system (System No. 13) and all the augmented versions of this system would satisfy the performance specifications. For this reason, a second set of Minimal Systems given in Table XIX, was generated. The two sets are referred to as Option A in which no enlargement of C1 is allowed and Option B in which such an enlargement is permitted.

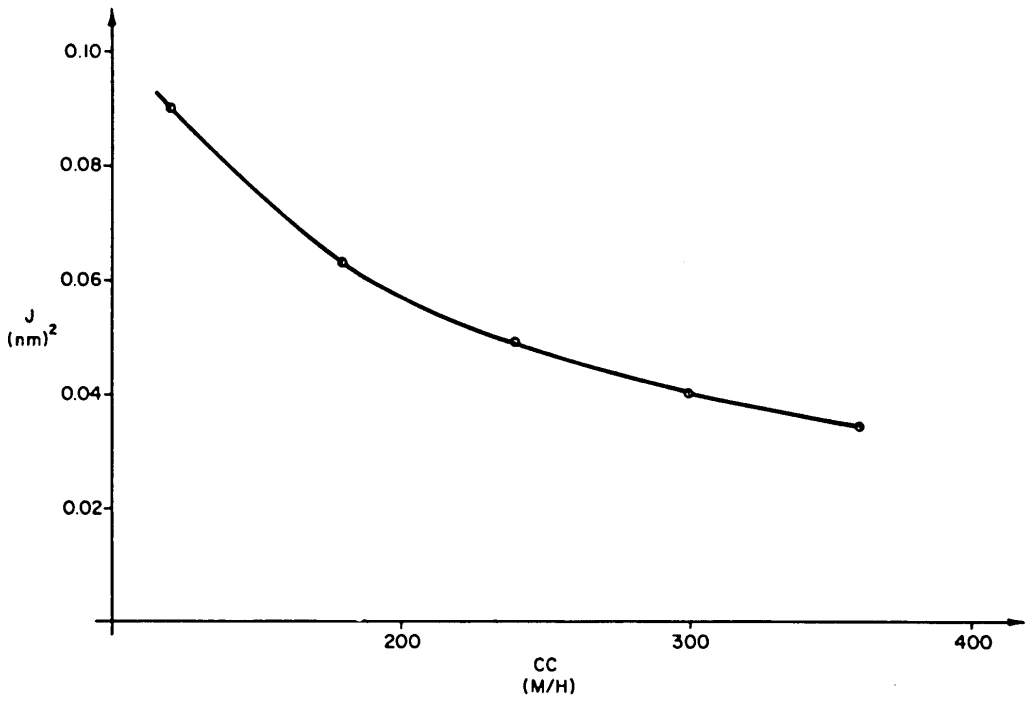


Figure 39.- Mean-squared terminal estimation error vs computer capacity for DME Doppler

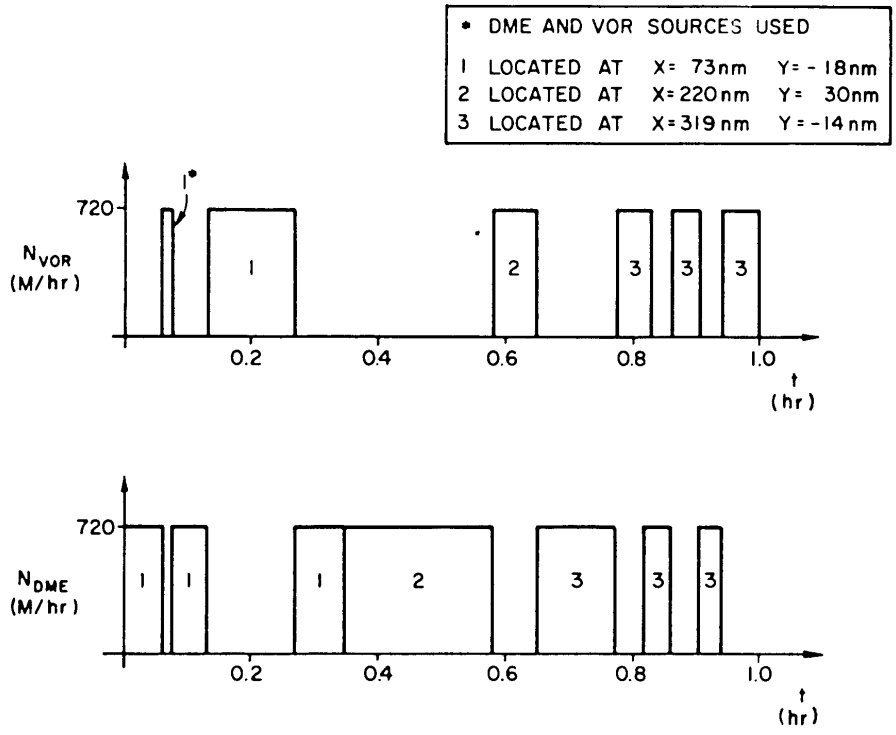


Figure 40.- Optimal control history for DME-VOR-C3 configuration

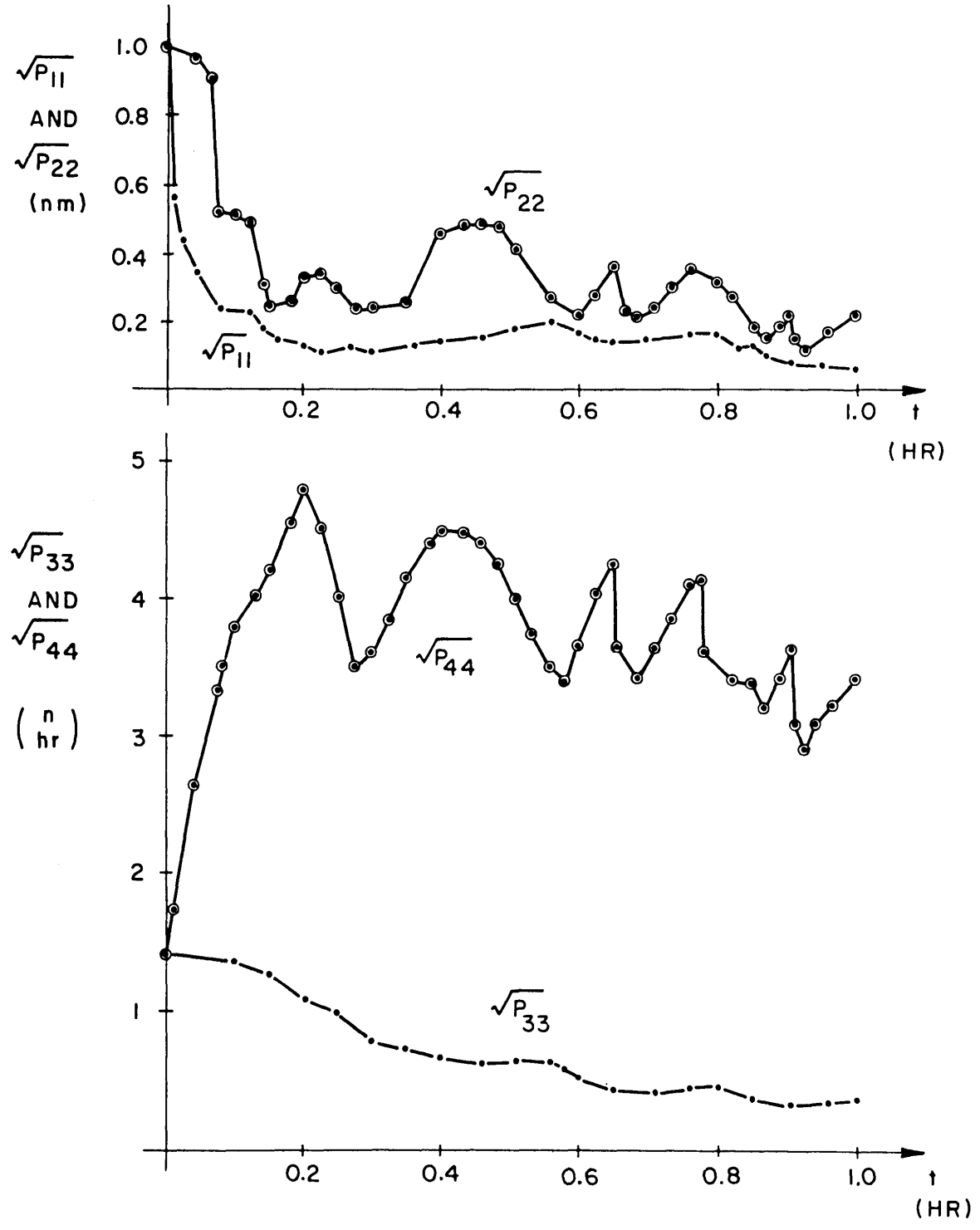


Figure 41.- RMS position and velocity estimation errors for VOR-DME-C3 system

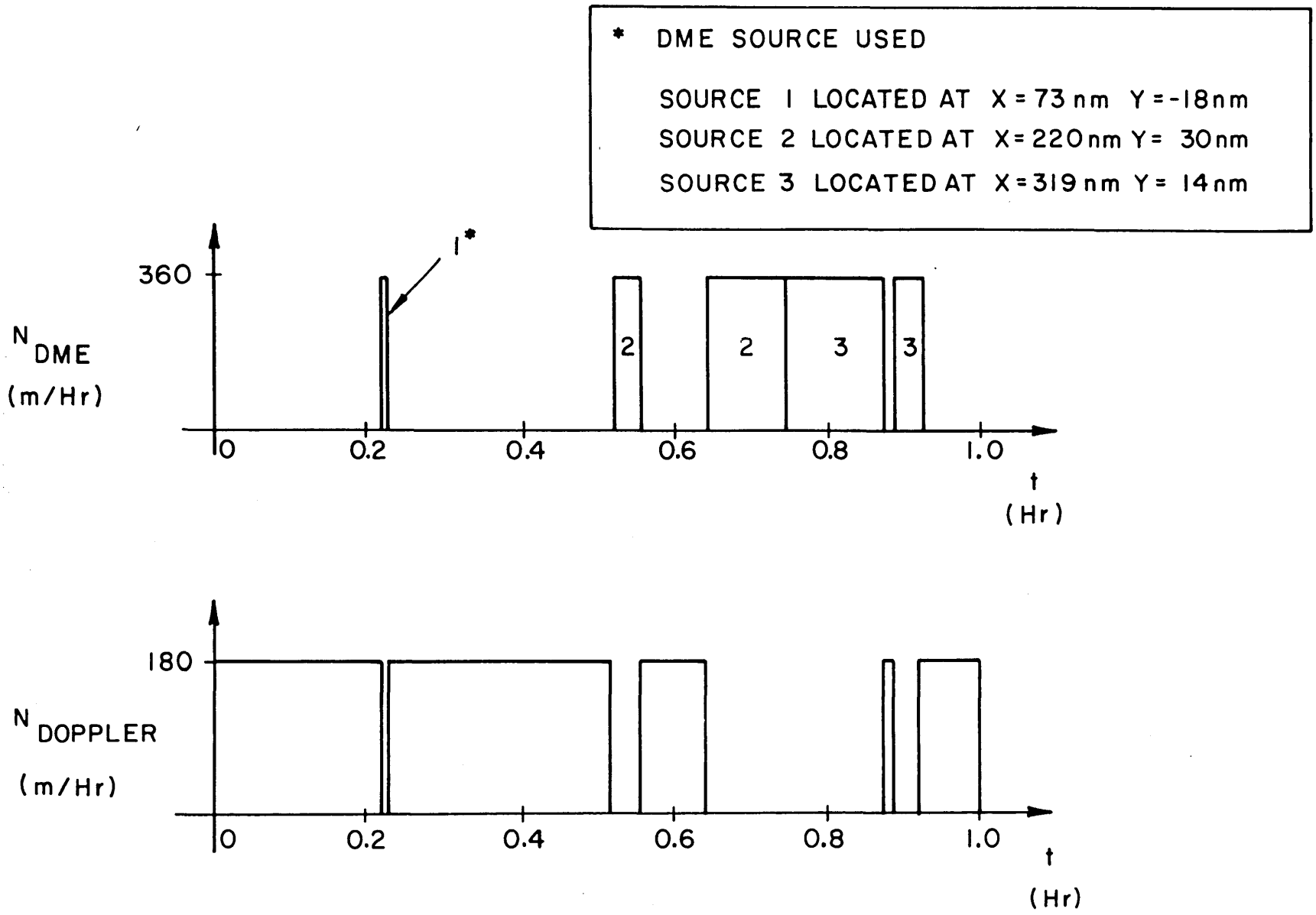


Figure 42.- Optimal control history for DME-Doppler-Cl configuration

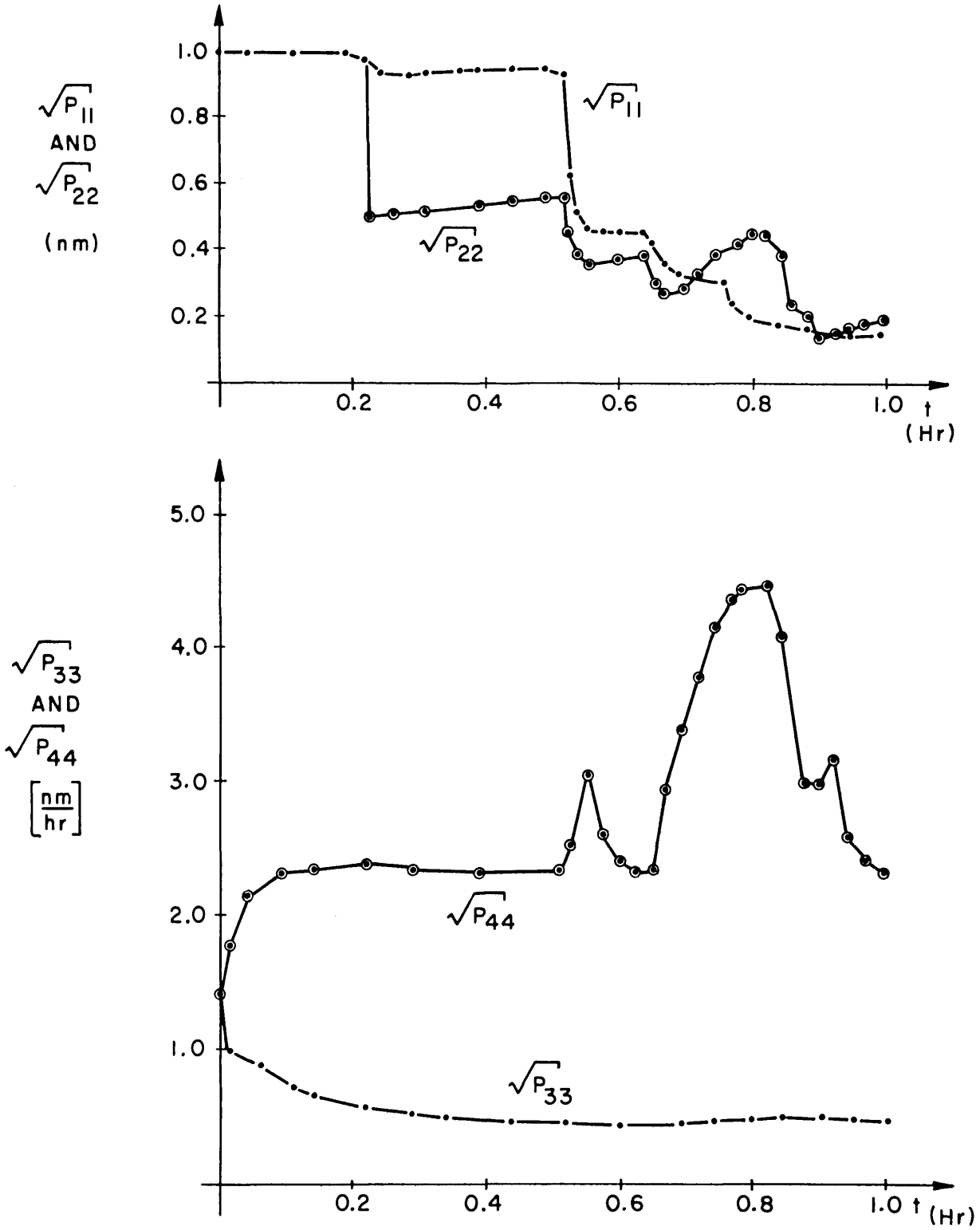


Figure 43.- RMS position and velocity estimation errors for DME-Doppler-Cl system

TABLE XVII

SET OF MINIMAL SYSTEMS (OPTION A)

CHAIN	MINIMAL SYSTEM	COST (DOLLARS X 10^3)	LIMITING CASE PERFORMANCE (nm)	OPTIMAL PERFORMANCE (nm)
VOR	VOR-DME-C3	69	0.1921	0.2265
DME	VOR-DME-C3	69	0.1921	0.2265
Doppler	VOR-Doppler-C2	72	0.1781	0.2467
Decca	VOR-DME-Decca-C3	83	0.1891	< 0.2265
C1	None	-	-	-
C2	VOR-Doppler-C2	72	0.1781	0.2467
C3	VOR-DME-C3	69	0.1921	0.2265

TABLE XVIII

ANALYSIS SUMMARY FOR SET OF MINIMAL SYSTEMS OPTION

SYSTEM NO.	CONFIGURATION	COST $ X 10^3	PERFORMANCE (nm)	ANALYSIS	ADDITIONAL DATA
1	VOR-C1	24	0.4153	L.C.	
2	DME-C1	25	0.4097	L.C.	
3	VOR-DME-C1	29	0.2980	L.C.	
4	Decca-C1	34	0.9308	L.C.	This is also optimal value
5	VOR-Decca-C1	38	0.3727	L.C.	
6	DME-Decca-C1	39	0.3204	L.C.	
7	DME-VOR-Decca-C1	43	0.2919	L.C.	
8	VOR-C2	44	0.3214	L.C.	
9	DME-C2	45	0.3610	L.C.	
10	Doppler-C1	48	1.5183	L.C.	This is also optimal value
11	DME-VOR-C2	49	0.2828	O.T.	Limiting Case 0.2405 nm
12	VOR-Doppler-C1	52	0.3405	O.T.	Limiting Case 0.2493 nm

TABLE XVIII (Continued)

SYSTEM NO.	CONFIGURATION	COST $ X 10^3	PERFORMANCE (nm)	ANALYSIS	ADDITIONAL DATA	
13	DME-Doppler-C1	53	0.2509	O.T.	Limiting Case 0.1959 nm	DME, Doppler and C1 Min. Syst. for Option B
14	Decca-C2	54	0.8616	L.C.	This is also optimal value	
15	DME-VOR-Doppler-C1	57	0.2505	O.T.	Limiting Case 0.1761	VOR Min. Syst. for Option B
16	VOR-Decca-C2	58	0.3068	L.C.		
17	DME-Decca-C2	59	0.3360	L.C.		
18	Decca-Doppler-C1	62	0.3763	L.C.		
19	DME-VOR-Decca-C2	63	0.2827	O.T.	Limiting Case 0.2349 nm	
20	VOR-C3	64	0.2585	O.T.	Limiting Case 0.2499 nm	
21	DME-C3	65	0.3176	L.C.		
22	VOR-Doppler-Decca-C1	66	0.3377	O.T.	Limiting Case 0.2402 nm	
23	DME-Doppler-Decca-C1	67	0.2506	O.T.	Limiting Case 0.1941 nm	Decca Min. Syst. for Option B

TABLE XVIII (Continued)

SYSTEM NO.	CONFIGURATION	COST $ X 10^3	PERFORMANCE (nm)	ANALYSIS	ADDITIONAL DATA	
24	Doppler-C2	68	1.4679	L.C.	This is also optimal value	
25	DME-VOR-C3	69	0.2265	O.T.	Limiting Case 0.1921 nm	VOR, DME, C3 Min. Syst. Syst. Option Option A C3 Min. Syst. for Option B
26	DME-VOR-Doppler-Decca-C1	71	0.2504	O.T.	Limiting Case 0.1750 nm	
27	VOR-Doppler-C2	72	0.2467	O.T.	Limiting Case 0.1781 nm	C2 Min. Syst. for Opt. A&B Doppler Min. for A
28	Decca-C3	74	0.6963	L.C.	This is also optimal value	
29	VOR-Decca-C3	78	0.2582	O.T.	Limiting Case 0.2409 nm	
30	DME-Decca-C3	79	0.2937	L.C.		
31	Doppler-Decca-C2	82	0.2688	L.C.		
32	DME-VOR-Decca-C3	83	< 0.2265	A.S.	Limiting Case o.1891 nm	Decca Min. Syst. for Option A

TABLE XIX

SET OF MINIMAL SYSTEMS (OPTION B)

CHAIN	MINIMAL	COST (DOLLARS X 10^3)	LIMITING CASE PERFORMANCE (nm)	OPTIMAL PERFORMANCE (nm)
VOR	VOR-DME-Doppler-C1	57	0.1761	0.2505
DME	DME-Doppler-C1	53	0.1959	0.2509
Doppler	DME-Doppler-C1	53	0.1959	0.2509
Decca	DME-Doppler-Decca-C1	67	0.1941	0.2506
C1	DME-Doppler-C1	53	0.1959	0.2509
C2	VOR-Doppler-C2	72	0.1781	0.2467
C3	VOR-DME-C3	69	0.1921	0.2265

From the lists of the minimal systems, the designer can easily identify the overall Minimal System. It is also possible to see the gains or penalties associated with demanding that a particular sensor or computer be used or rejected. For example, in Option B, a Decca sensor requirement gives a system cost of $14,000 higher than the DME-Doppler-C1 system, and a terminal RMS position uncertainity of 0.2506 nm, as compared to 0.2509 nm. It is evident that inclusion of Decca would be an inefficient choice. The inefficiency of Decca for this application is due to the fact that its information is limited to a small region early in the flight.

6.3.3 Satisfactory Systems

Of a total of 45 candidate systems identified at the start of the problem, 15 were found to be satisfactory. If the enlargement of the computer C1 is allowed, an additional four systems are satisfactory. A listing of the satisfactory systems ordered according to cost is given in Table XX. To derive this list required the following analyses:

Limiting Case Analysis - 34 systems

Optimization Technique - 14 systems

Augmented System Concept - 11 systems

A summary of the analysis is given in Table XXI. The data developed in the two provious Design Options are subsets of the information in Table XXI and can easily be developed. In addition, other useful results can be developed. If the designer decides to change the performance requirements, a glance at the information in Tables XX and XXI will furnish him with an idea of the impact of such changes on the system cost. It is also possible to use the data in Tables XX and XXI to develop a better understanding of the basic nature of the problem. An example of this can be seen regarding the utility of the DME and VOR sensors. For a given computer, say C2, the VOR-C2 combination is shown by a Limiting Case Analysis to be more efficient than the DME-C2. If a Doppler is added to both systems, the relative efficiencies of the augmented systems switch, and the DME-Doppler-C2 is more efficient than the VOR-Doppler-C2. This is due to the fact that the VOR gives better cross-track information than the DME, while the DME provides better along-track information. When only position information is used, the cross-track disturbances affect the DME generated information more than those from the VOR. The Doppler data take care of the cross-track disturbances, thus, letting the DME provide good along-track data. Another way of stating this effect is that the DME and the Doppler tend to complement each other better than the VOR and the Doppler.

TABLE XX

SATISFACTORY SYSTEMS

SYSTEM NO.	CONFIGURATION	COST $ X 10^3	PERFORMANCE (nm)	ANALYSIS	ADDITIONAL DATA
1	DME-Doppler-C1	53	0.2509*	O.T.	Limiting Case 0.1959 nm
2	DME-VOR-Doppler-C1	57	0.2505*	O.T.	Limiting Case 0.1761 nm
3	DME-Doppler-Decca-C1	67	0.2506*	O.T.	Limiting Case 0.1941 nm
4	DME-VOR-C3	69	0.2265	O.T.	Limiting Case 0.1921 nm
5	DME-VOR-Doppler-Decca-C1	71	0.2504*	O.T.	Limiting Case 0.1750 nm
6	VOR-Doppler-C2	72	0.2467	O.T.	Limiting Case 0.1781 nm
7	DME-Doppler-C2	73	0.1850	O.T.	Limiting Case 0.1419 nm
8	DME-VOR-Doppler-C2	77	< 0.1850	A.S.	
9	DME-VOR-C3 Decca	83	< 0.2265	A.S.	
10	VOR-Doppler-Decca-C2	86	< 0.2467	A.S.	

* These system satisfactory if C1 expanded.

TABLE XX (Continued)

SYSTEM NO.	CONFIGURATION	COST $ X 10^3	PERFORMANCE (nm)	ANALYSIS	ADDITIONAL DATA
11	DME-Doppler-Decca-C2	87	< 0.1850	A.S.	
12	DME-VOR-Doppler-Decca-C2	91	< 0.1850	A.S.	
13	VOR-Doppler-C3	92	< 0.2467	A.S.	
14	DME-Doppler-C3	93	< 0.1850	A.S.	
15	DME-VOR-Doppler-C3	97	< 0.1850	A.S.	
16	Doppler-Decca-C3	102	0.2474	O.T.	Limiting Case 0.1918 nm
17	VOR-Doppler-Decca-C3	106	< 0.2467	A.S.	
18	DME-Doppler-Decca-C3	107	< 0.1850	A.S.	
19	DME-VOR-Doppler Decca-C3	111	< 0.1850	A.S.	

TABLE XXI

SATISFACTORY SYSTEM DESIGN OPTION ANALYSIS SUMMARY

SYSTEM NO.	CONFIGURATION	COST $ X 10^3	PERFORMANCE (nm)	ANALYSIS	ADDITIONAL DATA
1	VOR-C1	24	0.4153	L.C.	
2	DME-C1	25	0.4097	L.C.	
3	VOR-DME-C1	29	0.2980	L.C.	
4	Decca-C1	34	0.9308	L.C.	This also optimum value
5	VOR-Decca-C1	38	0.3727	L.C.	
6	DME-Decca-C1	39	0.3204	L.C.	
7	DME-VOR-Decca-C1	43	0.2919	L.C.	
8	VOR-C2	44	0.3216	L.C.	
9	DME-C2	45	0.3610	L.C.	
10	Doppler-C1	48	1.5183	L.C.	This also optimum value
11	DME-VOR-C2	49	0.2828	O.T.	Limiting case 0.2405 nm
12	VOR-Doppler-C1	52	0.3405	O.T.	Limiting Case 0.2493 nm

TABLE XXI (Continued)

SYSTEM NO.	CONFIGURATION	COST $ X 10^3	PERFORMANCE (nm)	ANALYSIS	ADDITIONAL DATA
13	DME-Doppler-C1	53	0.2509	O.T.	Limiting case 0.1959 nm
14	Decca-C2	54	0.8616	L.C.	This also optimum value
15	DME-VOR-Doppler-C1	57	0.2505	O.T.	Limiting case 0.1761 nm
16	VOR-Decca-C2	58	0.3068	L.C.	
17	DME-Decca-C2	59	0.3360	L.C.	
18	Doppler-Decca-C1	62	0.3763	L.C.	
19	DME-VOR-Decca-C2	63	0.2827	O.T.	Limiting case 0.2349 nm
20	VOR-C3	64	0.2585	O.T.	Limiting case 0.2499 nm
21	DME-C3	65	0.3176	L.C.	
22	VOR-Doppler-Decca-C1	66	0.3377	O.T.	Limiting case 0.2402 nm
23	DME-Doppler-Decca-C1	67	0.2506	O.T.	Limiting case 0.1941 nm
24	Doppler-C2	68	1.467	L.C.	This also optimal value

TABLE XXI (Continued)

SYSTEM NO.	CONFIGURATION	COST $ X 10^3	PERFORMANCE (nm)	ANALYSIS	ADDITIONAL DATA
25	DME-VOR-C3	69	0.2265	O.T.	Limiting case 0.1921 nm
26	DME-VOR-Doppler-Decca-C1	71	0.2504	O.T.	Limiting case 0.1750 nm
27	VOR-Doppler-C2	72	0.2467	O.T.	Limiting case 0.1781
28	DME-Doppler-C2	73	0.1850	O.T.	Limiting case 0.1419
29	Decca-C3	74	0.6963	L.C.	This also optimal value
30	DME-VOR-Doppler-C2	77	< 0.1850	A.S.	
31	VOR-Decca-C3	78	0.2582	O.T.	Limiting case 0.2409 nm
32	DME-Decca-C3	79	0.2937	L.C.	
33	Doppler-Decca-C2	82	0.2688	L.C.	
34	DME-VOR-Decca-C3	83	< 0.2265	A.S.	
35	VOR-Doppler-Decca-C2	86	< 0.2467	A.S.	
36	DME-Doppler-Decca-C2	87	< 0.1850	A.S.	

TABLE XXI (Continued)

SYSTEM NO.	CONFIGURATION	COST $ X 10^3	PERFORMANCE (nm)	ANALYSIS	ADDITIONAL DATA
37	Doppler-C3	88	1.441	L.C.	This also optimal value
38	DME-VOR-Doppler-Decca-C2	91	< 0.1850	A.S.	
39	VOR-Doppler-C3	92	< 0.2467	A.S.	
40	DME-Doppler-C3	93	< 0.1850	A.S.	
41	DME-VOR-Doppler-Ce	97	< 0.1850	A.S.	
42	Doppler-Decca-C3	102	0.2474	O.T.	Limiting case 0.1918
43	VOR-Doppler-Decca-C3	106	< 0.2467	A.S.	
44	DME-Doppler-Decca-C3	107	< 0.1850	A.S.	
45	DME-VOR-Doppler-DECCA-C3	111	< 0.1850	A.S.	

The designer can request auxilliary data either at the start of the Design Procedure or after examination of the data presented in Tables XX and XXI.

6.4 SUMMARY

The purpose of this example was the demonstration of the utility and efficiency of the Design Procedure when applied to a realistic design problem. The efficiency of the Procedure can be seen when the total number of systems analyzed for each option is compared with the total number of candidate systems (45); e.g., the Minimal system required the analysis of only 25 systems. A second and more important indicator of efficiency is the small number of optimizations required. For example, of the 45 systems evaluated in the determination of the Satisfactory Systems, only 14 systems required the Optimization Technique.

The utility of the procedure was demonstrated by the variety of analyses and auxillery data that the designer can use in selection of the system of systems that will be analyzed in further detail.

Chapter 7

SUMMARY AND RECOMMENDATIONS

7.1 SUMMARY

The Design Procedure developed in this report represents the first application of automatic computation to the design of Multi-Sensor Navigation Systems. In the process of the formulation of the Design Procedure, several important decisions were required. After a general examination of the total design process, it was decided that the portion of the process which involves the iterative evaluation of systems was best suited for application of automatic computation techniques. Also, the system accuracy and cost were selected as the measures of system performance (other factors such as maintainability and reliability can be introduced by the system designer in his selection from the results of this Design Procedure). The important design parameters affecting navigation system accuracy and cost were identified and modeled mathematically. This work involved the technique of linearization of the nonlinear vehicle dynamics and measurements about a nominal trajectory to obtain linearized system dynamics, as well as measurement errors and geometric sensitivity of the navigation sensors. The model of the sensors includes sampling rate limiting which recognizes the fact that the rate at which the sensor can be sampled is limited by the physical availability of information or by computer sampling limitations. The onboard computer was also modeled. The computer's finite processing capability was modeled as an instantaneous constraint acting throughout the flight. The computer model also recognizes the different computer loadings of the various navigation measurements. These models are combined in a mathematical framework in which the measurements are processed using a Least-Squares Estimation routine.

Once the basic model of the navigation system was formulated, a technique was required to determine the accuracy limitation of any choice of navigation system configuration; i.e., any choice of a set of onboard sensors plus an onboard computer. A numerical optimization procedure was developed that iteratively adjusts the times at which the sensors are turned on and off. This procedure makes use of a formulation that models the measurement process in terms of continuous measurement rates. This formulation of the measurement process is useful in that it allows the sensors sampling rates and the computer processing constraints to assume their natural form. This greatly reduces the complexity involved in determining the optimal switching histories.

It was recognized early in the development of the Design Procedure that to be of genuine use to a designer it must be flexible (to allow the designer to tailor it to his application) and it must be efficient (to be able to perform the evaluation of a large number of candidate systems).

The desired flexibility was achieved by defining three design options and a set of auxiliary design data. Each design option provides the designer with a different list of systems. The first option determines the Minimal system; i.e., the system that satisfies the design accuracy requirements and has the lowest total cost. Defining a component chain as a list of all systems which contain the component, the second option determines the minimal system for each sensor and computer chain. The third option determines all those candidate systems that satisfy the system accuracy requirements. The auxiliary data includes the time histories of the estimation errors, the optimal measurement schedules and the corresponding sensor switching functions, and computer sensitivity data. By selecting among the design options and auxiliary data, the designer can tailor the Design Procedure to the application.

To permit efficient evaluation of the candidate systems, the Design Procedure contains three system evaluation techniques. One technique exercises the system using measurement schedules which minimize the system navigation uncertainty. To determine the optimal measurement schedules, a numerical optimization procedure was developed. This procedure uses first-order information generated by an application of the Maximum Principle to iterate on the times at which navigation sensors are sampled. The second evaluation technique exercises the system using non-optimal measurement schedules, which ignore the computer constraint, to determine the system's limiting performance. The third technique uses the fact that a system's performance is never degraded if the system is augmented by additional sensors or computer capacity. Application of the two non-optimal evaluation techniques often allows candidate systems to be eliminated or determined acceptable without the need of determining the optimal measurement schedule. To make efficient use of these three evaluation techniques, a different selection logic was generated for each of the design options. These sets of logic determine both the order in which the candidate systems are evaluated and also the order in which the evaluation techniques are applied to each system.

In order to demonstrate both the efficiency of the Procedure in terms of reduced analysis requirements and the utility of the design data generated, the Design Procedure was applied to the design of an aircraft navigation system.

7.2 RECOMMENDATIONS

To increase the general utility of the Design procedure, research is recommended directed toward improving the efficiency and flexibility of the Design Procedure and toward broadening the class of navigation systems to which the procedure applies.

7.2.1 Procedure Efficiency and Flexibility

The major measure of the efficiency of the Design Procedure is the time required to determine the outputs of the design options and auxiliary data. The portion of the Design Procedure that uses the most time is the Optimization Technique. Two methods exist for reducing the time required to arrive at an optimal measurement schedule. An obvious method for reducing the time to generate an optimization is to run the program on a faster computer. For example, if an IBM 360 were used instead of the SDS 9300, it is estimated the time to perform an optimization could be reduced by a factor of four. A second method which gives a reduced optimization time is the application of hybrid computational techniques (refs. 27, 28) to the problem. A properly used hybrid computer takes advantage of the strong points of both the analog and digital computation processes. The analog computer is very efficient at integrating differential equations and carrying out parallel operations. The digital computer provides very accurate calculation. For the present problem, the same general optimization procedure would be recommended as presented in Chapter 4. This involves iteration on only a few switchpoints at a time. The integration of the covariance equation, however, would be done rapidly on the analog computer. This would greatly reduce the time required to perform one iteration, since this iteration, when done digitally, uses about two-thirds of the time required to perform one iteration. The lower accuracy of the analog integration as compared with that performed on the digital computer is not a problem for at least the initial iterations. The time history of the covariance matrix is sampled and transmitted to the digital machine for storage. The backward integration of the costate equation, the calculation of the switching curves, and the application of the optimal switching logic are done in the digital computer, due to the large dynamic range and required accuracy. If, at some point, the analog integration were not accurate enough, the process could be then switched over to full digital solution for the final few iterations. The time savings resulting from the use of such a hybrid procedure could be substantial.

Increasing the flexibility of the Design Procedure would require new design options and auxiliary design data. The generation of these options and data would most naturally occur as the result of applying the Design Procedure to actual system designs. Another avenue of investigation that could lead to increased flexibility of the Design Procedure is the study of the interaction of the designer and the Design Procedure. In its present form, the designer inputs data to the Design Procedure and reviews the data at the completion of the Design Procedure. It would be useful if the designer could view internal or intermediate results and be able to modify the problem that the Design Procedure is doing. Examples of these modifications might be the addition or deletion of a candidate component, a request for additional auxiliary data, or a change in the desired output. If this were possible and if the time required to apply the procedure was small enough (on the order of several hours), then automatic computation applied to navigation system design would have started to realize its full potential as a design tool.

7.2.2 Related Applications

The final area in which further investigation is recommended is the extension of the techniques developed in this work so that the Design Procedure can be applied to a larger class of applications.

The model of the navigation system used in this work did not contain costs associated with taking measurements or constraints on the estimation error times $0 \leq t < T$. To apply the Design Procedure to applications which have one or both of these features would require only a modification of the optimization procedure presented in Chapter 4. Consider first applications which have measurement costs. Some work for simple cases of this problem have appeared in the Literature (refs. 25, 26). An example would be a space vehicle where measurements require the use of attitude fuel to either reorient or stabilize the vehicle. Because of the limited on-board attitude fuel, the minimum number of measurements must be used. There is still a requirement on the terminal uncertainty, but now it is in the form of an inequality constraint. The optimization problem is now the minimization of J where:

$$J = \int_0^T \sum_{i=i}^{m} K_i N_i \, dt$$

Subject to

$$\mathrm{tr}\left[AP(T)\right] \leq \hat{P}$$

An optimization procedure required to solve this problem is more complicated than that given in Chapter 4 for two reasons. First, the existence of optimal singular measurement sampling rates; i.e., sampling histories which do not use all the computer capacity, must be considered. Although techniques (ref. 10) exist that determine these singular controls, the logic required is complex. The second complication arises due to the fact that the terminal condition is a constraint rather than part of the cost function. Therefore, there is no specified terminal value of Λ, the costate matrix. An iterative loop must be added which determines the value of $\Lambda(T)$ which gives $tr[AP(T)] = \hat{P}$.

A second extension of the problem is the inclusion of internal constraints on the estimation errors. These constraints could be at a finite number of discrete points along the trajectory or for continuous segments of the trajectory. In the case of constraints imposed at discrete points in the flight, one method of solution would be to determine the optimal measurement schedule between two way-points using the technique of Chapter 4. Although this would not necessarily give the optimal total flight measurement schedule, it would be a close approximation. If the optimal were required or if continuous constraints were imposed, then a new optimization procedure would be required. Although work has been done on this type problem (ref. 6), the development of such an optimization procedure would require original research in both the theoretical and numerical aspects of the problem.

APPENDIX A

THEORMS RELATING TO THE SWITCHING FUNCTIONS AND THE COVARIANCE PROPAGATION

Theorm 1: The diagonal elements of a positive semidefinite matrix are all greater than or equal to zero (ref. 22).

Theorm 2: For A an nxn positive semidefinite matrix ($\underline{x}\ A\ \underline{x}^T \geq 0$ for all $\underline{x}$) and M an mxn matrix the matrix B given by:

$$B = M\ A\ M^T \tag{A.1}$$

is positive semidefinite.

Proof: Forming a quadratic form for B using the 1xm vector $\underline{y}$

$$\underline{y}\ B\ \underline{y}^T = \underline{y}\ M\ A\ M^T y^T \tag{A.2}$$

Define $\underline{a} = \underline{y}M$ then

$$\underline{y}\ B\ \underline{y}^T = \underline{a}\ A\ \underline{a}^T \geq 0 \tag{A.3}$$

Q.E.D.

Theorm 3: If $\Lambda(T)$ is positive semidefinite, then

$$SW_{ii} = \left(-R^{-1}HP\Lambda PH^T\right)_{ii} \leq 0 \qquad i=1,\ldots m$$

Proof: For R a diagonal matrix with all positive diagonal elements only the matrix $-HP\Lambda PH^T$ need be considered. Given $\Lambda(T)$ positive semidefinite, the terminal value of the matrix Z

$$Z\ (T) = P(T)\Lambda(T)P(T) \tag{A.4}$$

is positive semidefinite by Theorm 2

Z(T) satisfies

$$\dot{Z} = \left(F + P^{-1}Q)\right)Z + Z\left(F^T + QP^{-1}\right) \tag{A.5}$$

or

$$Z(t) = \phi(t,T)\ Z(T)\ \phi^T\ (t,T) \tag{A.6}$$

where $\phi(t,T)$ satisfies

$$\dot{\phi} = \left(F + P^{-1}Q\right)\phi \text{ with } \phi\ (T,T) = I \tag{A.7}$$

Applying Theorm 2 to Eq. (A.6) indicates $Z(t)$ is positive semidefinite.
A final application of Theorm 2 to HZH^T gives $-SW = R^{-1}\ HP\Lambda PH^T$ as positive semidefinite. Applying Theorm 1 to -SW gives

$$-(SW)_{ii} \geq 0 \qquad i = 1,\ldots,m \tag{A.8}$$

or

$$SW_{ii} \leq 0 \qquad i = 1,\ldots,m$$

Q.E.D.

Theorm 4: For the estimation error covariance matrix $P(t)$ which satisfies

$$\dot{P} = FP+PF^T - PH^TNR^{-1}HP + Q \tag{A.9}$$

with $P(t_o) = P_o$ and performance index $J = tr[A\ P(T)]$, the following is true. For A a positive semidefinite matrix and $\delta P_o = 0$ then $\delta N \geq 0$ implies $\delta J \leq 0$.

Proof: Taking the first variation of Eq. (A.9) assuming no variation in F, H, R or Q

$$\dot{\delta P} = \left(F - PH^TNR^{-1}H\right) + \delta P\left(F^T - H^TNR^{-1}HP\right) \tag{A.10}$$

$$- PH^T\ \delta NR^{-1}HP$$

Defining the projected variation in the covariance matrix $\overline{\delta P} = \phi(t,T)\ \delta P(t)\phi^T(t,T)$ an expression for the value of $\delta P(T)$ is derived in Appendix F as

$$\delta P(T) = -\int_0^T \phi P H^T \delta N R^{-1} H P \phi^T dt \qquad (A.11)$$

The variation in J is given by

$$\delta J = tr\left[A \delta P(T)\right] \qquad (A.12)$$

Using the property of the trace operator and the diagonal nature of δN, and R, δJ can be written

$$\delta J = -\int_0^T \sum_{i=1}^{m} R_{ii}^{-1} \left(H P \phi^T A \phi P H^T\right)_{ii} \delta N_{ii} \, dt \qquad (A.13)$$

For A positive semidefinite, repeated applications of Theorm 2 gives $HP\phi^T A \phi P H^T$ positive semidefinite. Using the fact that $R_{ii} > 0$ and $\delta N_{ii} \geq 0$ and Theorem 1, each element in the summation in Eq. (A.13) is greater than or equal to zero. Therefore, $\delta J \leq 0$.

Q.E.D.

APPENDIX B

NAVIGATION IN A BENIGN ENVIRONMENT

An interesting special case of the scheduling of navigation measurements is navigation in a benign environment; that is when there is no external driving noise on the system. This problem arises in the navigation of a vehicle in free space when the disturbing effects of solar pressure, gravitational perturbations, or for near earth trajectories, aerodynamic drag are small enough to be ignored.

In addition to being physically meaningful, this special case has several interesting mathematical properties. For $Q = 0$, Eq. (4.2) governing the propagation of the estimation error covariance matrix, $P(t)$, simplifies to

$$\dot{P} = FP + PF^T - PH^T NR^{-1} HP \tag{B.1}$$

This equation is still a non-linear differential equation, but it is now possible to derive an equivalent linear differential equation in the matrix S where $S = P^{-1}$. Since P is a measure of the uncertainty in the estimation of state variables, S corresponds to the knowledge of the state variables. Using this transformation in Eq. (B.1), it can be shown that

$$\dot{S} = - F^T S - SF + H^T NR^{-1} H \tag{B.2}$$

For this equation, the information rate $\dot{I} = H^T NR^{-1} H$ acts as a driving function which tends to increase the knowledge of the state. Also for a stable dynamic system where F has negative characteristic roots, the natural mode of the system is to diverge toward infinite knowledge (the uncertainties decay toward zero).

The necessary condition for optimal $N(t)$ can be determined as in Section 4.2.2 (Necessary Conditions, by applying the Maximum Principle to the system Hamiltonian. In terms of S and its costate matrix ϕ, $\mathscr{H}$ is

$$\mathscr{H} = \mathrm{tr}\left\{\psi\left[-F^T S - SF + H^T NR^{-1} H\right]\right\}$$

or

$$\mathscr{H} = \mathrm{tr}\left\{\left(R^{-1} H\psi H^T\right)N - \psi\left(F^T S + SF\right)\right\} \tag{B.3}$$

The costate ψ must satisfy

$$\dot{\psi} = F\psi + \psi F^T \tag{B.4}$$

Both Eqs. (B.2) and (B.4) look familiar. In fact, if the equations for the switching function and the special costate presented in Section 4.2.2, are simplified by setting $Q = 0$, it is seen that $Z(t) = \psi(t)$. Therefore, the special costate defined in the formulation of the problem in terms of the uncertainty in the estimates of the state is the natural costate for the problem formulated in terms of $S(t)$. This is true even if $Q \neq 0$, but in this case the propagation of S is also governed by the nonlinear differential equation.

One final point of interest that is true only if $Q = 0$ is that the costate matrix Z is influenced by the value of the state variables P only through the boundary condition $Z(T) = P(T)\Lambda(T)P(T)$. This, combined with the linear nature of Eq. (B.4), indicates that the shape of Z is fixed with different $P(T)$ just providing scaling.

APPENDIX C

CHARACTERISTICS OF DIGITAL PROGRAM

The iterative optimization procedure of Chapter 4 was programmed on a Scientific Data System 9300 digital computer. The characteristics of the SDS 9300 are given in Table (C.1). Because of the short word length, the computer is hard wired so that double precision operations and storage are used automatically throughout the program. With this arrangement, the computations had eleven dicimal digits of accuracy, but only 16 K words of memory. The program was written in *FORTAN IV*. It required a deck of approximately 1000 cards and 10 K words of storage. In addition some 16 K words of memory were required for variable storage, most of which was required to store the time history of the 4 x 4 covariance matrix P.

The number of iterations required to find an optimal measurement schedule requires approximately 2 to 4 times the number of switch times in the optimal measurement history. Each iteration requires 300-400 times steps to integrate from t = 0 to t = 1 hr. and this takes 4 to 5 minutes in real-time.

TABLE (C-1)

Double Precision Characteristics of SDS 9300 Digital Computer

Wordlength	48 bits
Add Time	5.25 μsec.
Multiply Time	8.75 μsec.
Cycle Time	1.75 μsec.
Memory	16,000 words

APPENDIX D

MODEL OF ENVIRONMENTAL DISTURBANCES

For the geometry shown in Figure D-1 with nominal velocity V along the x axis, the effects of gust velocities δV_x and δV_y are to produce accelerations along x and y axes. For small δV_x and δV_y the resulting accelerations are developed in the following sections.

D.1 LONGITUDINAL ACCELERATION PERTURBATION

The nominal longitudinal acceleration is

$$a_x = \frac{F_x}{m} = \frac{T - \frac{1}{2}\rho V^2 C_D A}{m} \qquad (D.1)$$

where ρ = air density (slugs/ft^3)

V = nominal velocity (ft/sec.)

C_D = drag coefficient (non dimensional)

A = characteristic area (ft.^{2})

m = mass of vehicle (slugs)

T = thrust (lbs.)

Assuming no variation in thrust due to the gust velocity δV_x, the first order longitudinal perturbation acceleration δa_x is

$$\delta a_x = \frac{\rho V C_D A}{m} \delta V_x$$

or

$$\delta a_x = \frac{2D}{Vm} \delta V_x \qquad (D.2)$$

Assuming δV_x is a zero mean random variable with mean squared value $\sigma^2 \delta V_x$, the mean squared longitudinal acceleration is

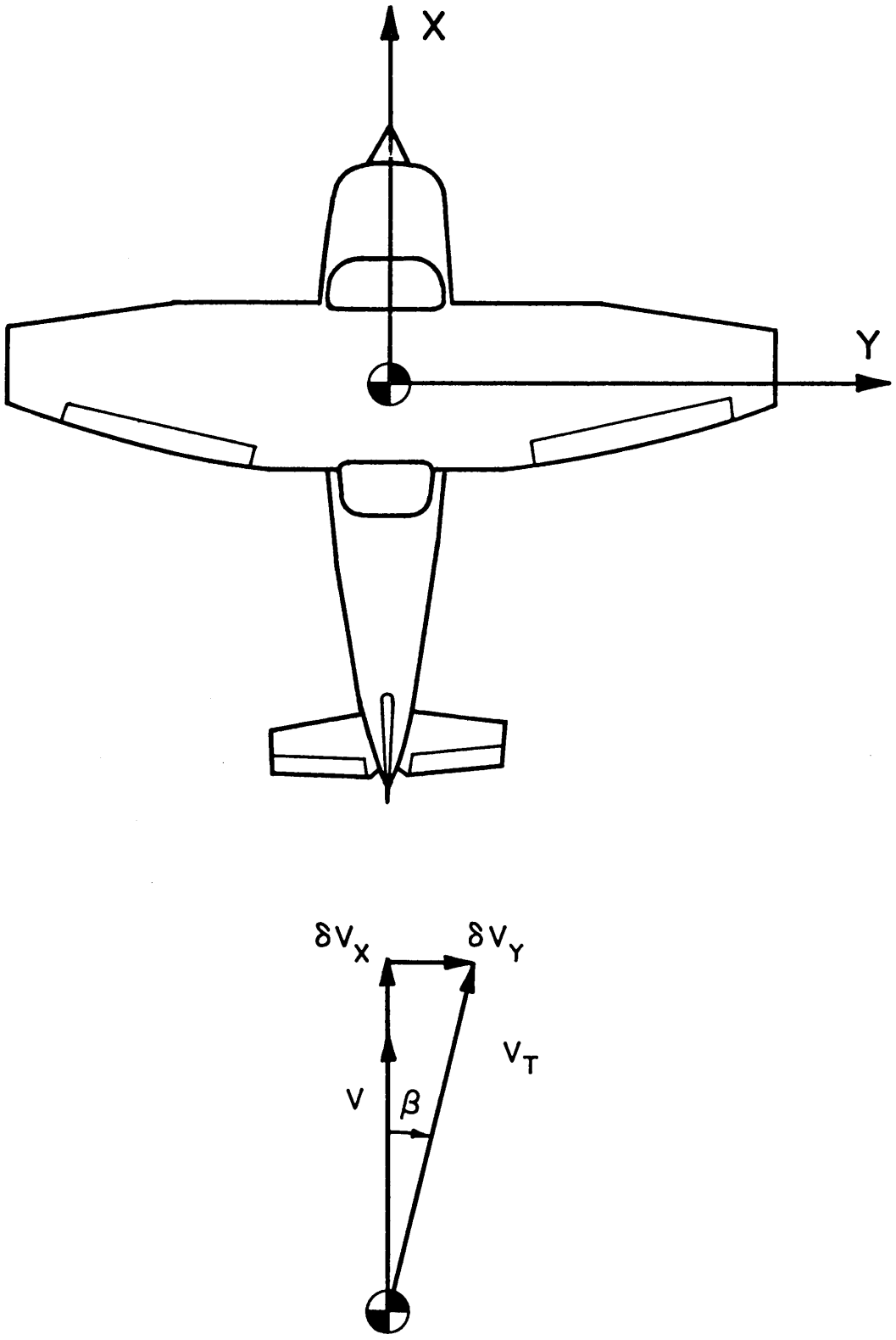


Figure D-1.- Vehicle geometry

$$\sigma_{\delta a_x}^2 = \frac{4D^2}{V^2 m^2} \sigma_{\delta V_x}^2 \qquad (D.3)$$

D.2 LATERAL ACCELERATION PERTURBATION

The nominal lateral acceleration is

$$a_y = \frac{F_y}{m} = \frac{\frac{1}{2} \rho V^2 C_y A_S}{m} \qquad (D.4)$$

where C_y = side force coefficient

A_S = aide plan form area (ft.^{2})

The perturbation side acceleration due to a side gust δV_y is

$$\delta a_y = \cancel{\frac{\rho V C_y A}{m}}^{\,0} \delta V_y + \frac{\frac{1}{2}\rho V^2 A_S}{m} \frac{\partial C_y}{\partial \beta} \beta$$

where β = side slip angle

The first term is equal to zero because the nominal value of $C_y = 0$; i.e., the vehicle is trimmed to have zero side force. Therefore, assuming β small so that $\sin\beta \simeq \beta$ this can be written in terms of the side gust δV_y as

$$\delta a_y = \frac{\frac{1}{2}\rho V A_S}{m} C_{y\beta} \delta V_y \qquad (D.5)$$

where

$$C_{y\beta} = \frac{\partial C_y}{\partial \beta}$$

For δV_y a zero mean random variable with mean squared value $\sigma_{\delta a_y}^2$ the mean squared lateral acceleration $\sigma_{\delta a_y}^2$ is

$$\sigma^2_{\delta a_y} = \left[\frac{\frac{1}{2}\rho V A_S}{m} C_{y\beta} \right]^2 \sigma^2_{\delta V_y} \tag{D.6}$$

D.3 EQUIVALENT WHITE NOISE ACCELERATION PERTURBATION

The white noise power spectral density of the longitudinal (Q_{33}) and the lateral (Q_{44}) gust generated accelerations can be written (ref. 6)

$$Q_{33} = 2\, \sigma^2_{\delta a_x}\, \tau_x \tag{D.7}$$

and

$$Q_{44} = 2\, \sigma^2_{\delta a_y}\, \tau_y \tag{D.8}$$

where τ_x and τ_y are the characteristic times for the x and y gusts. Assuming the gust field is isotropic, then

$$\sigma^2_{\delta V_x} = \sigma^2_{\delta V_y} = \sigma^2_V \tag{D.9}$$

and

$$\tau_x = \tau_y = \tau \tag{D.10}$$

and finally

$$Q_{33} = \frac{2D^2}{V^2 m^2}\, \tau \sigma^2_V \tag{D.11}$$

$$Q_{44} = \frac{1}{8} \left[\frac{\rho V A_S}{m} C_{y\beta} \right]^2 \tau \sigma^2_V \tag{D.12}$$

APPENDIX E

MEASUREMENT SENSITIVITY

The quantity measured and the first variation of this quantity for the DME, VOR, Doppler Radar and Decca Navigation Aids are listed below. Z corresponds to the total measurement which is a function of X and Y. z corresponds to the perturbation in the measurement Z which is a function of δx and δ_y,

E.1 DME SENSOR

Referring to Figure E-1,

$$Z_{DME} = D = \sqrt{(x-x_S)^2 + (y-y_S)^2}$$

$$z_{DME} = \left[\frac{x-x_S}{D}\right]_{nom} \delta x + \left[\frac{y-y_S}{D}\right]_{nom} \delta y$$

E.2 VOR SENSOR

$$Z_{VOR} = \theta = \tan^{-1}\left[\frac{y-y_S}{x-x_S}\right]$$

$$z_{VOR} = \left[\frac{y-y_S}{D^2}\right]_{nom} \delta x + \left[\frac{x-x_S}{D^2}\right]_{nom} \delta y$$

E.3 DOPPLER RADAR

Referring to Figure (E-2), the measurement and geometric sensitivity for each of the two beams is given by

$$Z_{Doppler} = V_A = \left[V_x \cos\phi - V_y \cos(90-\phi)\right] \cos\beta$$

$$z_{Doppler} = \left[\cos\beta\cos\phi\right]_{nom} \delta V_x - \left[\cos\beta\cos(90-\phi)\right] \delta V_y$$

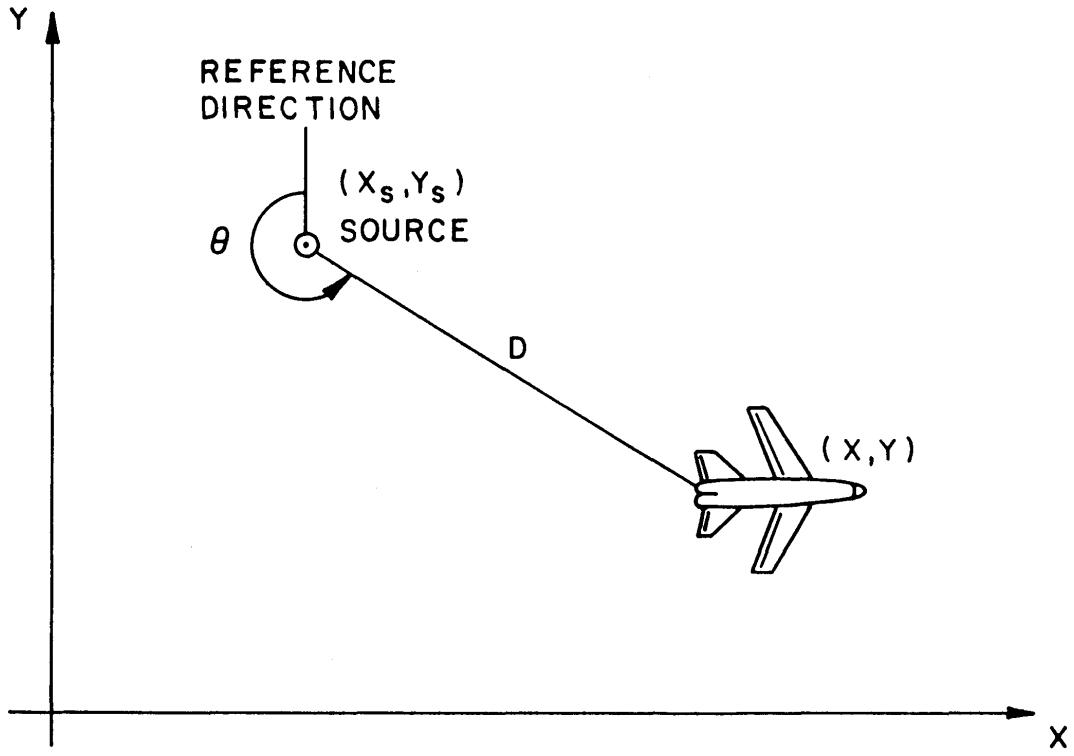


Figure E-1.- Geometry for VOR and DME navigation aids

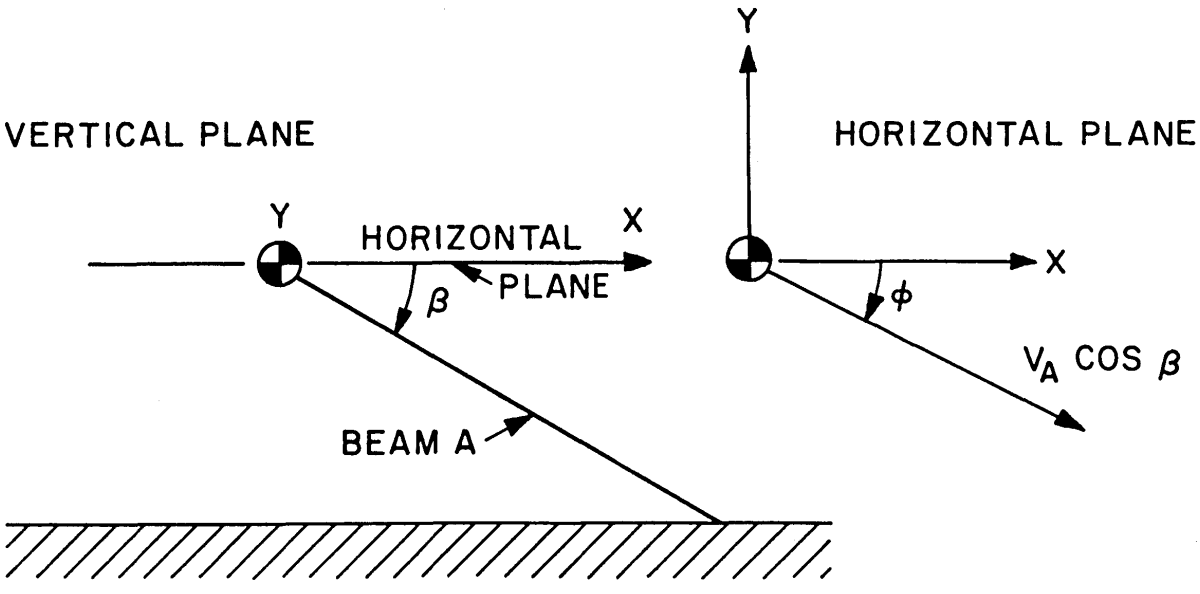


Figure E-2.- Doppler radar geometry

E.4 DECCA SENSOR

Referring to Figure E-3 the measurement and geometric sensitivity for one pair of Decca baselines is given by

$$z_{Decca} = \sqrt{(x-x_2)^2 + (y-y_2)^2} - \sqrt{(x-x_1)^2 + (y-y_1)^2}$$

$$z_{Decca} = \left[\frac{(x-x_2)}{D_2} - \frac{(x-x_1)}{D_1}\right]\delta x + \left[\frac{(y-y_2)}{D_2} - \frac{(y-y_1)}{D_1}\right]\delta y$$

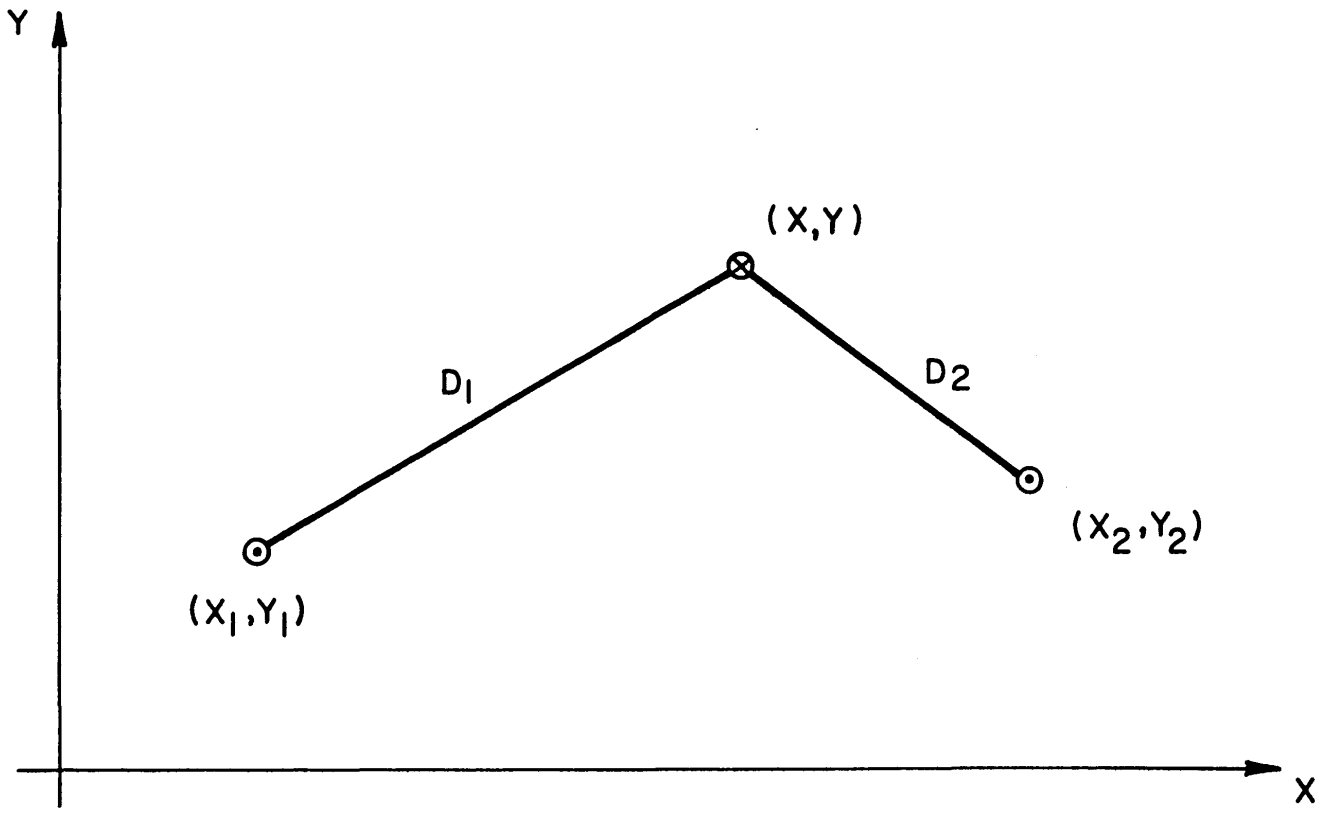


Figure E-3.- Decca geometry

APPENDIX F

PERFORMANCE INDEX SENSITIVITY FOR VARIATIONS IN CONTROL HISTORY

The equation satisfied by the estimation error covariance matrix $P(t)$ is

$$\dot{P} = FP + PF^T - PH^T NR^{-1}HP + Q \tag{F.1}$$

with $P(o) = P_o$

Taking the first variation of Eq. (F.1) considering F, H, R and Q fixed gives

$$\dot{\delta P} = F\delta P + \delta PF^T - PH^T NR^{-1}H\delta P - \delta PH^T NR^{-1}HP$$

$$- PH^T \delta NR^{-1}HP$$

or

$$\dot{\delta P} = \left(F - PH^T NR^{-1}H\right)\delta P + \delta P\left(F^T - H^T NR^{-1}HP\right)$$

$$-PH^T \delta NR^{-1}HP \tag{F.2}$$

Define the projected variation in the covariance matrix $\overline{\delta P}$ as

$$\overline{\delta P} = \phi \delta P \phi^T \tag{F.3}$$

where ϕ is the transition matrix defined by

$$\dot{\phi} = -\tilde{F}\phi \tag{F.4}$$

with $\phi(T,T) = I$ and $\tilde{F} = F - PH^T NR^{-1}H$

Using Eqs. (F.2, F.3, and F.4) the differential equation $\overline{\delta P}$ satisfies is

$$\dot{\overline{\delta P}} = -\phi PH^T \delta NR^{-1}HP\ \phi^T \tag{F.5}$$

with $\overline{\delta P}(o) = \phi(o,T)\delta P_o\ \phi^T(o,T)$. Separating variables and integrating from t=o to t=T gives

$$\delta P(T) = \overline{\delta P(T)} = \overline{\delta P_o} - \int_o^T \phi P H^T \delta N R^{-1} H P \phi^T \, dt \qquad (F.6)$$

Using the fact that $\delta P_o = 0$, the change in the system performance index is

$$\delta J = tr\left[A\delta P(T)\right] = - tr\left[A \int_o^T \phi P H^T \delta N R^{-1} H P \phi^T \, dt\right]$$

For A a constant matrix and using the property of the trance operation

$$\delta J = - tr\left[\int_o^T R^{-1} H P \phi^T A \phi P H^T \delta N \, dt\right] \qquad (F.7)$$

Using the diagonal nature of δN this can be written in summation form as

$$\delta J = - \int_o^T \sum_{i=1}^{m} \left(R^{-1} H P \phi^T A \phi P H^T\right)_{ii} \delta N_{ii} \, dt \qquad (F.8)$$

APPENDIX G

DESIGN PROCEDURE SYSTEM LISTING AND ANALYSIS SUMMARY

A list of the 45 candidate systems ordered according to cost is given in Table G.1. Also included in this table are the results of the analyses. The type of analysis used is indicated by the abbreviations L.C. - Limiting Case, O.T. - Optimization Technique and A.S. - Augmented System. When the Augmented System concept is used, the performance is only an upper bound. This is indicated by the use of the less than inquality sign (<).

TABLE G.1

DESIGN PROCEDURE SYSTEM LISTING AND ANALYSIS SUMMARY

SYSTEM NO.	CONFIGURATION	COST $ X 10^3	PERFORMANCE (nm)	ANALYSIS	ADDITIONAL DATA
1	VOR-C1	24	0.4153	L.C.	
2	DME-C1	25	0.4097	L.C.	
3	VOR-DME-C1	29	0.2980	L.C.	
4	Decca-C1	34	0.9308	L.C.	This also optimum value
5	VOR-Decca-C1	38	0.3727	L.C.	
6	DME-Decca-C1	39	0.3204	L.C.	
7	DME-VOR-Decca-C1	43	0.2919	L.C.	
8	VOR-C2	44	0.3216	L.C.	
9	DME-C2	45	0.3610	L.C.	
10	Doppler-C1	48	1.5183	L.C.	This also optimum value
11	DME-VOR-C2	49	0.2828	O.T.	Limiting case 0.2405 nm
12	VOR-Doppler-C1	52	0.3405	O.T.	Limiting case 0.2493 nm

TABLE G.1 (Continued)

SYSTEM NO.	CONFIGURATION	COST $ X 10^3	PERFORMANCE (nm)	ANALYSIS	ADDITIONAL DATA
13	DME-Doppler-C1	53	0.2509	O.T.	Limiting case 0.1959 nm
14	Decca-C2	54	0.8616	L.C.	This also optimum value
15	DME-VOR-Doppler-C1	57	0.2505	O.T.	Limiting case 0.1761 nm
16	VOR-Decca-C2	58	0.3068	L.C.	
17	DME-Decca-C2	59	0.3360	L.C.	
18	Doppler-Decca-C1	62	0.3763	L.C.	
19	DME-VOR-Decca-C2	63	0.2827	O.T.	Limiting case 0.2349 nm
20	VOR-C3	64	0.2585	O.T.	Limiting case 0.2499 nm
21	DME-C3	65	0.3176	L.C.	
22	VOR-Doppler-Decca-C1	66	0.3377	O.T.	Limiting case 0.2402 nm
23	DEM-Doppler-Decca-C1	67	0.2506	O.T.	Limiting case 0.1941 nm
24	Doppler-C2	68	1.467	L.C.	This also optimal value

TABLE G.1 (Continued)

SYSTEM NO.	CONFIGURATION	COST $ X 10^3	PERFORMANCE (nm)	ANALYSIS	ADDITIONAL DATA
25	DME-VOR-C3	69	0.2265	O.T.	Limiting case 0.1921 nm
26	DME-VOR-Doppler-Decca-C1	71	0.2504	O.T.	Limiting case 0.1750
27	VOR-Doppler-C2	72	0.2467	O.T.	Limiting case 0.1781 nm
28	DME-Doppler-C2	73	0.1850	O.T.	Limiting Case 0.1419
29	Decca-C3	74	0.6963	L.C.	This also optimal value
30	DME-VOR-Doppler-C2	77	< 0.1850	A.S.	
31	VOR-Decca-C3	78	0.2582	O.T.	Limiting case 0.2409 nm
32	DME-Decca-C3	79	0.2937	L.C.	
33	Doppler-Decca-C2	82	0.2688	L.C.	
34	DME-VOR-Decca-C3	83	< 0.2265	A.S.	
35	VOR-Doppler-Decca-C2	86	< 0.2467	A.S.	
36	DME-Doppler-Decca-C2	87	< 0.1850	A.S.	
37	Doppler-C3	88	1.441	L.C.	This also optimal value

TABLE G.1 (Continued)

SYSTEM NO.	CONFIGURATION	COST $ X 10^3	PERFORMANCE (nm)	ANALYSIS	ADDITIONAL DATA
38	DME-VOR-Doppler-Decca-C2	91	< 0.1850	A.S.	
39	VOR-Doppler-C3	92	< 0.2467	A.S.	
40	DME-Doppler-C3	93	< 0.1850	A.S.	
41	DME-VOR-Doppler-C3	97	< 0.1850	A.S.	
42	Doppler-Decca-C3	102	0.2474	O.T.	Limiting case 0.1918 nm
43	VOR-Doppler-Decca-C3	106	< 0.2467	A.S.	
44	DME-Doppler-Decca-C3	107	< 0.1850	A.S.	
45	DME-VOR-Doppler-Decca-C3	111	< 0.1850	A.S.	

REFERENCES

1. Denham, W. F., and Speyer, J. L.: "Optimal Measurement and Velocity Correction Programs for Midcourse Guidance." AIAA Journal, vol. 2, no. 5, May 1964.

2. Battin, R. H.: A Statistical Optimizing Navigation Procedure for Space Flight. ARA Journal, November 1962.

3. Fagan, J. H., and Whitlow, D. W.: Timing Schedule Optimization for Earth Orbit. M.I.T., Masters Thesis, 1965.

4. Meier, L., Peschon, J., and Dressler, R. M.: Optimal Control of Measurement Subsystems. IEEE Trans. Auto Control, vol. AC-12, no. 5, October 1967.

5. Tung, F., Rauch, H. E., and Striebel, C. T.: Maximum Likelihood Estimates of Linear Dynamic Systems. AIAA Journal, vol. 3, no. 8, August 1965.

6. Bryson, A. E. and Ho, Y. C.: Applied Optimal Control. Blaisdell Company, Massachusetts, 1969.

7. Lapidus, L. and Luus, R.: Optimal Control of Engineering Processes. Blaisdell Company, Massachusetts, 1967.

8. Abramowitz, M. and Stegun, I. A.: Handbook of Mathematical Functions. United States Department of Commerce, National Bureau of Standards, 1964.

9. Jacobson, D. H.: New Second-Order and First-Order Algorithms for Determining Optimal Control: A Differential Dynamic Programming Approach. Journal of Optimization Theory and Applications, vol. 2, no. 6, 1968.

10. Robbins, H. M.: A Generalized Legendre-Clebsch Condition for Singular Cases of Optimal Control. IBM, Federal Systems Division, Owego, New York, report no. 66-825, 1966.

11. Jacobson, D. H.: A New Necessary Condition of Optimality for Singular Control Problems. Harvard University, Division of Applied Physics, report no. 576, 1968.

12. McCloskey, L. M.: Integrated Navigation System Design for Deep Submergence Vehicles. M.I.T. Instrumentation Laboratory report R-594, 1967.

13. Kayton, M. and Fried, W. R.: Avionics Navigation Systems. New York, Wiley and Sons, 1969.

14. DeGroot, L. E. and Polhemus, W. L.: Navigation Management: The Integration of Multiple Sensor Systems. Navigation, vol. 14, no. 3, 1967-68.

15. Dodington, S. H.: Ground-Based Radio Aids to Navigation. Navigation, vol. 14, no. 4, 1967-68.

16. Blakelock, J. H.: Automatic Control of Aircraft and Missiles. New York, Wiley and Sons, Inc., 1965.

17. Babister, A. W.: Aircraft Stability and Control. New York, MacMillan Company, 1961.

18. Etkin, B.: Dynamics of Flight. New York, Wiley and Sons, Inc., 1959.

19. Taylor, J. W. R.: Jane's All the World's Aircraft. New York, McGraw-Hill Co., 1967-68.

20. Press, H., Medows, M., Hadlock, I.: A Re-Evaluation of Data on Atmospheric Turbulence and Airplane Gust Loads for Application in Spectral Calculations. NASA report 1272, 1956.

21. Cramer, H.: The Elements of Probability Theory. New York, Wiley & Sons, 1955.

22. Hildebrand, F. B.: Methods of Applied Mathematics. Prentice-Hall, Inc., N. J., 1952.

23. Gaines, H. T., Hilal, A. K., and Kell, R. J.: Computer Recommendations for an Automatic Approach and Landing System for V/STOL Aircraft. Vol. 1, NASA/ERC Contractors Report, Contract Number NAS 12-615, June 1968.

24. Ergin, E. I.: Advanced SST Guidance and Navigation System Requirements Study Final Report. Vol. 1-3, NASA/ERC Contractors Report, Contract Number NAS 12-510, April 1967.

25. Aoki, M. and Ki, M. T.: Optimal Discrete-Time Control System with Cost for Observation. IEEE Trans. on Auto Control, vol. AC-14, no. 2, April 1969.

26. Kushner, H. J.: On the Optimum Timing of Observations for Linear Control Systems with Unknown Initial State. IEEE Trans. Automatic Control, vol. AC-9, April 1964.

27. Bekey, G. A. and Karplus, W. J.: Hybrid Computation. Wiley and Sons, New York, 1968.

28. Gilbert, E. G.: The Application of Hybrid Computers to the Iterative Solution of Optimal Control Problems in Computing Methods in Optimization Problems. Academic Press, New York, 1964.

BIOGRAPHICAL SKETCH

David Royal Downing was born on July 21, 1939 in Lima, Ohio. His family moved to Lincoln Park, Michigan where he attended elementary and high school graduating from Lincoln Park High School in 1958. He then entered the University of Michigan and received a BSE (Aeronautical Engineering) in August 1962 and a MSE (Instrumentation Engineering) in December 1963. He entered MIT in February 1964.

While at the University of Michigan he was a Research Assistant working on aerodynamic turbulence research and Hybrid Inertial-Doppler aircraft navigation systems. At MIT he was a Research Assistant concerned with ICBM booster guidance. He has been a Teaching Follow at the University of Michigan in an Aerodynamics laboratory and a Teaching Assistant in linear and nonlinear control theory at MIT. He was an Instructor for the summer term 1966 teaching Linear Control theory. He is now connected with NASA Electronics Research Center engaged in strapdown guidance systems and avionics research.

Mr. Downing is a member of Tau Beta Pi and Sigma Xi honary fraternities. He currently resides in Acton, Massachusetts, with his wife, the former Barbara Mathews of Lincoln Park, Michigan.